

AIR TECHNICAL INTELLIGENCE STAT TRANSLATION

STAT

RADIO ENGINEERING —
(RADIOTECHNIQUE)
VOL. 10, NO. 12, 1955
pp. 3-80

SVYAZ'IZDAT - MOSCOW

STAT



STAT

Table of Contents	<u>Page</u>
Pulse Spark Excitation of Oscillations in the Microwave Band, by I.V.Ivanov.....	1
The Reaction of Square Pulses with Random Duration and Separation on a Line Detector, by V.I.Tikhonov.....	14
The Transitory Characteristics of a Compound Pulse System made up of Nonuniform Sections, by S.N.Krize.....	22
An Analysis of Intermediate-Frequency Amplifiers in Semiconductor Triodes, by Ye.Ya.Pumper, Ye.M.Petrov.....	29
High-Frequency Broad-Band Transformers, by S.G.Kalikhman.....	47
Calculation of an Ionic Voltage Stabilizer, by G.S.Veksler.....	61
A Method for Increasing the Accuracy of Frequency Analyzers with an Electron-Beam Indicator, by N.F.Vollerner.....	73
The Effect of Capacitance of a Space Charge and Nonlinearity of a Tube Characteristic on the Frequency of a Self- Oscillator, by G.T.Shitikov.....	78
Calculation of the Amplitude Characteristics of Limiters, by Ya.Z.Tsytkin.....	104
List of Articles which Appeared in "Radio Engineering" Journal in 1955.....	110
New Books.....	117

PULSE SPARK EXCITATION OF OSCILLATIONS IN THE MICROWAVE BAND

by

I.V.Ivanov

The report describes the method for spark excitation of oscillations in cavity resonators. The energy level of the fundamental oscillation is given. The design of the resonator is described, giving to the charge HF pulses of an exponential form whose duration is of the order of 0.1μ sec in the 8 - 13 cm band. The pulse output power of the resonator reaches 10 watts.

In connection with scanning by new methods for generating microwaves, interest has lately been revived in the Hertzian spark method for exciting oscillations in the SHF band.

G.Anders (Bibl.1) describes an oscillator whose basic member is a Hertz doublet in the video alteration inspired by P.N.Lebedev (Bibl.2). In the Anders oscillator, the dipole is placed in a cylindrical circular cavity. The dipole radiation excites the entire spectrum of the cavity oscillations, and the energy of one of the oscillations of this spectrum is filtered out and emitted further on. The shortcoming of this method is that the oscillator works on the principle of extracting, from a continuous spectrum, a narrow strip of the dipole oscillations, whose width is determined by a quality factor of the cavity. There is no oscillating interaction of the dipole and cavity, so that the fundamental energy of the dipole emission is wasted on equal excitation of all the other oscillations of the cavity spectrum. Besides, the power which the oscillator puts into the load has an insignificantly small value.

Oscillators, working on a similar principle of extracting a narrow strip from

a continuous spectrum of narrow pulse current, are described by Davis and others (Bibl.3 and 4). As in Anders's case, there is little utilization of the energy entering the oscillator from the modulator.

The problem of the given operation consists in increasing the degree of utilized energy from the modulator in a system, consisting of a cavity resonator with a Hertz vibrator placed inside it. Speculation on the possibility of resonant interaction between these two members led to the result that, when there is a coincidence of the dipole and cavity resonant frequency, it is already impossible to consider them separately. The dipole proportions become in this case comparable to the resonator proportions, so that the dipole, together with the resonator, forms a certain complicated topology of the conducting surfaces, a resonator of a new form. If in such a resonator, it is possible to charge the component conductors at various voltages, then static electric fields arise in the system with corresponding reserves of energy. When the charged conductors are brought into the resonant circuit, currents and alternating electromagnetic fields are created, bringing into the closed system the character of standing waves. In the capacity of a closing key, a spark discharge can be used, whose operation time is much less than the period of the cavity oscillations. Such a discharge arises between the charged conductors of the resonator when the voltage drop between them is large enough for disruption.

As is well known (cf. for example the works in Bibl.5 and 6), the development of a spark discharge in air at atmospheric pressure has a streamer character. During this, in the process of forming the discharge, two stages can be observed. In the first stage, a spread of the initial avalanche and streamers crosses the spark gap between the electrodes. In the final stage, the stage of forming the main discharge, the electrodes are well overlapped by a conducting bridge, by which the pulse of the current crosses with a speed of the order of 10^{10} cm/sec, completing the disruption of the gap. For gaps of 1 mm width, the formation time for the main discharge has an order of 10^{-11} sec. So short a duration for the closing process

guarantees the possibility of using the spark as a low-inertia key for the entire microwave range. The explained calculations allow us to develop the Hertzian method for exciting oscillations usable in electromagnetic cavity resonators.

As an resonant system, in our opinion the most convenient for spark excitation in actual operation is a coaxial cylindrical cavity, a diagram of which is given

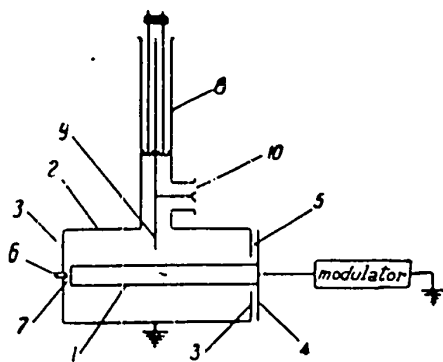


Fig.1

in Fig.1. The cavity is made up of two concentric cylinders (1) and (2) and end planes (3). The central conductor (1), because of the fact that its direct current has no contact with the outer cylinder of the end planes and enters through an opening in one of the ends. Between the disk (4), in contact with the central rod of the oscillator and one of the end surfaces (3), there is a clearance (5), forming a capacitor of fairly large capacitance. Between the points of the rod (6), in contact with the outer conductor, and the end surface of the inner conductor there is a spark gap (7). In this diagram, the following designations are used: 8 - coaxial two-wire circuit of the sonde, 9 - sonde, connected with the charge, 10 - HF outlet plug.

The inner conductor of the resonator is connected with the modulator, giving pulses of 1μ sec duration and 3 - 5 kv amplitude. An artificial line is used as modulator, which is charged by a high-voltage rectifier and connected across a thyatron to the characteristic impedance. As a consequence of the characteristic impedance of the line, the spark gap of the resonator is closed. During the firing of the thyatron, the central conductor of the resonator is charged to the disruptive potential of the spark gap U_0 ; during this time, energy is stored in the coaxial part of the resonator

$$W_0 = \frac{C_0 U_0^2}{2},$$

where C_0 is the distributed capacitance of the coaxial part of the oscillator.

While the disruption occurs, the spark gap is closed and the artificial line discharges into the characteristic impedance. The square pulse of the current, flowing through the spark channel, guarantees constant closing conditions for the last oscillation of the cavity. The resonator, closed at one end by the spark channel and at the other end by the fairly large capacitance of the central conductor entrance, on account of the stored energy W_0 accomplishes the damped oscillation.

The fundamental oscillation - an oscillation of the Lecher type with a wavelength of $\lambda = 2L$, where L is the length of the resonator, and all the odd harmonics with $\lambda = \frac{2}{2n+1}L$ ($n = 1, 2, 3, \dots$) - is excited, as will be shown below, by preferential means by comparison with the even Lecher harmonics ($\lambda = \frac{L}{n}$) and with all oscillations of the waveguide types H and E. Preference excitation of odd harmonics is related to the fact that the configuration of the electric fields of the odd harmonics is contained in the structure of the initial field of the resonator, so that the initial field can be analyzed in terms of the fields of the odd harmonics. Such an analysis, making it possible to determine the share of the initial energy entering into the fundamental oscillation (the first odd harmonic) can be nearly completed on the following supposition: We will suppose that the configuration of the initial field in the resonator is equivalent to the field in a cylindrical capacitor. Actually a longitudinal component field extends to the limits of the cavity, and consequently there is room for a certain deviation from the field of a cylindrical capacitor. After mirror-reflecting the charges, forming the field of the inner cavity relative to the two end planes, developing the fields, and repeating such operations an infinite number of times, we obtain such a periodically spaced structure of the field that:

$$f(z) = E_r = \begin{cases} \dots \dots \dots \\ E_{r_0} \text{ for } -2L < z < -L \\ -E_{r_0} \text{ for } L < z < 0 \\ E_{r_0} \text{ for } 0 < z < L \\ E_{r_0} \text{ for } L < z < 2L \\ E_{r_0} \text{ for } 2L < z < 3L \\ \dots \dots \dots \end{cases}; \quad E_{r_0} = \frac{U_0}{r \cdot \ln x},$$

where, as in the case of a cylindrical capacitor:

U_0 is the potential of the inner conductor relative to the outer,

r is the distance from the axis of the cavity,

$x = \frac{r_2}{r_1}$ is the ratio of the radii of the resonator cylinders.

Expanding $f(z)$ into a Fourier series according to sines, we get

$$f(z) = \sum_{\kappa=1}^{\infty} C_{\kappa} \sin \kappa \frac{\pi}{L} z,$$

where

$$C_{\kappa} = \frac{1}{L} \int_0^{2L} f(z) \sin \kappa \frac{\pi}{L} z \cdot dz.$$

After integrating, we get the following expressions for the amplitudes of the harmonics:

$$\begin{aligned} C_{\kappa} &= \frac{4 E_{r_0}}{\kappa \pi} \quad \text{for } \kappa = 2n - 1 \quad (n = 1, 2, \dots) \\ C_{\kappa} &= 0 \quad \text{for } \kappa = 2n \quad (n = 1, 2, \dots) \end{aligned}$$

Knowing now the distribution of the field of the fundamental oscillation

$$E_r^{(1)} = \frac{4 E_{r_0}}{\pi} \sin \frac{\pi}{L} z = \frac{4 U_0}{\pi \cdot 2 \cdot \ln x} \cdot \sin \frac{\pi}{L} z,$$



the energy entering part of this wave can be obtained. For this, it is essential to take the integral for the entire volume of the cavity from the energy density $w^{(1)} = \frac{|E_r^{(1)}|^2}{8\pi}$. On completing the integration, we obtain

$$W^{(1)} = \frac{4 U_0^2 L}{\pi^2 \ln x};$$

and neglecting the capacitance of the oscillator coaxial part $C_0 = \frac{1}{2 \ln x}$, we get

$$W^{(1)} = \frac{8}{\pi^2} \frac{C U_0^2}{2} \approx 0,8 W_0.$$

In this manner, roughly 80% of all the energy stored in the oscillator enters part of the fundamental oscillation. An analogous calculation gives a value of 10% and 3%, respectively, for the energy of the third and fifth harmonics.

The above calculation gives the initial energy for the odd harmonics of Lecher type oscillations. Excitation of even harmonics and waveguide type oscillations in an absolutely symmetrical distribution of the initial field is impossible. Their excitation is tied to a deviation of the initial field of the resonator from the field of the cylindrical capacitor, to an asymmetric distribution of the initial field (one end of the cavity has a spark gap, the other end has a lead-in capacitance), and to the presence of elements linking the cavity with the charge, deforming the initial field. Secondary types of oscillation excitation are possible on account of the radiation of the spark itself. It can be demonstrated that, by a corresponding selection of the oscillator geometry, the intensity of the fundamental oscillation can significantly heighten the intensity of secondary type oscillations; besides, the wavelengths of the secondary oscillations are at such a distance from the wavelengths of the fundamental oscillation $\lambda = 2L$ that filtering out the fundamental frequency presents no difficulty.

The oscillations of the resonator, beginning at the moment the spark gap closes at maximum amplitude, have a damped character. Let us agree to denote the duration

STAT

of the HF pulse by τ , being the time in which the oscillations will be damped e^n times. Such damping takes place, as is well known, in Q periods so that $\tau = QT$, where Q is the quality factor of the charged oscillator. The quality factor of the resonator, appearing as a prime factor and influencing the duration of the HF pulse depends on the magnitude of the loss of oscillating energy of the resonator. The following basic sources of loss in the cavity can be pointed out: useful expenditure of energy in the load, loss along the cavity walls and loss in the spark resistance, included necessarily in the circuit of the resonator current. Finally, a certain amount of energy leaks from the resonator into the external space through the capacitance lead-in. This capacitance, formed by two conductive planes (cf. 5 in Fig. 1) separated by a dielectric spacer, represents a certain waveguide device, connected with the resonator across the slit; a certain leakage of energy through this system is unavoidable. It is useful to introduce the concept of "frequency quality factors," defining them as the ratio of the energy stored in the cavity to the energy lost during this period due to each of the enumerated sources of loss. In this case:

$Q_i = \frac{2r W^{(1)}}{w_i^{(1)}}$ is the internal quality factor of the cavity relative to losses in the walls;

$Q_e = 2\pi \frac{W^{(1)}}{w_e^{(1)}}$ is the external quality factor relative to the expenditure of energy on the load;

$Q_{load} = 2\pi \frac{W^{(1)}}{w_{spark}^{(1)}}$ is the quality factor determining the losses in the spark channel;

$Q_c = 2\pi \frac{W^{(1)}}{w_c^{(1)}}$ is the quality factor of the capacitance lead-in.

The general quality factor of the charged resonator Q is defined by the relationship:

$$\frac{1}{Q} = \frac{1}{Q_i} + \frac{1}{Q_e} + \frac{1}{Q_{spark}} + \frac{1}{Q_c}$$

The internal quality factor of the coaxial oscillator can be determined by conventional computing formulas (cf. for example Bibl. 7). The external quality factor

can be computed if given the mode and magnitude of the oscillator links with the load. In the given operation, an electric link with the load is used, accomplished with the aid of a sonde (9) (Fig.1), led into the oscillator radially to the loop of the electric field of the fundamental oscillation. The energy from the sonde enters the 50-ohm outlet plug (10). The coaxial two-wire circuit (8) serves as an element matching the load with the sonde, and also as a filter for the fundamental frequency.

If d is the depth of immersion of the sonde in the cavity then, as computation shows, the external quality factor has the form:

$$Q_e = \frac{\pi}{30} \cdot \frac{\ln \frac{r_2}{r_1}}{\ln^2 \frac{r_2}{r_2 - d}} R_0. \quad (1)$$

The quality factors, connected with losses in the spark channel and in the capacitance lead-in, cannot be calculated in advance, but can be determined experimentally.

Computing by eq.(1) shows that the external quality factor drops rapidly with an increase in the depth of immersion of the sonde. This leads to a decrease in the general quality factor, even in the case of a small loss in the spark and capacitance lead-in. If the link with the load is great so that the general quality factor is small, there is no sense in striving for an infinitesimally small value of loss in the resonator walls, expressed by the ratio of the cylinder radii $\frac{r_2}{r_1} = 3.6$. In this case, it is advantageous to increase the diameter of the central conductor; a certain impairment of the internal quality factor with a comparatively small Q will not lead to a noticeable change in the general Q -factor; however, the energy expended on the load becomes greater because of the increase in the capacitance of the resonator, with a resultant increase in initial energy.

The problem concerning the magnitude of the link between resonator and load and the quality factor of the resonator is especially real, if the resonator is working

on a narrow-band load. In that case, the power dissipated in the load is determined by the value of a spectral density scanning of the resonator HF pulse at the fundamental frequency. Computation shows that an optimum coupling exists, by which maximum power is obtained. While increasing the depth of immersion of the sonde up to the optimum, the external Q-factor drops, the HF pulse is shortened, its energy is "blurred" along the spectrum, and the spectral density value at the fundamental frequency decreases. Together with this, the power supplied to the load drops.

Experimental Part

The design of a resonator used for spark excitation and illustrated in Fig.2, in

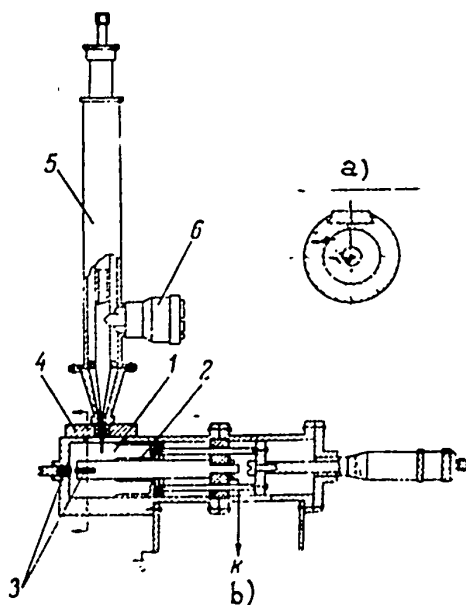


Fig.2

a) Section through AA; b) To the modulator

general follows the diagram of Fig.1 with the difference, that here a tuning plunger is used, which permits a continuous retuning of the resonator frequency in the 8 - 13 cm range. In the resonator, a contact piston (2) is installed, whose depth is equal to $\frac{\lambda}{4}$ for the medium frequency band. The sonde, with whose help the resonator was connected to the load, is led in through a slit cut into the resonator (1) during manufacture and is mounted to a carriage (4) able to travel within the boundary limits. Due to the displacement of the carriage, the sonde could be mounted in the antinode of the electric field of the fundamental oscillation and

in the node of the field of the even harmonics. The filtering out of the fundamental oscillation from the disruptive oscillations was effectively accomplished with

the help of the two-wire tuning of the sonde (5). The dimensions of the resonator are: diameter of the outer cylinder, $2r_2 = 3$ cm; diameter of the inner rod, $2r_1 = 1$ cm; length of the resonator, varying during retuning, within the limits of $L = 4 \div 6.5$ cm. The piston displacement for tuning the resonator was accomplished with the aid of a micrometer screw. The dependence of the wavelength of the fundamental oscillation and of the lowest-frequency **secondary** oscillations on the length of the cavity is plotted in Fig.3. For computing these wavelengths, the influence of the capacitance lead-in, necessarily included in the resonator circuit and producing certain changes in the characteristic frequencies of the resonator, was disregarded; the permissibility of such neglect is confirmed by experiment.

The dependence of the wavelength of the fundamental oscillation on the length of the resonator and the mean power transferred by the resonator to a 50-ohm load was tested experimentally. With the help of the change in Q-factor of the operating resonator, the duration of the HF pulse and the magnitude of the peak output power were evaluated.

The wavelength of the oscillations of the resonator was measured with the help of a wavemeter FTK-332. The voltage from the output of the detector of the wavemeter, a pulse envelope for HF oscillations is fed to an amplifier with a band in the order of 5 megacycles and an amplification equal to 100, and then to the cathode-voltmeter VKS-7B. The measurements showed that the wavelength of the resonator follows a plotted linear curve (the experimental points are plotted on the computed curve in Fig.3).

The duration of the HF pulse, necessary for evaluating the output power of the resonator pulse, was determined by measuring the general Q-factor of the working resonator. For this, a signal oscillator is used for starting the oscillating curve of the band, by which the amplitude of the forced oscillation is measured at the instant when the spark gap is closed by a discharge. For measuring the forced oscillations, the resonator sonde is connected with the detector, whose output is fed to

the oscillograph IO-4. The sweep of the oscillograph is triggered by the pulse after firing the thyatron of the modulator.

The measurements in a varied circuit under load showed that, beginning with a

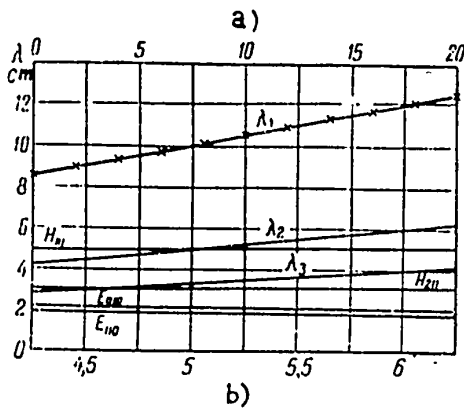


Fig.3

a) Scale of the oscillator, in mm;

b) Length of resonator L, in cm

certain determined value for the depth of immersion of the sonde $d_0 = 2.5$ mm, the general Q-factor of the resonator drops rapidly. The minor dependence of the general Q-factor on the magnitude of the circuit when $d < d_0$ speaks for a low consumption of energy by the load, compared with parasitic losses. The circuit, when $d \approx d_0$ corresponds to an approximation of the energy consumption by the load to the internal losses in the resonator. During further increase of the circuit, the gener-

al Q-factor drops rapidly together with the external Q-factor of the resonator. The general Q-factor, measured at $d = d_0$, was equal to $350 \pm 10\%$ when $\lambda = 10.7$ cm. By several preventions of losses in the resonator, including losses in the spark channel by short-circuiting the spark gap, losses in the capacitance lead-in by using a piston with a shorted capacitance, and external losses by constructing a minimum link with the load, it became possible to measure the values of the frequency Q-factors. These measurements were made while the modulator was turned off, and the resonance curves were plotted in the usual manner. This resulted in the following readings: internal Q-factor of the resonator, $Q_i = 1200 \pm 5\%$; Q-factor of the capacitance lead-in, $Q_c = 900 \pm 5\%$. The results of measuring the Q-factor of the resonator during a hot spark (the general quality factor Q) and during a shorted spark gap are accurate within the measuring error. This guarantees a value above 2000 for the Q-factor Q_{spark} of the spark. In this way, the spark is a completely satisfactory

key, also from the point of view of its resistance.

Concerning the general Q-factor $Q = 350$, the HF pulse duration ($\tau = QT$) of the order $0.1 \mu \text{ sec}$ corresponds to a wavelength of $\lambda = 10 \text{ cm}$. Inasmuch as the resonator pulse has an exponential shape, it is essential for determining the pulse power in a general sense, to determine the duration of the equivalent square pulse, carrying the energy forming the pulse of the resonator. It can be shown that the duration of the equivalent square pulse τ_e , having an amplitude equal to the initial amplitude of the HF exponential pulse, has the form

$$\tau_e = \frac{\tau}{2\pi},$$

where $\tau = QT$ is the duration of the exponential pulse.

For determining the value of the peak output power, the mean power emitted by

the resonator in a 50-ohm load. The measurements were carried out with the aid of a thermistor microwattmeter IMM-10M. At a pulse frequency repetition of 200 cycles, with the modulator pulses having an amplitude of 3 kw, and a link with the load (the microwattmeter) corresponding to a general Q-factor of $Q = 350$, the mean power is $P_{\text{mean}} = 5 \mu \text{ w}$. On conversion to the equivalent square pulse, the pulse output power was of the order of 1.5 w. The same measurements with the modulator pulses at

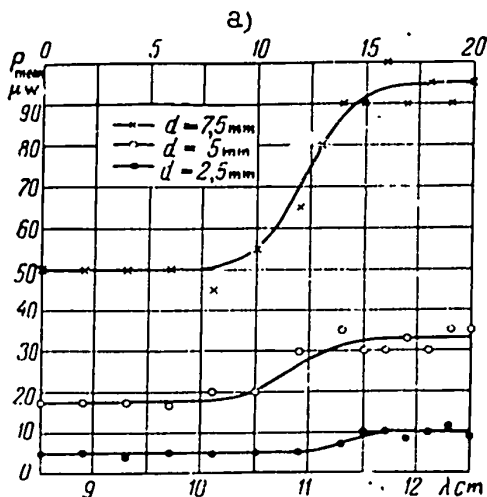


Fig. 4

a) Scale of the Resonator, in mm

an amplitude of 5 kw gave $P_{\text{pulse}} = 5 \text{ w}$.

By increasing the depth of immersion of the sonde, the emitted power is sharply increased. This is illustrated in Table 1, whose values were obtained with the 3-kw modulator pulses at a wavelength of $\lambda = 10.7 \text{ cm}$ and a frequency repetition of

200 cycles.

The dependence of the mean output power of the resonator at the generated wavelength is plotted in Fig.4 for three values of the depth of immersion of the sonde.

Table 1

Depth of immersion of the sonde d , in mm	2.5	5	7.5
General Q-factor Q	370	220	140
Duration of HF pulse, in sec^{-6}	0.13	0.08	0.05
Mean power P_{mean} , in μw	5	20	60
Pulse output power P_{pulse} , in w	1.5	8	35

The increase in emitted power with an increase in wavelength is explained by an increase in capacitance of the resonator and, as a result, an increase in the storing of initial energy.

The actual operation was carried out in the Department of Oscillations of the Physics Faculty at MGU under the supervision of Professor V.V.Migulin, who had proposed this work program. I use this occasion to express my deep gratitude to V.V. Migulin.

Article received by the Editors 8 April 1955.

BIBLIOGRAPHY

1. Anders, G. - Zeitschrift der Physik, Vol.129, No.1 (1951) pp.45-55.
2. Lebedev, P.N. - Collected Works. Gostekhizdat (1949)
3. Davis, G.L., Peer, K.B., and White, P.E.R. - Electronics. July (1950)
4. - Electronics, (Oct.1946), p.140
5. Kaptsov, N.A. - Electronics. Gostekhizdat (1953)
6. Balygin, I.E. - ZhTF No.7 (1954) pp. 1-87.
7. - The Technique of Measuring Microwaves, Vol.1, Soviet Radio (1949)

THE REACTION OF SQUARE PULSES WITH RANDOM DURATION AND SEPARATION ON
A LINE DETECTOR

by

V.I.Tikhonov

A general expression is obtained of the density probability for the voltage on a line detector load when subjected to the effect of random pulses of square shape.

The question of the sensitivity and accuracy of integrating devices for measuring the intensity of radioactive emissions (Bibl.1 and 2) and certain special radio-technological problems (Bibl.3 and 4) lead to the following problem in the theory of probability; The voltage $u(t)$ (Fig.2), presenting itself as a random sequence of square pulses of identical height h with random durations τ and intervals T , reacts on the line detector (Fig.1). Assuming as known the density probabilities $\omega_1(\tau)$ and $\omega_2(T)$, it is necessary to find the density probability $w(v)$ for the voltage at

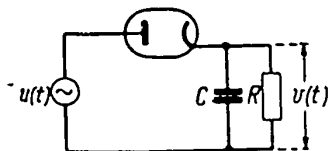


Fig.1

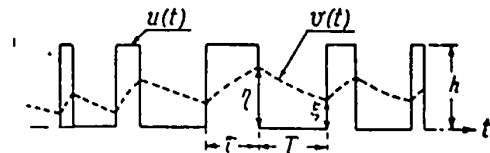


Fig.2

the detector output, by which, as it is stipulated in radio engineering for the case of a "line" detector, the volt-ampere characteristic of a tube is considered linearly broken, i.e.,

$$I = f(U) = \begin{cases} \frac{1}{r} U & \text{for } U > 0 \\ 0 & \text{for } U < 0, \end{cases} \quad (1)$$

where I is the current flowing through the tube during the reaction on it of the voltage U .

Later in the text, we will give a practical study of the most important case, where the random quantities τ and T appear independently, and consequently the voltage $u(t)$ presents a marked random process.

The differential equation correlating the output voltage $u(t)$ with the voltage $v(t)$ in the circuit RC has the form

$$\frac{dv}{dt} + \frac{v}{RC} = \frac{1}{C} f(u - v). \quad (2)$$

Since all pulses have an identical height h , eq.(2) can be resolved into two equations, valid, respectively, during the action of the pulse and during the interval between pulses,

$$\left. \begin{aligned} \dot{v} &= -\alpha v + \frac{1}{rC} h \\ \dot{v} &= -\beta v \end{aligned} \right\} \quad (2a)$$

where

$$\alpha = \frac{1}{C} \left(\frac{1}{R} + \frac{1}{r} \right), \quad \beta = \frac{1}{RC}. \quad (3)$$

The solution of the first of these equations under the initial conditions ϵ , t_1 (Fig.2) has the form

$$v = (\epsilon - a) e^{-\alpha(t-t_1)} + a. \quad (4)$$

while the solution of the second equation, under initial conditions η , t_2 , has the form

$$v = \eta e^{-\beta(t-t_2)}. \quad (5)$$

Here

$$a = \frac{h}{1 + \frac{r}{R}} \quad (6)$$

is the maximum possible value of the voltage in the circuit RC which can be attained during the active period of the pulse.

Let A denote the case when $u(t) \neq 0$, i.e., when a pulse enters the detector; let B denote the opposite case, i.e., when there is no pulse. Let us fix any instant of time t . Then, with the independent quantities τ and T , according to the complete probability equation, we have

$$w(v) = P(A) w_t(v/A) + P(B) w_t(v/B), \quad (7)$$

where $P(A)$ and $P(B)$ are the probabilities of the cases A and B, $w_t(v/A)$ and $w_t(v/B)$ are the conditional functions for the distribution of the density probability of the output voltage v on the assumption that, at the selected instant of time t , there is or is not a pulse at the input.

For the probabilities $P(A)$ and $P(B) = 1 - P(A)$ we have the obvious expressions

$$P(A) = \frac{\int_0^t \tau w_1(\tau) d\tau}{\int_0^{\infty} \tau w_1(\tau) d\tau + \int_0^{\infty} T w_2(T) dT},$$

$$P(B) = \frac{\int_0^{\infty} T w_2(T) dT}{\int_0^{\infty} \tau w_1(\tau) d\tau + \int_0^{\infty} T w_2(T) dT}. \quad (8)$$

In this way, the problem of finding $w(v)$ leads to calculating $w_t(v/A)$ and $w_t(v/B)$. For this we use the correlations (4) and (5).

Correlation (4) can be considered an equation between the random quantities ξ and $(t - t_1)$ on the one hand, and $v - c$ on the other. Actually, let $P_1(\xi)$ be the density probability for the lower ordinate of the inflection points of the curve $v(t)$ (Fig.2), while $P_A(\Delta)$ is the density probability for the random quantity $\Delta = t - t_1$, under the condition that the event A takes place at the instant of time t . Then, on the basis of eq.(4), we can write

$$\begin{aligned}
 w_t(v/A) &= \int_0^{\infty} P_1 [a + (v-a)e^{ax}] P_A(x) \left| \frac{\partial(\xi, \Delta)}{\partial(v, x)} \right| dx = \\
 &= \int_0^{\infty} P_1 [a + (v-a)e^{ax}] P_A(x) e^{ax} dx.
 \end{aligned} \tag{9}$$

This expression for $w_t(v/A)$ is obtained if, during the conversion of the variables to the order of the new variable v determined by eq. (4), the other new variable x is equal to Δ . If $x = \xi$, then $w_t(v/A)$ is expressed in another form:

$$\begin{aligned}
 w_t(v/A) &= \int_v^a P_1(x) P_A \left(\frac{1}{a} \ln \frac{x-a}{v-a} \right) \left| \frac{\partial(\xi, \Delta)}{\partial(v, x)} \right| dx = \\
 &= \frac{1}{a(a-v)} \int_v^a P_1(x) P_A \left(\frac{1}{a} \ln \frac{x-a}{v-a} \right) dx.
 \end{aligned} \tag{10}$$

By analogous reasoning, two expressions for $w_t(v/B)$ can be obtained

$$w_t(v/B) = \int_0^{\infty} P_2(v e^{\beta y}) P_B(y) e^{\beta y} dy, \tag{11}$$

$$w_t(v/B) = \frac{RC}{v} \int_v^a P_2(y) P_B \left(\frac{1}{\beta} \ln \frac{y}{v} \right) dy. \tag{12}$$

Here $P_2(\eta)$ is the density probability for the upper ordinate of the inflection points of the curve $v(t)$, and $P_B(\Delta)$ is the density probability for the random quantity $\Delta = t - t_2$ in the state B.

Equations (9) ÷ (12) give an expression for the function of the density probability $w_t(v/A)$ and $w_t(v/B)$ through the still unknown distribution functions $P_1(\xi)$, $P_2(\eta)$, $P_A(\Delta)$, and $P_B(\Delta)$. Let us find these functions.

$P_A(\Delta)$ is a function of the interval distribution between the initial pulse and the fixed instant of time t under the condition that, at the instant of time t , there is a pulse. It is obvious that

$$P_A(\Delta) = \int_0^{\infty} P_A(\Delta/\tau) w_1(\tau) d\tau, \tag{13}$$

where $P_A(\Delta/\tau)$ is the conditional function of the density probability for the quantity Δ under the condition that the duration of the pulse τ is given. However, for the fixed duration of the pulse τ , the quantity Δ is included within the limits $0 < \Delta < \tau$ so that equal distribution takes place within these limits, i.e.,

$$P_A(\Delta/\tau) = \begin{cases} \frac{1}{\tau} & \text{for } \Delta < \tau \\ 0 & \text{for } \Delta > \tau. \end{cases} \quad (14)$$

Therefore,

$$P_A(\Delta) = \int_{\Delta}^{\infty} \frac{1}{\tau} w_1(\tau) d\tau. \quad (15)$$

Such reasoning leads to the following expression for $P_B(\Delta)$:

$$P_B(\Delta) = \int_{\Delta}^{\infty} \frac{1}{T} w_2(T) dT. \quad (16)$$

Let us now turn to calculating the functions $P_1(\xi)$ and $P_2(\eta)$. We notice first of all that it is necessary to find only one of these, since the other function is determined from the first function by integration. Let us discuss this connection between $P_1(\xi)$ and $P_2(\eta)$.

If in eq.(4) we substitute the duration of the pulse τ for $(t - t_1)$, we obtain the connection between the ordinate ξ of the lower break of the curve $v(t)$ and the ordinate η corresponding to the upper break of the same curve. Using the same method employed for obtaining the distribution $w_t(v/A)$ through $P_1(\xi)$ and $P_A(\Delta)$, two expressions are obtained corresponding to two methods for converting the variables. These two means are obtained, obviously, from the correlations (9) and (10) if we substitute in them $w_1(x)$ for the function $P_A(x)$:

$$P_2(\eta) = \int_0^{\infty} P_1[a + (\eta - a)e^{ax}] w_1(x) e^{ax} dx, \quad (17)$$

$$P_2(\eta) = \frac{1}{a(a-\tau)} \int_{\eta}^a P_1(x) \omega_1 \left(\frac{1}{a} \ln \frac{x-a}{\eta-a} \right) dx. \quad (18)$$

Using eqs.(11) and (12) and eq.(5), we get

$$P_1(\xi) = \int_0^{\infty} P_2(\xi e^{\beta y}) \omega_2(y) e^{\beta y} dy, \quad (19)$$

$$P_1(\xi) = \frac{RC}{\xi} \int_{\xi}^a P_2(y) \omega_2 \left(\frac{1}{\beta} \ln \frac{y}{\xi} \right) dy. \quad (20)$$

Any pair of equations, either the one taken from the system (17) and (18) or from the system (19) and (20), can serve for determining $P_1(\xi)$ and $P_2(\eta)$.

Analogous correlations will be valid both in the case when successive pulses have a fixed duration but a random height h and in the case when, in the examined system, pulses of the harmonic voltage with a frequency f and random duration τ and intervals T are acting, if the condition

$$f \gg \alpha, f \gg \beta,$$

is satisfied, permitting the use of the averaging method (Bibl.3).

In practice, often one particular case is used, when in the circuit of Fig.1 pulses of identical height h and fixed duration $\tau_0 = \text{const}$ are active, arriving independent of time. In this case, the original density probability for the duration and intervals of the pulses is given by the expressions

$$\omega_1(\tau) = \delta(\tau_0 - \tau), \quad (21)$$

$$\omega_2(T) = m e^{-mT} dT, \quad (22)$$

where δ is the delta function, $m = \frac{n}{1 + n\tau_0}$ is the mean number of pulses arising in unit time.

For the given case, eq.(17) will yield

$$P_2(\eta) = e^{a\tau_0} P_1[a + (\eta - a)e^{a\tau_0}]. \quad (23)$$

Having substituted this value in eq.(20), we get the following integral equation:

$$P_1(\xi) = mRC e^{a\xi} \xi^{\frac{m-\beta}{\beta}} \int_{\xi}^a P_1 [a + (y-a)e^{a\xi}] y^{-\frac{m}{\beta}} dy. \quad (24)$$

We failed to find an analytical solution not only for eqs. (17) - (20), but even for this particular equation, establishing a probability connection between the upper η and lower ϵ ordinates of the inflection points of the curve of the output voltage $v(t)$. This does not permit obtaining demonstrable analytic expressions for $w_t(v/A)$ and $w_t(v/B)$ and, consequently, for $w(v)$. Therefore, during the solution of problems of the examined type, numerical methods should be used.

Therefore, the way of solving the problem of the reaction of random pulses on a line detector is to use the above method. In spite of not succeeding in solving this problem analytically to the end, we believed it useful to publish this article. The fact is that the examined problem is of interest to radio physics and, at present, such problems are involved in many instances. However, up to this time there is no clarity with respect to the correct way of solving the problem under discussion. More than that, in some papers (Bibl.4) incorrect results are cited. The error in the paper referred to is due to the fact that the voltage values in the capacitor C at the end of pulse K and of pulse $K + 1$ are considered equal, regardless of the magnitude of the random interval T between them. Such a supposition is correct in the case of regular pulses with steady operating conditions of the detector but unreliable for a random sequence of pulses. Certain critical remarks in this respect can be made even on the recently published paper by A.G.Frantsuz (Bibl.5).

Article received by the Editors 7 February 1955.

BIBLIOGRAPHY

1. Sanin, A.A. - Radio Technological Methods for Research on Radiation. GITTL (1951)

2. Elmor, V. and Sends, M. - Electronics in Nuclear Physics. IIL (1953)
3. Bogolubov, N.N. - Concerning Certain Statistical Methods in Mathematical Physics.
AN USSR (1945)
4. Burgess, R.E. - Wireless Engineer. Vol.28, No.338 (1951)
5. Frantsuz, A.G. - Radio Engineering, Vol.9, No.6 (1954)

THE TRANSITORY CHARACTERISTICS OF A COMPOUND PULSE SYSTEM MADE UP OF
NONUNIFORM SECTIONS

by

S.N.Krize

Active Member of the Society

In this article, the transitory characteristics of a multisectional line pulse system made up of nonidentical sections of arbitrary form with lumped constants are examined. Likewise a link is established between the transitory characteristics of the most general form and simpler particular cases.

The widespread use of spectral analysis in radio engineering methods permits a thorough study of the equations for the frequency characteristics of many systems. But for calculating the assembly processes in pulse systems it is essential to calculate their transient characteristics; therefore, in many papers (Bibl.1, 2, 3, 4, and others) a connection is established between the frequency and transitory characteristics of the system. In the general form, this connection can be found for line circuits, as is well known, by the methods of operational calculation or through Fourier integrals.

The majority of authors in their investigations calculate the transitory characteristics for comparatively simple systems, made up of identical sections, for example amplifier stages with the same pass band, etc. But often the necessity arises, dictated by practical demands, to find the transitory characteristics for more complicated systems, formed of nonidentical sections with various pass bands.

We will calculate the transient function for a system consisting of N sections with various time constants. An N -stage video amplifier with dissimilar cascades or its high-frequency analog, an N -stage resonance amplifier with various separate-step

pass bands, can serve as an example of such a system. In the latter case, as S.I. Yevtyanov (Bibl.1) demonstrated, the transient function determines the law for setting up the high-frequency voltage envelopes at the amplifier output.

The equation for the frequency characteristics of such a system has the form

$$m(i\omega) = \frac{1}{(1 + i\omega\tau_1)(1 + i\omega\tau_2) \dots (1 + i\omega\tau_N)} = \prod_{k=1}^N \frac{1}{(1 + i\omega\tau_k)} \quad (1)$$

For calculating the transient function we will use the Fourier integral

$$h(t) = \frac{1}{2\pi} \int_{-\infty}^{+\infty} \frac{e^{i\omega t} d\omega}{i\omega \prod_{k=1}^N (1 + i\omega\tau_k)} \quad (2)$$

The integral (2) is the simplest to be found, if the theorem of deductions is used; it will be equal to the sum of the deductions at individual points in the considered case - in the poles of the first order:

$$\left. \begin{array}{l} \omega_1 = 0 \\ \omega_2 = \frac{i}{\tau_1} \\ \dots \\ \omega_N = \frac{i}{\tau_N} \end{array} \right\} \quad (3)$$

As a result of integrating we find

$$h(t) = 1 - \sum_{k=1}^N \frac{e^{-\frac{t}{\tau_k}}}{\prod_{n=1}^{k-1} \left(1 - \frac{\tau_n}{\tau_k}\right) \cdot \prod_{n=k+1}^N \left(1 - \frac{\tau_n}{\tau_k}\right)} \quad (4)$$

The formula obtained appears more general in comparison to Ageyev's well-known formula. Kobzarev's formula is correct for systems with identical sections.

The transient characteristic (4) describes the process for setting up the amplitudes at the output of the high-frequency resonance amplifier with single cir-

circuits, or for setting up the instantaneous voltage value at the video amplifier output; in the latter case, eq.(4) is correct for the front build-up of the pulse, since we used the equation for the frequency characteristic (1), valid for the higher frequency region.

In the particular case of a two-stage amplifier with nonidentical parameters, eq.(4) takes the form

$$n_2(t) = 1 + \frac{\tau_2 e^{-\frac{t}{\tau_2}} - \tau_1 e^{-\frac{t}{\tau_1}}}{\tau_1 - \tau_2},$$

where τ_1 and τ_2 are the time constants of the first and second stage, determining the frequency characteristic at higher frequencies.

If each of the sections of the system has two time constants, then its frequency characteristic formula has the form

$$\bar{m}(i\omega) = \frac{1}{1 + i\omega\tau_v + \frac{1}{i\omega\tau_n}}. \quad (5)$$

Let us find the transient function

$$h(t) = \frac{1}{2\pi} \int_{-\infty}^{+\infty} \frac{e^{i\omega t} \cdot d\omega}{i\omega \left(1 + i\omega\tau_v + \frac{1}{i\omega\tau_n} \right)}. \quad (6)$$

After integration and certain transformations, we arrive at the result

$$h(t) = \frac{2}{F} e^{-\frac{t}{2\tau_v}} \cdot \text{sh} \left(\frac{t}{2\tau_v} \cdot F \right), \quad (7)$$

$$\text{where } F = \sqrt{1 - 4 \frac{\tau_v}{\tau_n}}.$$

The transient function (7) has a maximum when

$$t = t' = \frac{\tau_v}{2F} \ln \frac{1+F}{1-F} = \frac{\tau_v}{F} \cdot \text{Arth } F. \quad (8)$$

A graph of the transient function $h(t)$ is given in Fig.1, plotted according to eq.(7).

For two-section systems, each of whose sections is described by eq.(5), we obtain the following relation on the basis of Dyamel's integral:

$$h(t) = \frac{2}{F^2} e^{-\frac{t}{2\tau_v}} \left[\left(F \frac{t}{2\tau_v} + \frac{1}{F} \right) \text{sh } F \frac{t}{2\tau_v} - \frac{t}{2\tau_v} \text{ch } F \frac{t}{2\tau_v} \right], \quad (9)$$

where

$$F = \sqrt{1 - 4 \frac{\tau_v}{\tau_n}}.$$

Equation (9) is correct, for example, for the system of a double-differentiated

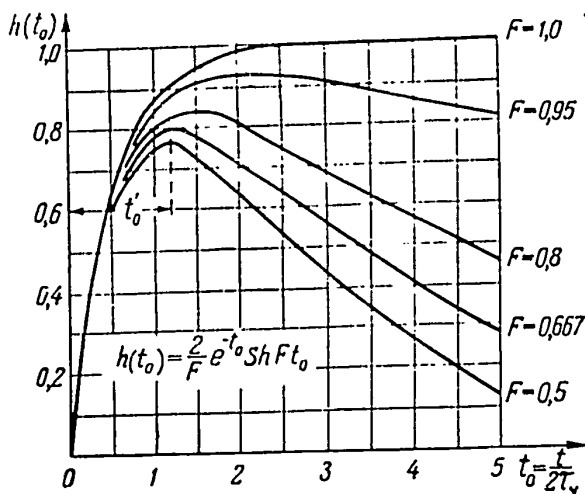


Fig.1

pulse, accomplished in two adjacent cascades of the amplifier. In Fig.2 a graph of the transient functions is presented, plotted according to eq.(9).

Equation (4) was obtained above for determining the transient function of the system, consisting of an arbitrary combination of sections, each of which is characterized by the frequency-characteristic equation of the form

$$m_{\kappa}(i\omega) = \frac{1}{1 + i\omega\tau_{\kappa}},$$

corresponding to the cascades of the aperiodic video amplifier or of the high-frequency tuned amplifier with single circuits. The obtained result is easily ex-

tended to the most general case of the linear electric system with lumped constants, an equation of the frequency characteristic which can be presented in the form of a ratio of two rational polynomials of the frequency:

$$m(i\omega) = \frac{\sum_{q=0}^p \beta_q (i\omega)^q}{\sum_{n=0}^N \alpha_n (i\omega)^n} = \frac{1}{\sum_{n=0}^N \alpha_n (i\omega)^n} + \frac{\beta_1 i\omega}{\sum_{n=0}^N \alpha_n (i\omega)^n} + \dots + \frac{\beta_p i\omega^p}{\sum_{n=0}^N \alpha_n (i\omega)^n} \quad (10)$$

For a linear system, the transient process can be considered as the sum of the processes, based on the separate components of eq.(10),

$$h_0(t) = h_1(t) + h_2(t) + \dots + h_p(t) \quad (11)$$

Let us first find the initial component of this sum $h_1(t)$, having used the Fourier transformation

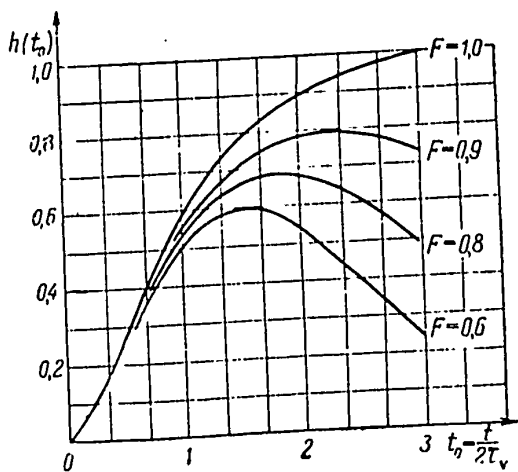


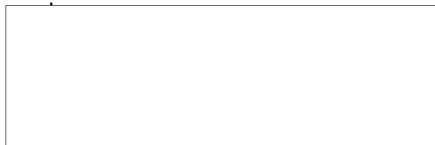
Fig.2

$$h_1(t) = \frac{1}{2\pi} \int_{-\infty}^{+\infty} \frac{e^{i\omega t}}{i\omega} \cdot \frac{d\omega}{\sum_{n=0}^N \alpha_n (i\omega)^n} \quad (12)$$

The first member of the sum (10), entering into the subintegral expression (12), on the basis of the nature of the polynomial of the n^{th} degree, can be converted to the form

$$\frac{1}{\sum_{n=0}^N \alpha_n (i\omega)^n} = \frac{1}{\alpha_N \prod_{\kappa=1}^N (i\omega - \omega_\kappa)} \quad (13)$$

where ω_κ are the roots of the given polynomial.



The structures of eqs.(13) and (1) are completely identical; consequently, for calculating $h_1(t)$ the earlier obtained eq.(4) can be used, being

$$h_1(t) = 1 - \sum_{\kappa=1}^N \frac{e^{i\omega_{\kappa}t}}{\prod_{n=1}^{\kappa-1} (1 - i\omega_{\kappa}\tau_n) \cdot \prod_{n=\kappa+1}^N (1 - i\omega_{\kappa}\tau_n)}. \quad (14)$$

After having found the first term of the sum (11), it is not difficult to determine all of its following terms if we disregard the fact that each of the subsequent terms of this sum differs from its predecessor by a constant coefficient and a factor $i\omega$. Factoring $i\omega$ out of the subintegral function in eq.(12), it can be analyzed by differentiation to t , so that

$$h_q(t) = \beta_q \frac{d^{(q-1)}}{dt^{(q-1)}} [h_1(t)] = \frac{\beta_q}{\beta_{q-1}} \cdot \frac{d}{dt} [h_{q-1}(t)]. \quad (15)$$

The unknown sum (11) can be expressed through its first term, while the derivatives of the term according to time can be determined in the following manner:

$$h_0(t) = h_1(t) + \beta_q \sum_{q=2}^p \frac{d^{(q-1)}}{dt^{(q-1)}} [h_1(t)]. \quad (16)$$

The obtained expression establishes the connection between the transient process in a linear system with lumped constants, having an arbitrary form of the frequency characteristic equation, and the transient process in systems with a simpler form, described by eqs. (1) and (13), for which the transient function can be calculated with the help of eq.(4). The obtained results, obviously, are equally suitable for calculating transient instantaneous values in video networks and for determining transient amplitudes in high-frequency networks, having abridged symbolic equations of a corresponding form.

Article received by the Editors 18 February 1955.

BIBLIOGRAPHY

1. Yevtyanov, S.I. - Transient Processes in Receiving-Amplifying Networks.
Svyazizdat (1948)
2. Gonorovskiy, I.S.- Radio Signals and Transient Processes in Radio Circuits.
Svyazizdat (1954)
3. Riskin, A.A. - Fundamentals of the Theory of Amplifying Networks. Soviet
Radio (1954)
4. Krize, S.N. - Low-Frequency Voltage Amplifiers. Gosenergoizdat (1953)

AN ANALYSIS OF INTERMEDIATE-FREQUENCY AMPLIFIERS IN SEMICONDUCTOR TRIODES

by

Ye.Ya.Pumper, Ye.M.Petrov

An analysis is given of certain networks with tuned amplifiers in point-contact, semiconductor triodes in matching conditions. The features of a technical account of such systems are shown and compared with a discussion of vacuum-tube amplifiers.

1. Introduction

At present, widespread use is made of semiconductor triode tubes in radio receiving equipment. Therefore, there is an interest in analyzing the operation of the various components of such installations. In the present paper, an analysis and a possible method are given for a technical calculation of certain resonance IF circuits in point-contact semiconductor triodes.

This problem leads to an analysis of the amplification factor for the state of maximum power transmission in the narrow frequency spectrum on a relatively low-resistance output load, linked by tuned circuits to the output of the preceding cascade, having a higher resistance. The analyzing method used and the corresponding results obtained are adaptable to any other system, characterized by the indicated features.

In calculating systems with semiconductor triodes, a specific difficulty always arises, namely that the input resistance R_{in} of the triode depends on the characteristics of its output circuit, while the output resistance R_{out} of the triode correspondingly depends on the characteristics of the input circuit. Disregarding these dependences will seriously complicate the computing of R_{in} and R_{out} . The problem is simplified in the case where complete matching takes place in the examined sys-

tem. Then R_{in} and R_{out} depend only on the triode parameters and are calculated by the well-known formulas (Bibl.3)

$$R_{in} = R_{11} \sqrt{1 - \frac{R_{12}R_{21}}{R_{11}R_{22}}} \text{ and } R_{out} = R_{22} \sqrt{1 - \frac{R_{12}R_{21}}{R_{11}R_{22}}},$$

where R_{11} , R_{12} , R_{21} , and R_{22} are the resistances of the quadripole, equivalent to the examined triode.

In the present work, R_{in} and R_{out} are assumed to be known. This is justified by the fact that the system is considered to be in a state of complete, or else partial quasi-complete balance, due to the low specific losses of the tuned circuits. If the output of the next stage and the input of the preceding stage match, then the calculation of R_{in} and R_{out} by the cited formulas is strictly valid. At partial matching, this leads to an error which decreases with decreasing losses of the circuit.

In the calculation, the problem concerning the inner capacitances of the semiconductor triode is not considered. The amplification factor along the triode current is considered independent of the frequency.

We will apply a thorough analysis, consequently, to triodes with point contacts, and for frequencies lower than 1 megacycle. At the beginning of a thorough analysis, the peculiarities of technical computations are shown, and a comparison is made of various IF amplifier circuits networks. The proposed methods for calculating intermediate-frequency amplifiers of the same degree are applicable to any network including a semiconductor triode, satisfying the conditions of stability. The resistances of the quadripole, therefore, will be determined by the circuit diagram of the triode (Bibl.1).

2. Amplifier with a Single Circuit

The IF amplifier hookup with a single circuit, in which the semiconductor tri-

ode is replaced by an active quadripole, is shown in Fig.1. In this hookup, R_{in} is the input resistance of the following triode stage. We will designate the cut-in factor on the end of the collector and the emitter, respectively, by $m_1 = \frac{L_1'}{L_1}$ and $m_2 = \frac{L_1}{L_1'}$. We will find the conditions for obtaining the maximum amplification factor of the voltage for the entire stage.*

The fundamental equations of the quadripole give the amplification factor of the triode for the voltage with open output terminals 2 - 2 (Bibl.3):

$$K_{U_{xx}} = \frac{U_{xx}}{U_1} = \frac{R_{21}}{R_{11}}$$

where U_{xx} is the value of U_2 under no-load conditions. We will split the schematic in Fig.1 along the lines 2 - 2 and 3 - 3 and apply successively to these sections the theory of the equivalent generator.

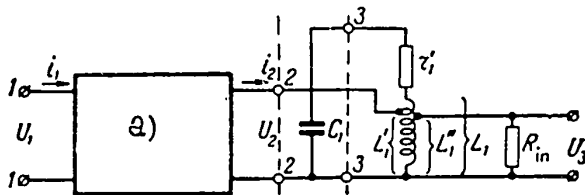


Fig.1

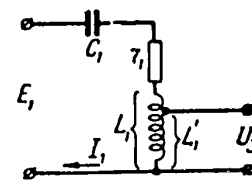


Fig.2

a) Quadripole, replacing the semiconductor triode

end, equivalent to an increase in the shunting resistance by $\frac{1}{m_1^2}$ times in comparison with a complete cut-in, the schematic in Fig.1 is converted to the schematic in Fig.2, with the following parameters:

$$r_1 = r_1' + \frac{m_1^2 \rho^2}{R_{out}} + \frac{m_2^2 \rho^2}{R_{in}} \quad (1)$$

*At small amplitudes, they will correspond to the conditions for maximum amplification of current and power.

when

$$\frac{\omega^2 C_1^2 R_{out}^2}{m_1^2} \gg 1 \text{ and } \frac{\omega^2 C_1^2 R_{in}^2}{m_2^2} \gg 1,$$

where

$$\rho = \sqrt{\frac{L_1}{C_1}}.$$

The second term represents the resistance introduced into the circuit by the triode of the given cascade, and the third term is the resistance introduced into the circuit by the input resistance of the succeeding triode. The voltage is

$$E_1 = \frac{U_{rr}}{m_1 \sqrt{1 + \frac{\omega^2 C_1^2 R_{out}^2}{m_1^2}}} \approx \frac{U_1 m_1}{\omega C_1 R_{out}} \frac{R_{21}}{R_{21}}.$$

The amplification factor of the cascade, in voltage, will be equal to

$$K_U = \frac{U_2}{U_1} = \frac{m_1 m_2 \rho^2 \frac{R_{21}}{R_{11}}}{R_{out} \sqrt{r_1^2 + \left(\omega L_1 - \frac{1}{\omega C_1}\right)^2}} \quad (2)$$

The amplification curve has the form of a resonance curve.

The condition of balance in the circuit of the collector is written as follows:

$$\frac{m_1^2 \rho^2}{R_{out}} = r_1' + \frac{m_2^2 \rho^2}{R_{in}} \quad (3)$$

and, correspondingly, in the circuit of the emitter

$$\frac{m_2^2 \rho^2}{R_{in}} = r_1' + \frac{m_1^2 \rho^2}{R_{out}} \quad (4)$$

The equations are not compatible, i.e., in a single circuit it is impossible to attain complete matching. We will derive the approximate condition of complete matching at least for the case where the resistances introduced into the circuit by

the shunts R_{in} and R_{out} are much greater than the characteristic resistance of the circuit.

Then,

$$\frac{m_1^2}{m_2^2} = \frac{R_{out}}{R_{in}}. \quad (5)$$

The voltage amplification factor, in the presence of resonance and of matching across the input (emitter) or output (collector) circuit, takes the forms, respectively,

$$K_{oe} = \frac{1}{2} \frac{R_{21}}{R_{11}} \sqrt{\frac{R_{in}}{R_{out}}} \frac{m_{1e} \rho}{\sqrt{\left(r_1' + \frac{\rho^2 m_{1e}^2}{R_{out}} \right) R_{out}}} \quad (6)$$

or

$$K_{ok} = \frac{1}{2} \frac{R_{21}}{R_{11}} \sqrt{\frac{R_{in}}{R_{out}}} \frac{m_{2k} \rho}{\sqrt{\left(r_1' + \frac{\rho^2 m_{2k}^2}{R_{in}} \right) R_{in}}} \quad (7)$$

In the case of almost complete matching, when $\frac{m_{1e}^2}{R_{out}} \gg r_1'$ or $\frac{m_{2k}^2}{R_{in}} \gg r_1'$ the amplification factors in the presence of balance across the input or output circuits coincide and have the form

$$K_{oe} = K_{ok} = \frac{1}{2} \frac{R_{21}}{R_{11}} \sqrt{\frac{R_{in}}{R_{out}}} = \frac{1}{2} \sqrt{\frac{R_{out}}{R_{in}}} \alpha = K_{op}, \quad (8)$$

where α is the current amplification factor of the triode.

We will express the voltage amplification factor by the ratio: $\frac{Q_{xx}}{Q_{work}} = \gamma$, where $Q_{xx} = \frac{\omega L_1}{r_1'}$ is the quality factor of the no-load condition, and $Q_{work} = \frac{\omega L_1}{r_1}$ is the work quality factor.

We will first consider the case of matching across the emitter circuit. From the expression for the work Q-factor of the circuit and from eqs.(1) and (4) we have

$$m_{2e} = \sqrt{\frac{R_{in}}{2\rho Q_{work}}} \quad (9)$$

Substituting this expression in the condition of matching across the emitter circuit, we find

$$m_{1e} = \sqrt{\frac{R_{out}}{\rho} \left(\frac{1}{2Q_{work}} - \frac{1}{Q_{x.r}} \right)} \quad (10)$$

Analogously, in the presence of matching across the collector circuit, we have

$$m_{1k} = \sqrt{\frac{R_{out}}{2\rho Q_{work}}} \quad (11)$$

$$m_{2k} = \sqrt{\frac{R_{in}}{\rho} \left(\frac{1}{2Q_{work}} - \frac{1}{Q_{x.r}} \right)} \quad (12)$$

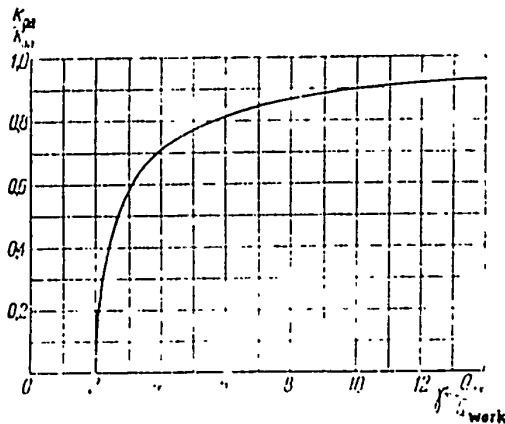


Fig.3

From eqs.(6), (7), and (8) we will determine voltage amplification factors K_{oe} and K_{ok} in the presence of matching across the emitter circuit or across the collector circuit through the values of γ :

$$K_{ok} = K_{oe} = K_{op} \sqrt{1 - \frac{2}{\gamma}} \quad (13)$$

at $\gamma \gg 1$ $K_{ok} = K_{oe} \approx K_{op}$.

It follows from eq.(13) that the value K_{op} has the meaning of a limiting amplification, which can be attained for the given triodes as $\gamma \rightarrow \infty$.

Matching across the emitter and across the collector leads to the same amplification at the same values of γ . The dependence of the amplification on γ is shown in Fig.3. The growth of γ to four or five does not lead to a significant increase in amplification. For the selected value of γ the amplification does not depend on the frequency within the limits of accuracy of the inequality (1).

Using the expression for the generalized detuning α_1 , applicable to the given case, we will obtain an expression linking Q_{XX} with the intermediate frequency and the pass band P:

$$Q_{XX} = \frac{\gamma \alpha_1 f_0}{P} \quad (14)$$

From this it follows that a decrease in f_0 permits scaling Q_{XX} , while keeping γ , α_1 , and P constant.

The difference between calculating the amplification of a cascade with a single circuit in a semiconductor triode and calculating the amplification of an electron tube consists of the following:

- 1) The values of γ are selected to match the curve in Fig.3 within the limits $4 - 6$;
- 2) The choice of an intermediate frequency is made while disregarding eq.(14);
- 3) The work Q-factor;

$$Q_{work} = \frac{f_0}{P} \alpha_1;$$

$$4) Q_{XX} = \gamma Q_{work};$$

- 5) The cut-in factors are chosen in the presence of matching across the emitter agreeing with eqs.(9) and (10) and of matching across the collector agreeing with eqs.(11) and (12);

- 6) The amplification factor at matching across the emitter and collector are determined by eq.(13).

3. Amplifier with a Band Filter

A diagram of amplification with a band filter is shown in Fig.4. As before, the semiconductor triode is replaced by an active quadripole. The resistance R_{in} is the input resistance of the succeeding triode, while $m_1 = \frac{L_1}{I_1}$ and $m_2 = \frac{L_2}{I_2}$ are the cut-in factors from the collector and emitter end, respectively.

Splitting the network along the lines 2 - 2 and 3 - 3 and applying successively the theory of the equivalent generator, we arrive at the equivalent network in Fig.5. Having used the basic formulas of the quadripole and having

$$\frac{\omega^2 C_1^2 R_{out}^2}{m_1^4} \gg 1 \text{ and } \frac{\omega^2 C_2^2 R_{in}^2}{m_2^4} \gg 1$$

we obtain the following values for the parameters of the network in Fig.4:

$$r_1 = r_1' + \frac{m_1^2 p_1^2}{R_{out}}, \quad r_2 = r_2' + \frac{m_2^2 p_2^2}{R_{in}} \quad (15)$$

where r_1' and r_2' are the characteristic resistances of the first and second circuits

$$p_1^2 = \frac{L_1}{C_1}, \quad p_2^2 = \frac{L_2}{C_2}. \quad \text{The value } E_1 \text{ is equal to}$$

$$E_1 = \frac{U_1 m_1}{\omega C_1 R_{out}} \frac{R_{21}}{R_{11}} \quad (16)$$

For a network with a partial cut-in, the voltage amplification factor of the

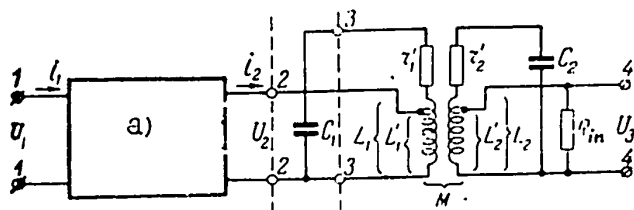


Fig. 4

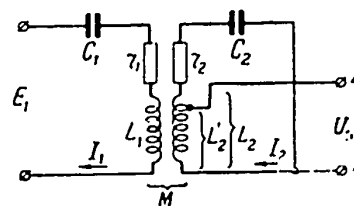


Fig. 5

a) Quadripole, replacing the semiconductor triode

cascade as a whole will have the following value:

$$K_U = \frac{M R_{21} m_1 m_2}{C_2 R_{11} [\omega^2 M^2 + r_1 r_2 (1 + iy Q_{work_1}) (1 + iy Q_{work_2})] \omega C_1 R_{out}} \quad (17)$$

where



$$y = \frac{\omega}{\omega_0} - \frac{\omega_0}{\omega}; \quad Q_{work_1} = \frac{\omega_0 L_1}{r_1}, \quad Q_{work_2} = \frac{\omega_0 L_2}{r_2}.$$

The amplification factor in the presence of resonance has a maximum with the values m_1 and m_2 , corresponding to matching conditions, which can be written in the following manner:

1) for the emitter circuit

$$\frac{m_2^2 \rho_2^2}{R_{in}} = r_2' + \frac{\omega_0^2 M^2}{r_1' + \frac{m_1^2 \rho_1^2}{R_{out}}}, \quad (18)$$

2) for the collector circuit

$$\frac{m_1^2 \rho_1^2}{R_{out}} = r_1' + \frac{\omega_0^2 M^2}{r_2' + \frac{m_2^2 \rho_2^2}{R_{in}}}. \quad (19)$$

In the given case, complete matching is possible, which results in two conditions

$$\gamma_1 = \gamma_2 = \gamma, \quad \gamma = \frac{2}{1 - \beta_1 \beta_2}, \quad (20)$$

where

$$\gamma_1 = \frac{Q_{xx1}}{Q_{work_1}}; \quad \gamma_2 = \frac{Q_{xx2}}{Q_{work_2}}; \quad \beta_1 = Q_{work_1} K \text{ and } \beta_2 = Q_{work_2} K,$$

$$Q_{xx1} = \frac{\omega_0 L_1}{r_1}; \quad Q_{xx2} = \frac{\omega_0 L_2}{r_2}; \quad Q_{work_1} = \frac{\omega_0 L_1}{r_1}; \quad Q_{work_2} = \frac{\omega_0 L_2}{r_2}.$$

Here K is the coupling coefficient.

For circuits with the same parameters, we have $r_1' = r_2' = r$ and $Q_{xx1} = Q_{xx2} = Q_{xx}$. From eq.(20), it thus follows that

$$\left. \begin{aligned} Q_{work_1} &= Q_{work_2} = Q_{work} \\ \beta_1 &= \beta_2 = \beta \end{aligned} \right\} \quad (21)$$

where β is the coupling factor.

At complete balance, not only is maximum amplification attained but also the work Q-factors become equal for contours with the same parameters.

The second matching condition for the case of identical circuits leads to an expression connecting γ and β :

$$\gamma = \frac{2}{1 - \beta^2} \quad (22)$$

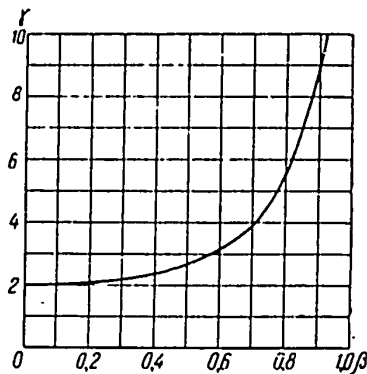


Fig.6

At complete matching, the choice of β determines the value of γ . When $2 < \gamma < \infty$, we correspondingly have $0 < \beta < 1$.

From eq.(22) whose graph is given in Fig.6, it follows that, at full matching, it is difficult to express $\beta > 0.7 - 0.8$

since $\gamma = 4$ already at $\beta = 0.707$ and $\gamma = 6$ at $\beta = 0.82$.

From the expressions for the work Q-factor the switching-in factors can be found:

$$\left. \begin{aligned} m_1 &= \frac{1}{\rho} \sqrt{r R_{out} (\gamma - 1)} \\ m_2 &= \frac{1}{\rho} \sqrt{r R_{in} (\gamma - 1)} \end{aligned} \right\} \quad (23)$$

Having substituted the expressions for the cut-in factors of eq.(23) in eq.(17) under conditions of resonance and using eq.(22), we get the following expression for the voltage amplification at complete balance and with identical circuits of the filter:

$$K_{U_0} = \frac{1}{2} \frac{R_{21}}{R_{11}} \sqrt{\frac{R_{in}}{R_{out}}} \beta = K_{OP} \beta = K_{OP} \sqrt{1 - \frac{2}{\gamma}} \quad (24)$$

The magnitude K_{OP} coincides with eq.(8). It has the meaning of a limiting coefficient for the voltage amplification at complete matching and when $\gamma \rightarrow \infty$.

The calculation of cascades with a band filter differs from the conventional calculation of vacuum-tube amplifiers, studied specifically by V.I.Siferov (Bibl.2), by the following characteristics:

- 1) The values of the coupling factor β and the ratio of the Q-factors $\gamma = \frac{Q_{\text{ext}}}{Q_{\text{work}}}$ are selected according to the curves in Figs.3 and 6;
- 2) The intermediate frequency f_0 is selected while disregarding eq.(14);
- 3) From the generalized detuning, the intermediate frequency and the given pass band are determined

$$Q_{\text{work}} = \frac{f_0}{\beta} \alpha_1.$$

- 4) $Q_{\text{ext}} = \gamma Q_{\text{work}}$;
- 5) The cut-in factors m_1 and m_2 are found according to eq.(23);
- 6) The amplification factor at complete matching is determined in agreement with eq.(24).

4. Band Filter with Parallel and Series Circuits

A diagram of such an amplifier is shown in Fig.7. By means of successive application of the equivalent generator theory, this leads to the diagram in Fig.8, we have, for $\frac{\omega^2 C_1^2 R_{\text{out}}^2}{m_1^4} \gg 1$,

$$r_1 = r_1' + \frac{m_1^2 \rho_1^2}{R_{\text{out}}}, \quad (25)$$

$$E_1 = \frac{U_1 m_1}{C_1 R_{\text{out}}} \cdot \frac{R_{21}}{R_{11}}. \quad (26)$$

Such a cascade has as a voltage amplification factor of

$$K_U = \frac{MR_{\text{in}} \frac{R_{21}}{R_{11}} m_1}{C_1 R_{\text{out}} [\omega^2 M^2 + Z_1 (Z_1 + R_{\text{in}})]}, \quad (27)$$

where

$$Z_1 = r_1 + i \left(\omega L_1 - \frac{1}{\omega C_1} \right); Z_2 = r_2 + i \left(\omega L_2 - \frac{1}{\omega C_2} \right).$$

The matching conditions for the collector circuit of the schematic in Fig.7 is expressed in the following manner:

$$\frac{m_1^2 \rho_1^2}{R_{out}} = r_1' + \frac{\omega_0^2 M^2}{r_2' + R_{in}} \tag{28}$$

An analysis demonstrates that the maximum power in the emitter circuit is obtained under the condition of an optimum link:

$$R_{in} + r_2' = \frac{\omega_0^2 M^2}{r_1' + \frac{m_1^2 \rho_1^2}{R_{out}}} \tag{29}$$

The given system in the general case is incompatible with m_1 and the coupling factor K . When $r_1' < \frac{\omega_0^2 M^2}{R_{out}}$ and $r_2' < R_{in}$ the condition of eq.(29) coincides with

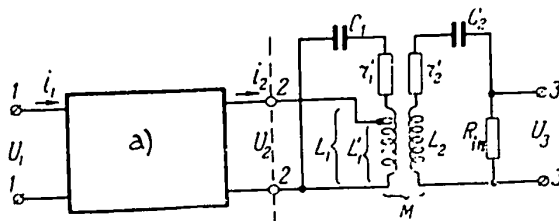


Fig.7

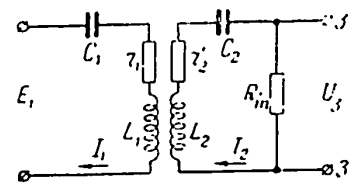


Fig.8

a) Quadripole, Replacing the Semiconductor Triode

matching across the collector. In this case complete matching takes place, whose condition is expressed by

$$\frac{m_1^2 \rho_1^2}{R_{out}} = \frac{\omega_0^2 M^2}{R_{in}} \tag{30}$$

We will determine the voltage amplification factor with balance across the collector circuit, using eq.(27) during resonance and the congruence condition (28):

$$K_{ok} = K_{oP} \sqrt{1 - \frac{1}{\gamma_1 - 1}} \sqrt{1 - \frac{1}{\gamma_2}} \quad (31)$$

At optimum coupling we get from eq.(27) for the condition of resonance and from eq.(29)

$$K_{oe} = K_{oP} \sqrt{1 - \frac{1}{\gamma_1}} \sqrt{1 - \frac{1}{\gamma_2}} \quad (32)$$

At $\gamma_1 \gg 1$ and $\gamma_2 \gg 1$, we get $K_{ok} = K_{oe} = K_{oP}$.

We will then define the general conditions which permit determining the coupling factor $\beta = K_{work}$, taking into account that $Q_{work1} = Q_{work2} = Q_{work}$, $C_1 \neq C_2$, $L_1 \neq L_2$, $r_1 \neq r_2$ and $Q_{xx1} \neq Q_{xx2}$. At balance across the collector, eq.(28) will

yield, as in the case of the band filter,

$$\gamma_1 = \frac{Q_{xx1}}{Q_{work}} = \frac{2}{1 - \beta^2} \quad (33)$$

From eq.(33) it follows that $\beta < 1$. In the opposite case the condition of congruence breaks off.

For the case of optimum coupling, after dividing both parts of eq.(29) by $\omega_0 L_1$ and verifying that $Q_{work1} = Q_{work2}$, we

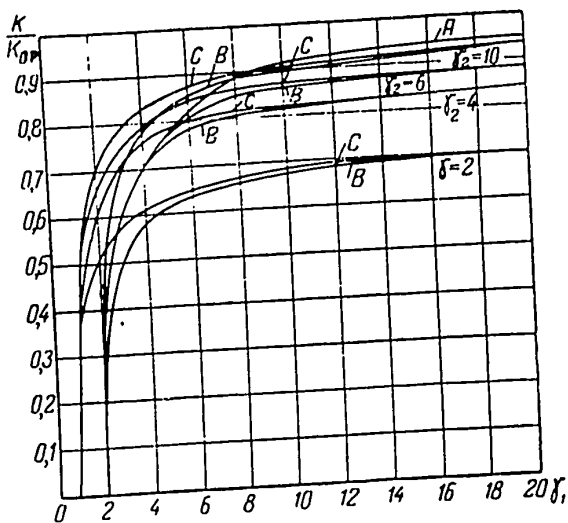
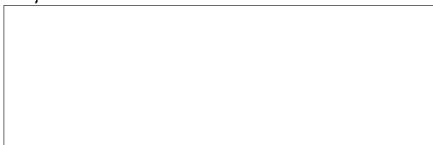


Fig.9

get:

$$\beta = 1. \quad (34)$$

Selecting values of γ_1 at optimum coupling, according to eq.(32) permits determining the value $\sqrt{1 - \frac{1}{\gamma_1}}$ when $\gamma_1 = 4$, $K_{oe} = 0.87 K_{oP} \sqrt{1 - \frac{1}{\gamma_1}}$.



.41

STAT

An increase in γ_1 to 4, 5, or 6 does not lead to a significant increase in amplification.

The dependence of the amplitude on γ_2 , in the case of balance across the collector and of optimum coupling, has the same form. An increase in γ_2 to 4, 5, or 6 likewise does not result in a significant increase in amplification.

Having assumed the ratio of K_{oe} and K_{ok} according to eqs.(31) and (32), at the same relationship of Q-factors, it is possible to compare the amplification magnitude during balance across the collector with the case of optimum coupling

$$\frac{K_{oe}}{K_{ok}} = \sqrt{1 + \frac{1}{\gamma_1(\gamma_1 - 2)}} \quad (35)$$

The case of optimum coupling thus leads to a slightly larger amplification. When $\gamma_1 = 4$, we have $\frac{K_{oe}}{K_{ok}} = 1.06$. When $\gamma_1 \rightarrow \infty$, we have $\frac{K_{oe}}{K_{ok}} \rightarrow 1$.

We will next consider a general schematic for calculating an amplifier with series and parallel circuits under the condition of $Q_{work1} = Q_{work2} = Q_{work}$. As in former cases, the amplifier should guarantee the wanted pass band P with frequency distortions σ_1 in the cascade and an adjacent-channel selectivity S_e .

1. For calculating such an amplifier:

a) We select a capacitance C_1 equal to 200 - 400 μf , corresponding to the Q-factors γ_1 ;

b) We determine the coupling factor β [with matching across the collector corresponding to eq.(33); at optimum coupling $\beta = 1$];

c) We select an intermediate frequency and a Q-factor at no-load conditions Q_{xx1} , derived from the expression $Q_{xx} = f_0 \frac{\gamma_1 \alpha_1}{P}$. It is possible to calculate the generalized detuning α_1 according to the curve plotted in the book by V.I. Siforov "Radio Receiving Systems," p.111, Fig.82.

2. From the capacitance C_1 and the intermediate frequency we compute L_1 and ρ_1 .

3. We calculate $Q_{work} = \frac{Q_{xx1}}{\gamma}$.

4. We determine the coupling factor $K = \frac{\beta}{Q_{work}}$.

5. From the expression for the work Q-factor we determine the cut-in factor

$$m_1^2 = \omega_0 C_1 R_{out} \left(\frac{1}{Q_{work}} - \frac{1}{Q_{x.x1}} \right).$$

6. Given γ_2 , we determine r_2' from the equation

$$r_2' = \frac{R_{in}}{\gamma_2 - 1}.$$

7. Starting with the equality of the work Q-factors of both circuits, we determine

$$p_2 = p_1 \frac{r_2' + R_{in}}{r_1 + \frac{m_1^2 p_1^2}{R_{out}}}.$$

8. Inductance of the second circuit $L_2 = \frac{p_2}{\omega_0 p_1}$.

9. Capacitance of the second circuit $C_2 = \frac{1}{\omega_0 p_2}$.

10. The limiting voltage amplification of the cascade:

$$K_{0P} = \frac{1}{2} \sqrt{\frac{R_{out}}{R_{in}}} \alpha.$$

11. The cascade voltage amplification with matching across the collector is found according to eq.(31).

12. The cascade voltage amplification at optimum coupling is in agreement with eq.(32).

13. We determine $\alpha_2 = \frac{2P_{Qwork}}{f_0}$.

14. We determine the value of the adjacent-channel selectivity:

$$S_c = \frac{\sqrt{(1 + \alpha_2^2 - \beta^2)^2 + 4\beta^2}}{1 + \beta^2}. \quad (36)$$

This formula for the hookup in question is justified by the fact that its amplification curve coincides in form with the amplification curve in the resonance zone for the usual band filter.

5. Comparison and Numerical Rating of the Circuits in Question

From eqs.(13), (24), (31), and (32) for the amplification factor of the three hookups in question, it follows that, at $\gamma \rightarrow \infty$, they are all characterized by the same amplification which is equal to the limiting value of the amplification K_{OP} eq.(8). Such a result is physically understandable, since the case of $\gamma \rightarrow \infty$ leads to reducing the characteristic losses of the circuits to a value imperceptibly small with respect to the losses introduced into the circuits by the input and output resistances of the triodes. In this case, the limiting power, which can be segregated into the outer load from the triode output circuit, is transmitted to the triode input resistance. The quantity K_{OP} is determined exclusively by the triode parameters.

For a home-made triode with point contacts, introduced into the circuit from a master point in the base, the following data is possible: $R_{21} = 6 \times 10^4$ ohm; $R_{11} = 300$ ohms; $R_{in} = 232$ ohms; $R_{out} = 15,500$ ohm (Bibl.3). Then according to eq.(8), $K_{OP} = 12.2$. For the last value of γ , the amplification has a lower value. The amplification values depending on γ are plotted in Fig. 9. According to eqs.(24) and (13) an amplifier with a band filter with two identical circuits during complete balance, and an amplifier with a single circuit, balanced across the emitter or collector, are characterized by identical amplification when the Q-factors of γ have an identical relationship. The dependence of the amplification on γ for these cases in Fig.9 is depicted by curve A.

With the same values of m_1 , a hookup with a single circuit gives greater amplification in the presence of matching than a network with a band filter. From eqs.(10), (11), and (23) it follows that, at the same m_1 the value of γ appears large for a hookup with a single circuit.

1/4

STAT

In the case of a band filter with parallel and series circuits (curves B and C in Fig.9), the amplification has different values for the same values of γ_1 .

The curves C in Fig.9 correspond to the case of optimum coupling and the curves B to matching across the collector. In conformity with eq.(35) obtained above, the case of optimum coupling leads to a slightly larger amplification than matching across the collector. This is connected to the fact that, at optimum coupling, the coupling factor is $\beta = 1$ and, at the same time, to the fact of matching across the collector $\beta < 1$. In the presence of matching across the collector in a hookup with parallel and series circuits, the amplification K_{op} at $\gamma_1 = \gamma_2$ becomes equal to the amplification of systems considered above for the same values of γ_1 . This result follows directly from a comparison of eq.(31), under the corresponding assumption of $\gamma_1 = \gamma_2$, with eqs.(13) and (24). Actually, it can be seen in Fig.9 that the curves B intersect the curve A at $\gamma_1 = \gamma_2$. In this way, all the considered hookups, except the last with optimum coupling, lead in the presence of matching to the same amplification factor for the same values of γ . At $\gamma_1 < \gamma_2$, a hookup with a parallel and a series circuit gives, in this way, a greater amplification than a hookup with a simple band filter or than a hookup with a single circuit corresponding to a β -factor relationship equal to γ_1 . An increase in γ_2 leads to a rise in amplification for a hookup with parallel and series circuits. An increase in γ_2 may take place according to eq.(32), due to an increase in the input resistance of the succeeding triode R_{in} and due to a diminution in the characteristic losses r_2' . At normal values of γ_1 , equal to 4 - 6, a hookup with parallel and series circuits and optimum coupling (curves C in Fig.9 at $\gamma_2 = 4$ and $\gamma_2 = 6$) gives the greatest amplification.

A comparison of the adjacent-channel selectivity for all hookups under consideration, under the condition that frequency distortions along the edge of the band in 10 kc are equal to 3 db, and at $\gamma = 4$ leads to the following deduction (cf. the Table p 46).

For amplifiers with band filters, the adjacent-channel selectivity is here calculated according to eq.(36). It follows from these data that, with the same amplification, a hookup with a single circuit possesses the least selectivity.

A hookup with a band filter and a hookup with parallel and series circuits,

a)	S and Q	b)	c)	d)	
				e)	f)
$f_0 = 1,1 \cdot 10^6$	$S_c, \text{ db}$	7	7,8	7,8	8,45
	Q_{work}	11	16,1	16,1	20,5
$f_0 = 4,65 \cdot 10^6$	$S_c, \text{ db}$	7	7,6	7,8	8,45
	Q_{work}	46,5	68,5	68,5	87

- a) Frequency, b) Amplifier with single circuit; c) Amplifier with a band filter.
 d) Amplifier with parallel and series circuits. e) Balancing across the collector.
 f) Optimum coupling

matched along the collector and having the same amplification, are characterized by the same selectivity. A hookup with parallel and series circuits in the presence of optimum coupling is characterized by a higher adjacent-channel selectivity.

8

Article received by Editors 9 May 1955.

BIBLIOGRAPHY

1. - Problems in Radar Engineering. No.2 (1952), pp.68 - 86 (Crystal Triodes)
2. Siforov, V.I. - Radio Receiving Systems. Voenizdat (1951)
3. - Crystal Rectifiers and Amplifiers. Edited by Prof.S.G.Kalashnikov, p.49

HIGH-FREQUENCY BROAD-BAND TRANSFORMERS

by

S.G.Kalikhman

Active Member of the Society

On the basis of the well-known method for converting balanced filters into unbalanced ones, practical schematics for broad-band transformers are obtained, and the engineering formulas are derived for calculating their components. Experimental data are cited from actually constructed high-frequency broad-band transformers with flat frequency-response curves, designated for operation in the 0.15 - 100 megacycle band.

1. Basic Principles

In practice, the projecting of high-frequency radio receiving equipment often requires a matching of the resistances in the broad band of the received frequencies. Such problems are encountered, for example, in matching the antenna feeders with the input circuits of short-wave, ultrashort-wave, or of television receivers during the matching of vacuum-tube band amplifiers with the main line in the multichannel collective antenna (Bibl.1), etc.

The resonance methods, well-known from the theory of radio reception, used for solving problems of matching resistances on one frequency f_0 , are completely unsuitable in cases where the band of the transmitted frequencies ΔF becomes commensurable with its mean frequency. Under these conditions, the problem is solved by the use of band filters, based on the matching of the characteristic resistances. So that these filters may have the proper characteristic for the transformation of resistances, they should be unbalanced, i.e., their characteristic resistances at the

ends should be different.

The construction of unbalanced (transforming) band sections is based on two well-known equivalences (Bibl.2):

1. The ideal transformer with a (voltage) transformation factor n , whose primary winding is shunted by the resistance Z_0 , is equivalent to a T-shaped quadripole (Fig.1) whose components are determined by the equations

$$Z_A^T = (1 - n) Z_0, \quad (1)$$

$$Z_B^T = n(n - 1) Z_0, \quad (2)$$

$$Z_C^T = n Z_0. \quad (3)$$

2. The ideal transformer with a transformation factor n , whose primary winding is connected with the source emf across the resistance Z_0 , is equivalent to a Pi-

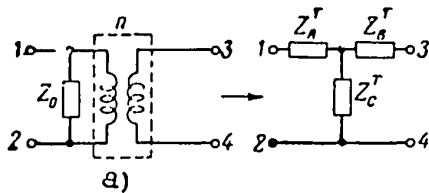


Fig.1

a) Ideal transformer - p

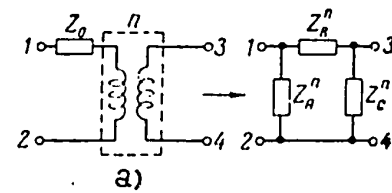


Fig.2

a) Ideal transformer - p

shaped quadripole (Fig.2) whose components are determined by the equations

$$Z_A^P = \frac{n}{n - 1} Z_0, \quad (4)$$

$$Z_B^P = n Z_0, \quad (5)$$

$$Z_C^P = \frac{n^2}{1 - n} Z_0. \quad (6)$$

2. Design of the Transformers

We will use the indicated equivalences for converting balanced filters (prototypes) with equal characteristic resistances into transforming band filters, having different characteristic resistances at the ends. Let us take as a prototype a T-shaped link whose characteristic resistances are

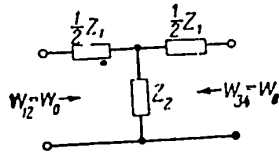


Fig. 3

$$Z_1 - Z_2 = Z_3 - Z_4 = Z_0 \text{ (Fig. 3).}$$

We will consider the links of types III₁, III₂, III₃, III₄ and IV_K,* presenting the greatest interest for high-frequency engineering (cf. Tables 1, 2, 3). We will split the circuit along

the line A - A and include the ideal transformer with a transformation factor equal to n (Figs. 4 and 5). Using the law of lumped resistances and having replaced, on the basis of the first equivalence, the system consisting of a parallel resis-

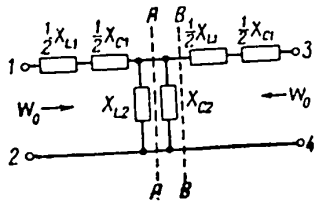


Fig. 4

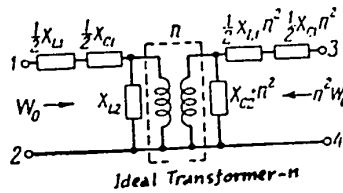


Fig. 5

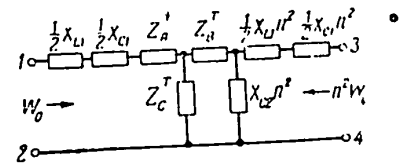


Fig. 6

tance X_{L2} and an ideal transformer by the T-shaped quadripole (Fig. 1), we will obtain an equivalent circuit (Fig. 6). The elements Z_A^T , Z_B^T , and Z_C^T of this hookup are determined by eqs. (1) - (3) with the substitution of Z_0 in $X_{L2} = \omega L_2$.

We will consider the particular case: $Z_2 = X_{L2}$, $X_{C2} = \infty$ (the prototype III₂, Table 1, No. 2). In this case, the circuit (Fig. 6) after summation of its elements, leads to a T-shaped unbalanced quadripole (Fig. 7), whose elements are

*Classification of filters according to T. Ye. Shi (Bibl. 2).

$$L_1 = \frac{L_1}{2} + (1 \cdot \dots \cdot n) L_2, \tag{7}$$

$$L_{11} = n \left[n \frac{L_1}{2} + (n-1) L_2 \right], \tag{8}$$

$$L_{1-11} = n L_2, \tag{9}$$

$$C_1 = 2 C_1, \tag{10}$$

$$C_{11} = \frac{2C_1}{n^2}. \tag{11}$$

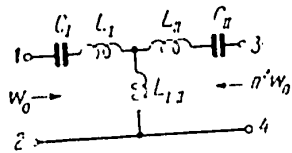


Fig. 7

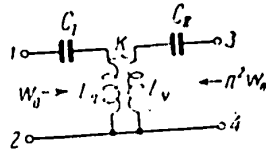


Fig. 8

The obtained conversion of the elements of prototype III₂ has a physical meaning at least when $L_I \geq 0$, $L_{II} \geq 0$, according to which the theoretically limiting transformation factor is determined by the inequality

$$\frac{1}{1 + \frac{L_1}{2L_2}} \leq n_{lim} \leq 1 + \frac{L_1}{2L_2}, \tag{12}$$

The limits in the ratio of the transformation factor can be principally defined by replacing the autotransformer circuit of the filter (Fig. 7) by a transformer circuit (Fig. 8); we then have

$$L_n = \frac{L_1}{2} + L_2, \tag{13}$$

$$L_v = n_2 \left(\frac{L_1}{2} + L_2 \right), \tag{14}$$

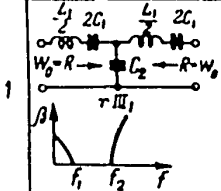
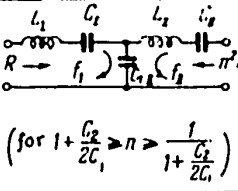
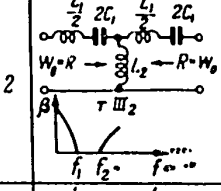
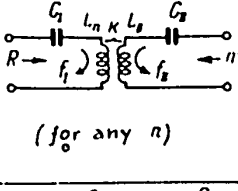
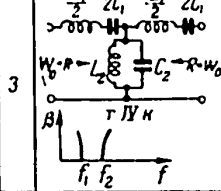
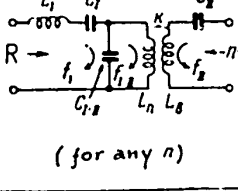
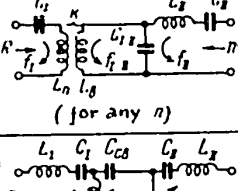
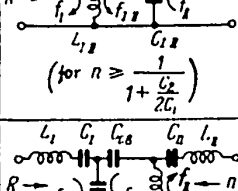
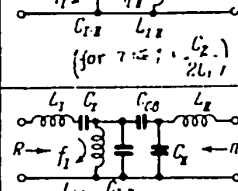
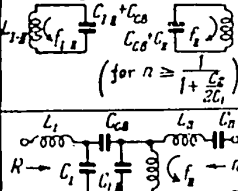
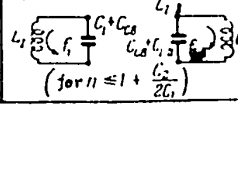
$$\kappa = \frac{1}{1 + L_1/2L_2}. \tag{15}$$

Equations (13) and (14) show that $L_n > 0$ and $L_v > 0$ for any value of n . By an analogous method, it is not difficult to convert into transformer filters the T-shaped and Pi-shaped links and the half-links of types III₁, III₃, III₄ and IV_K. It can be shown (Bibl.3) that:

a) For links with capacitance transformations



Table 1

#	a)	b)	c)	d)
1			$L_1 = \frac{L_2}{2}, C_1 = \frac{C_2}{1 + \frac{C_2}{2C_1}}, L_2 = \frac{R}{\pi(f_2 - f_1)}$ $L_2 = \frac{n^2 L_1}{2}, C_2 = \frac{C_1}{n^2 \sqrt{1 + \frac{C_2}{2C_1}}}, C_1 = \frac{1}{\pi R (f_1 + f_2)}$ $C_2 = \frac{C_1}{n}$	$f_1 = \sqrt{\frac{f_1^2 + f_2^2}{2}}$ $f_2 = \sqrt{\frac{f_1^2 + f_2^2}{2}}$
2			$L_1 = \frac{L_2}{2} + L_2; C_1 = 2C_2; L_2 = \frac{f_1 R}{\pi \sqrt{f_2^2 - f_1^2}}$ $L_2 = n^2 \left[\frac{L_1}{2} + L_2 \right]; C_2 = \frac{2C_1}{n^2}; L_2 = \frac{(f_1 + f_2) R}{4\pi f_0^2}; f_0 = \sqrt{f_1 f_2}$ $\kappa = \frac{1}{1 + \frac{L_1}{2L_2}}; C_1 = \frac{f_2 - f_1}{4\pi f_0^2 R}$	$f_1 = f_0 \sqrt{\frac{2f_0^2}{f_1^2 + f_2^2}}$ $f_2 = f_0 \sqrt{\frac{2f_0^2}{f_1^2 + f_2^2}}$
3			$L_1 = \frac{L_2}{2}, \kappa = \frac{1}{\sqrt{1 + \frac{L_1}{2L_2}}}, C_1 = C_2$ $L_1 = L_2, C_1 = 2C_2, C_2 = \frac{2C_1}{n^2}$ $L_2 = n^2 \left(\frac{L_1}{2} + L_2 \right)$	$f_1 = \sqrt{\frac{f_1^2 + f_2^2}{2}}$ $f_2 = f_0 \sqrt{\frac{2f_0^2}{f_1^2 + f_2^2}}$
4	$\tau IV \kappa$		$L_1 = \frac{L_2}{2} + L_2; C_1 = 2C_2$ $L_2 = n^2 L_1, C_2 = \frac{2C_1}{n^2}, \kappa = \frac{1}{\sqrt{1 + \frac{L_1}{2L_2}}}$ $L_1 = \frac{L_2}{2} n^2, C_1 = \frac{C_2}{n^2}$	$f_1 = f_0 \sqrt{\frac{2f_0^2}{f_1^2 + f_2^2}}$ $f_2 = f_0 \sqrt{\frac{2f_0^2}{f_1^2 + f_2^2}}$
5	$\tau IV \kappa$		$L_1 = \frac{L_2}{2}; C_1 = 2C_2$ $L_2 = \frac{1}{2} n^2, C_2 = \frac{C_1}{n}, C_2 = \frac{1}{n(1 + \frac{C_2}{2C_1})^{n-1}}$ $L_1 = L_2, C_1 = \frac{C_2}{n}$	$f_1 = f_0 \sqrt{\frac{2f_0^2}{f_1^2 + f_2^2}}$ $f_2 = f_0$ $f_2 = \sqrt{\frac{f_1^2 + f_2^2}{2}}$
6	$\tau IV \kappa$		$L_1 = \frac{L_2}{2}, C_1 = \frac{C_2}{1 + \frac{C_2}{2C_1}}, C_2 = \frac{C_1}{n(n-1)}$ $L_1 = \frac{L_2}{2} n^2, C_1 = \frac{C_2}{n}, C_2 = \frac{2C_1}{n^2}$ $L_1 = L_2 n^2$	$f_1 = \sqrt{\frac{f_1^2 + f_2^2}{2}}$ $f_2 = f_0$ $f_2 = f_0 \sqrt{\frac{2f_0^2}{f_1^2 + f_2^2}}$
7	$\tau IV \kappa$		$L_1 = \frac{L_2}{2}, C_1 = 2C_2$ $L_2 = \frac{L_1}{2} n^2, C_1 = C_2 + 2C_2 \frac{n-1}{n}$ $L_1 = L_2, C_2 = \frac{2C_1}{n}; C_1 = \frac{2C_2}{n^2} (1-n)$	$f_1 = f_0 \sqrt{\frac{2f_0^2}{f_1^2 + f_2^2}}$ $f_2 = f_0 \sqrt{\frac{2f_0^2}{f_1^2 + f_2^2}}$ $f_2 = f_0$
8	$\tau IV \kappa$		$L_1 = \frac{L_2}{2}, C_1 = 2C_2, \frac{n-1}{n}$ $L_1 = \frac{L_2}{2} n^2, C_2 = \frac{2C_1}{n}, C_1 = \frac{2C_2}{n^2}$ $L_1 = L_2 n^2, C_1 = \frac{C_2}{n^2} + \frac{2C_2(1-n)}{n^2}$	$f_1 = f_0$ $f_2 = f_0 \sqrt{\frac{2f_0^2}{f_1^2 + f_2^2}}$ $f_2 = f_0 \sqrt{\frac{2f_0^2}{f_1^2 + f_2^2}}$

a) Prototype (schematic and damping characteristic); b) Schematic of the transformer band, T-shaped link;

c) Computed values for the link elements; d) Natural frequencies of the link circuits;

e) For any n

Table 2

n	a)	b)	c)	d)
1			$C_1 = \frac{n-1}{n} C_2 + \frac{C_2}{2}; C_2 = \frac{F_1 + F_2}{4\pi F_0^2 R}$ $L_1 = 2L_2; C_2 = \frac{F_1}{\pi F_0(F_1 - F_2)R}$ $L_1 = 2L_2; C_2 = \frac{F_1}{\pi F_0(F_1 - F_2)R}$ $L_1 = 2L_2; C_2 = \frac{F_1}{\pi F_0(F_1 - F_2)R}$	$F_1 = F_0 \sqrt{\frac{2F_0^2}{F_1^2 + F_2^2}}$ $F_2 = F_0 \sqrt{\frac{2F_0^2}{F_1^2 + F_2^2}}$
2			$L_1 = 2L_2; C_1 = \frac{C_2}{2}; C_2 = \frac{F_1 + F_2}{4\pi F_0^2 R}$ $L_1 = 2L_2; C_1 = \frac{C_2}{2}; C_2 = \frac{F_1 + F_2}{4\pi F_0^2 R}$	$F_1 = F_0 \sqrt{\frac{2F_0^2}{F_1^2 + F_2^2}}$ $F_2 = F_0 \sqrt{\frac{2F_0^2}{F_1^2 + F_2^2}}$
3			$L_1 = 2L_2; C_1 = \frac{C_2}{2}; C_2 = \frac{F_1 + F_2}{4\pi F_0^2 R}$ $L_1 = 2L_2; C_1 = \frac{C_2}{2}; C_2 = \frac{F_1 + F_2}{4\pi F_0^2 R}$	$F_1 = F_0$ $F_2 = F_0$
4			$L_1 = 2L_2; C_1 = \frac{C_2}{2}; C_2 = \frac{F_1 + F_2}{4\pi F_0^2 R}$ $L_1 = 2L_2; C_1 = \frac{C_2}{2}; C_2 = \frac{F_1 + F_2}{4\pi F_0^2 R}$	$F_1 = F_0$ $F_2 = F_0$
5			$L_1 = 2L_2; C_1 = \frac{C_2}{2}; C_2 = \frac{F_1 + F_2}{4\pi F_0^2 R}$ $L_1 = 2L_2; C_1 = \frac{C_2}{2}; C_2 = \frac{F_1 + F_2}{4\pi F_0^2 R}$	$F_1 = F_0$ $F_2 = F_0$
6			$L_1 = 2L_2; C_1 = \frac{C_2}{2}; C_2 = \frac{F_1 + F_2}{4\pi F_0^2 R}$ $L_1 = 2L_2; C_1 = \frac{C_2}{2}; C_2 = \frac{F_1 + F_2}{4\pi F_0^2 R}$	$F_1 = F_0$ $F_2 = F_0$

a) Prototype (schematic and damping characteristic); b) Schematic of the transformer band T-shaped link; c) Computed values for the link elements; d) Natural frequencies of the link circuits; e) For any n

Table 3

a)	b)	c)	d)
	<p>(for $n \leq 1 + \frac{C_2}{4C_1}$)</p>	$L_1 = \frac{L_1}{2}; C_{1n} = \frac{2C_1}{n}; L_n = \frac{R}{\pi(f_2 - f_1)}$ $C_1 = 2C_1 \frac{n-1}{n}; C_n = \frac{f_2 - f_1}{4\pi f_1^2 R}$ $C_n = \frac{1}{n^2} \left[(1-n)2C_1 + \frac{C_2}{2} \right]; C_2 = \frac{1}{\pi(f_1 + f_2)R}$	$f_I = f_1$
	<p>(for any n)</p>	$L_n = \frac{L_1}{2} + 2L_2; K = \frac{1}{\sqrt{1 + \frac{L_1}{4L_2}}}$ $L_b = n^2 2L_2; C_1 = \frac{f_2 - f_1}{4\pi f_0^2 R}; L_1 = \frac{f_1 R}{\pi f_2 (f_2 - f_1)}$ $C_1 = 2C_1; L_2 = \frac{(f_1 + f_2)R}{4\pi f_0^2}; f_0 = \sqrt{f_1 f_2}$	$f_I = f_1$
	<p>(for $n \geq \frac{1}{1 + \frac{C_2}{4C_1}}$)</p>	$L_1 = 2L_2; C_n = \frac{1-n}{n^2} 2C_1$ $C_{1n} = \frac{2C_1}{n}; L_2 = \frac{(f_2 - f_1)R}{4\pi f_0^2}; C_1 = \frac{f_1 + f_2}{4\pi f_0^2 R}$ $C_1 = \frac{C_2}{2} + \frac{n-1}{n} 2C_1; C_2 = \frac{f_1}{\pi f_2 (f_2 - f_1) R}$ $f_0 = \sqrt{f_1 f_2}$	$f_I = f_1$
<p>T. IV K</p>	<p>(for any n)</p>	$L_n = 2L_2; K = \frac{1}{\sqrt{1 + \frac{L_1}{4L_2}}}; L_1 = \frac{R}{\pi(f_1 + f_2)}$ $L_b = (2L_2 + \frac{L_1}{2})n^2; C_1 = \frac{C_2}{2}$ $L_2 = \frac{(f_2 - f_1)R}{4\pi f_1^2}; C_2 = \frac{1}{\pi(f_2 - f_1)R}$	$f_I = f_1$
<p>T. IV K</p>	<p>(for any n)</p>	$L_n = \frac{L_1}{2} + 2L_2; K = \frac{1}{\sqrt{1 + \frac{L_1}{4L_2}}}; L_1 = \frac{R}{\pi(f_2 - f_1)}$ $L_b = n^2 2L_2; C_1 = 2C_1$ $C_n = \frac{C_2}{2n^2}; L_2 = \frac{f_2 - f_1}{4\pi f_0^2} R$	$f_I = \frac{f_0}{\sqrt{\frac{f_1^2 + f_2^2}{f_0^2} - 1}}$ $f_n = f_0$
<p>T. IV K</p>	<p>(for $n \leq 1 + \frac{C_2}{4C_1}$)</p>	$L_1 = \frac{L_1}{2}; C_{1n} = \frac{2C_1}{n}$ $L_n = 2L_2 n^2;$ $C_n = \frac{1}{n^2} \left[(1-n)2C_1 + \frac{C_2}{2} \right]; C_2 = \frac{1}{\pi(f_2 - f_1)R}$ $C_1 = \frac{n-1}{n} 2C_1;$	$f_I = f_0$ $f_n = \frac{f_0}{\sqrt{\frac{f_1^2 + f_2^2}{f_0^2} - 1}}$

a) Prototype (schematic and damping characteristic); b) Schematic of the transformer band T-shaped link; c) Computed values for the link elements; d) Natural frequencies of the link elements; e) For any n

$$\frac{1}{1 + \frac{C_2}{2C_1}} < n_{lim} < 1 + \frac{C_2}{2C_1}; \tag{16}$$

b) For half-links, the values of n_{lim} coincide with the corresponding eqs.(12) and (16) under the condition of changing $2L_2$ to $4L_2$ and $2C_1$ to $4C_1$.

The revisions of the computing formulas for more important types of links and half-links are cited in Tables 1, 2, and 3. For controlling the computed results,

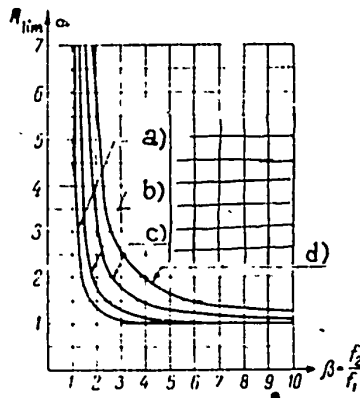


Fig.9

- a) Half-link of the prototypes; b) Links of the prototypes; c) Half-link of the prototype IV_K ; d) Link of the prototype

IV_K

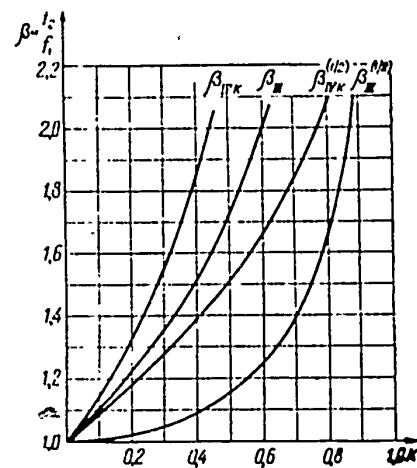


Fig.10

the values of the characteristic frequencies of the individual circuits of the filter are listed there.

After substituting into the expressions for n_{lim} , the values L_1 , L_2 , C_1 , and C_2 determine the limiting frequencies f_1 and f_2 and the load resistance $R = W_0$. From this it is clear that a dependence exists between n_{lim} and the pass band of the filter. These dependences, found by us for the considered types of links and half-links, are listed in Table 4 and in Fig.9.

Above it was mentioned that the transformer circuit of the filter, in principle,



can be completed with any transformation factor n . However, in reality the attainable value of n is determined by the possibility of obtaining a physical result from the computed values of the inductances, capacitances, and coupling factor K . The magnitude of K is determined by the ratio of the inductances L_1 and L_2 which, in turn, can be expressed by the cutoff frequency (cf Table 1 - 3).

Substituting the above expressions for L_1 and L_2 in the formula for K , we obtain the relationship establishing, for links and half-links, the following dependence (Fig.10) between the permissible pass bands (cutoff frequencies f_1 and f_2) and the given coupling factor K .

a) Transformer half-link and link of type III:

$$\beta_{III}^{(1)} = \frac{f_2}{f_1} = \frac{1}{\sqrt{1-K^2}}, \quad (17)$$

$$\beta_{III} = \frac{f_2}{f_1} = \sqrt{\frac{1+K}{1-K}}. \quad (18)$$

b) Transformer half-link and link of type IV_K

$$\beta_{IV_K} = \frac{2 - \kappa^2 + \kappa \sqrt{1 - 3\kappa^2}}{2\sqrt{1 - \kappa^2}}, \quad (19)$$

$$\beta_{IV_K} = \frac{1 + \kappa \sqrt{2 - \kappa^2}}{1 - \kappa^2}. \quad (20)$$

An analysis of the obtained dependences permits the following deductions:

1. The theoretical limiting coefficients of full transformation are determined by the limiting frequencies $\beta = \frac{f_2}{f_1}$, i.e., by the pass band of the filter.
2. The link of any type filter permits a significantly larger transformation of the resistances than a half-link.
3. The filter IV_K has the greatest efficiency for converting impedances. The gain in the transformation factor, guaranteed by a filter of this type in comparison with filters of other types, is characterized by the curves in Fig.9.
4. During an uninterrupted increase of the pass band, the transforming characteristics of all the filters are gradually flattened. Here it should be mentioned

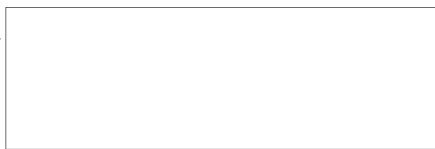
that the transformer developed by V.D.Kuznetsov for changing from a four-wire feeder to a coaxial cable (Bibl.1) can be considered as a particular solution of the above-

Table 4.

a)	b)	c)	d)
e)	a) $n > 1$ $n_{lim}^{(k)} < \frac{\beta^2 + 1}{(\beta - 1)^2}$	a) $n > 1$ $n_{lim} < \frac{\beta^2 + 1}{\beta^2 - 1}$	a) $n > 1$ $\frac{n_{lim}^{(k)}}{n_{lim}} = \frac{\beta + 1}{\beta - 1}$
	b) $n < 1$ $n_{lim}^{(k)} > \frac{(\beta - 1)^2}{\beta^2 + 1}$ $\beta = \frac{f_2}{f_1}$	b) $n < 1$ $n_{lim} > \frac{\beta^2 - 1}{\beta^2 + 1}$ $\beta = \frac{f_2}{f_1}$	b) $n < 1$ $\frac{n_{lim}^{(k)}}{n_{lim}} = \frac{\beta - 1}{\beta + 1}$ $\beta = \frac{f_2}{f_1}$
f)	a) $n > 1$ $n_{lim}^{(k)} < \frac{\beta^2 - \beta + 1}{(\beta - 1)^2}$	a) $n > 1$ $n_{lim} < \frac{\beta^2}{\beta^2 - 1}$	a) $n > 1$ $\frac{n_{lim}^{(k)}}{n_{lim}} = \frac{\beta^2 + 1}{\beta^2 (\beta - 1)}$
	b) $n < 1$ $n_{lim}^{(k)} > \frac{(\beta - 1)^2}{\beta^2 - \beta + 1}$ $\beta = \frac{f_2}{f_1}$	b) $n < 1$ $n_{lim} > \frac{\beta^2 - 1}{\beta^2}$ $\beta = \frac{f_2}{f_1}$	b) $n < 1$ $\frac{n_{lim}^{(k)}}{n_{lim}} = \frac{\beta^2 (\beta - 1)}{\beta^2 + 1}$ $\beta = \frac{f_2}{f_1}$

a) Form of the link; b) $n_{lim}^{(k)}$ is the limiting transformation factor in the filter of type IV_K; c) n_{lim} is the limiting transformation factor in the filters of types III₁, III₂, III₃, and III₄; d) $\frac{n_{lim}^{(k)}}{n_{lim}}$ is the relative efficiency of the filter of type IV_K; e) Complete link; f) Half-link

explained general problem of the designing transformer filters (in Table 2 this



transformer is listed as No.3).

3. Certain Features in the Designing of Transformer Filters in the 0.15 - 100 Mega-circle Band, and Experimental Data

As demonstrated above, transformers whose prototypes are links of type IV_K, possess maximum efficiency, so that types of transformers with a magnetic coupling (Tables 1 and 2, Nos.2 - 4) in principle permit any desired transformation of the resistances on any band.

In practice, however, as a result of the imperfect magnetic coupling between the coils, the actual pass band has a critical value. Therefore, an experimental determination of the coupling factor should precede the designing of transformers for a given case.

It is possible to list the following coupling factors reached in practice. In long-wave and medium-wave bands (0.15 - 1.6 mc), high coupling factors (90 - 98%) are obtained by using iron cores with an initial magnetic permeability of $\mu = 300$ to 500 gauss/oersted. In the short-wave band (6 - 20 mc), the use of carbon or iron cores with $\mu_0 \leq 400$ gauss/oe and of fine-wire windings guarantees obtaining coupling factors of the order of 75 - 80%. In the ultrashort-wave band (100 - 1000 mc), the limiting coupling factors have a magnitude of the order of 50%.

Knowing the actual magnitude of the coupling factor, the permissible pass band (Fig.10) can be determined from eq.(17) - (20). If the restriction as to pass band is less severe, filters with capacitance transformations should be used. In this case, using the curve in Fig.9, the magnitude of the transformation coefficient of one link n for the given pass band $\beta = \frac{f_2}{f_1}$ can be obtained. After this, it is not difficult to determine the number of links necessary for obtaining the desired coefficient of transformation. We may remark that a filter with capacitance transformation, despite a greater number of elements, is simpler in design. Therefore, in cases where economic considerations can be ignored, its use is more desirable.

Intense interest is exhibited in the use of transformer filters in the input

circuits or in the terminal stages of vacuum-tube amplifiers and receivers. In this case the critical value of the transformation of the resistances, as a rule, is determined by either the input or output capacitance. We will discuss certain practical considerations for choosing the cutoff frequencies and of the Q-factor of the filter coils.

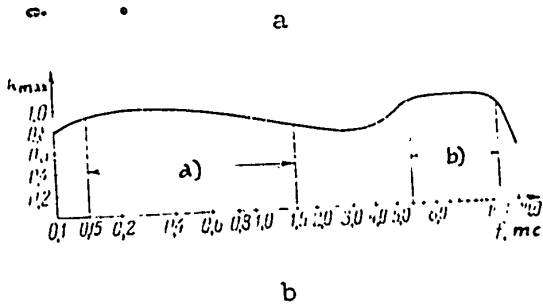
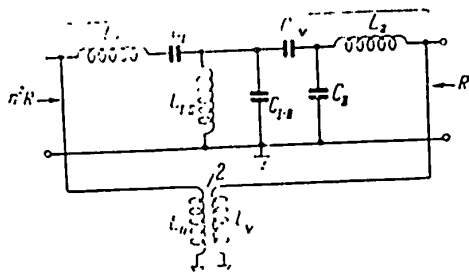


Fig.11

- a) Long-wave and medium-wave band;
- b) Short-wave band

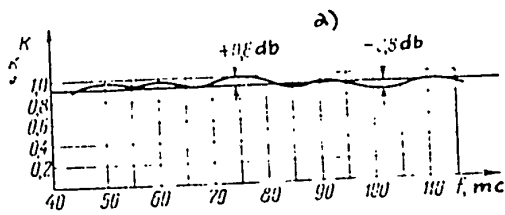


Fig.12

- a) Ultrashort-wave transformer,
75 - 25 ohms (n = 3)

The irregularity of the transformer frequency characteristic in the limiting pass bands is determined by the values chosen for the cutoff frequencies f_1 and f_2 and f_2 . Experience shows that irregularities in the frequency characteristics ± 1 db and ± 3 db are guaranteed at values of the cutoff frequencies f_1 and f_2 exceeding the pass band limiting frequencies by $\pm 20\%$ and $\pm 10\%$, respectively. At Q-factors of the coils of $Q \geq 50$ and at a pass band of $\frac{\Delta F}{f_0} \geq 0.15$ with damping, caused by active losses in the transformer sections, it can be disregarded.

To confirm the possibility of using the obtained relationships we will cite some experimental data. Figure 11a gives the schematic of an all-wave radio broad casting transformer. The diagram includes a ferrite transformer (2) with $\mu_0 = 4,00$ gauss/oe for operation on long and medium-wave bands (0.15 - 1.6 mc) and a band transformer filter (1) (denoted by No.7 in Table 1) for the short-wave band

(6 - 15 mc). In the long and medium-wave band, the ferrite transformer differs little from the ideal transformer (coupling factor $K = 98\%$, assigned capacitance of the coils 3 - 4 μf). Thanks to this, the replacement of a complicated transformer circuit by a simple ferrite transformer is permissible. As can be seen from the curves of Fig. 11b, the irregularity of the frequency characteristics in a given band does not exceed ± 0.6 db. The analogous frequency characteristics, obtained for ultrashort-wave transformers (75 - 25 ohms, $n = 3$) are cited in Fig. 12.

Not citing the characteristics, we point out that, with the help of analogous transforming filters in the input stage of each channel, amplifications were obtained equal to 14 db on an 8-megacycle band. In all cases, the practical frequency characteristics obtained were of the plane type.

1. Conclusion

On the basis of the cited theoretical and experimental material, the following deductions can be made. The considered method of designing band filters overcomes, to a significant degree, the shortcomings caused by the imperfections of high-frequency circuits (significant inductance diffusion in the inductively connected circuits, distributed capacitances of the coils, inductance of the wiring, and presence of other parasitic elements in the high-frequency circuits), and permits the construction of MF transformers on a given pass band of frequencies, which have parameters similar to those of ideal transformers.

Article received by the Editors 19 May 1954

BIBLIOGRAPHY

1. Kalikhman, S.G. - An All-Wave Antenna System for the Collective Reception of Radio Broadcast Programs of Ultrashort-Wave Broadcasting and Television. Paper read before the Session of BIOP and E imeni A.S. Popov, June (1954)
2. Shi, T. Ye. - Quadripoles and electric filters. Svyazizdat (1934)

3. Kalikhman, S.G. - The Transformation of Impedances in the Wide-Frequency Band.

Report IRPA. Issue II. Lenizdat (1954)

4. Aysenberg, G.Z. - Antennas for the National Radio Link Svyazizdat (1948)

CALCULATION OF AN IONIC VOLTAGE STABILIZER

by

G.S. Veksler

Active Member of the Society

The calculation of a stabilizer is presented in which the following factors are inter-related: integral stabilization factor of the hookup; firing voltage of the stabilivolt, its rated current; input voltage, and the efficiency of the stabilizer. The value of the possible maximum and minimum integral stabilization factors for each of the stabilivolts is established.

1. In designing an ionic stabilizer (Fig.1), the following denotations are used:

U_{2n} is the rated voltage at the load resistance; $+e$, $-f$ are the deviations of the voltage U_2 from U_{2n} in %; I_{2n} is the rated load current; $+c$, $-d$ are the deviations of the current I_2 from I_{2n} in %; $+a$, $-b$ are the deviations of the voltage U_1 at the input from the rated voltage U_{1n} in %; η is the efficiency of the stabilizing device (often not given); K_u is the integral stabilization factor for the input voltage, defined as

$$K_u = \frac{a + b}{c + f}$$

Besides this, the parameters of the stabilivolt are given: U_z is the firing voltage; I_c min perm., I_c max are the minimum and maximum permissible currents through the stabilivolt; R_i is the internal (dynamic) resistance, taken as constant in the stabilization band.

As a result of this calculation it is necessary to determine: the rated value of the input voltage U_{1n} and the value of the additional resistance r , which would

guarantee the firing of the stabilivolt at minimum input voltage $U_{1n} (1 - \frac{b}{100})$ and also at minimum load resistance $R(1 - \frac{e}{100})$, which would permit obtaining the wanted integral stabilization factor K_{η} with the given efficiency η , while preventing an output beyond the permissible current limits through the stabilivolt.

The published calculations of ionic stabilizers (Bibl.1, 2, 3, and 4) cannot be considered acceptable, since in these papers (Bibl.1, 2, and 4) the defined quanti-

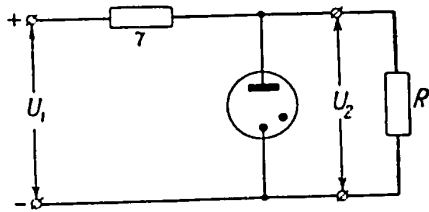


Fig.1

ties are not correlated with the voltage for firing the stabilivolt, while in other papers (Bibl.1 and 4) changes in the load are not considered, and in some papers (Bibl.3 and 4) the permissible oscillations of the output voltage are not taken into account.

Below, a method for calculating a voltage stabilizer, free of the indicated shortcomings is described, correlating stabilizer integral stabilization factor and its efficiency, and excluding the recalculations required by other methods of computing.

2. From the condition for obtaining the firing of the stabilivolt at minimum input voltage and load resistance, we have

$$r \leq \frac{U_{1n}}{I_{2n} (1 + \frac{c}{100})} \left[\frac{U_{1n} (1 - \frac{b}{100})}{U_s} - 1 \right]. \tag{1}$$

Let the deviation of the input voltage ΔU_1 from the rated value produce a deviation of the output voltage ΔU_2 from the rated value, and during this time the current through the stabilivolt changes its value by ΔI_c from the rated value.

Then,

$$\Delta U_1 = \left(\Delta I_c + \frac{\Delta U_2}{R} \right) r + \Delta U_2. \tag{2}$$

Since

$$\Delta U_2 = \Delta I_c R_i \quad (3)$$

then, substituting eq.(3) in eq.(2), we get

$$\Delta U_1 = \Delta I_c \left(1 + \frac{R_i}{r} + \frac{R_i}{R} \right) r.$$

Taking $R_i \ll R$ and $R_i \ll r$, we get

$$\Delta U_1 = \Delta I_c r. \quad (2a)$$

For the limiting deviation of the input voltage in the band of stabilization, eq.(2a) will yield

$$U_{1n} \frac{a+b}{100} = (I_{c_{max}} - I_{c_{min}}) r. \quad (2b)$$

From eq.(3), we get for the limiting deviation of the output voltage stabilization band

$$U_{2n} \frac{c+f}{100} = (I_{c_{max}} - I_{c_{min}}) R_i. \quad (3a)$$

We determine from eqs.(2b) and (3a) the integral stabilization factor for the input voltage, as follows:

$$K_u = \frac{a+b}{c+f} = \frac{1}{n} \cdot \frac{r}{R_i}, \quad (4)$$

where

$$n = \frac{U_{1n}}{U_{2n}}. \quad (5)$$

Considering eq.(1) to be an equality and substituting the value r from eq.(1) in eq.(4), we get from the condition guaranteeing the firing of the stabilivolt

$$n = \frac{U_{2n}}{U_3} \left(1 - \frac{b}{100} \right) - \frac{K_u R_i I_{2n}}{U_{2n}} \left(1 + \frac{c}{100} \right). \quad (6)$$

Equation (6) is a basic computation expression since, knowing n , it is possible to determine r from eq.(4) and U_{1n} from eq.(5).

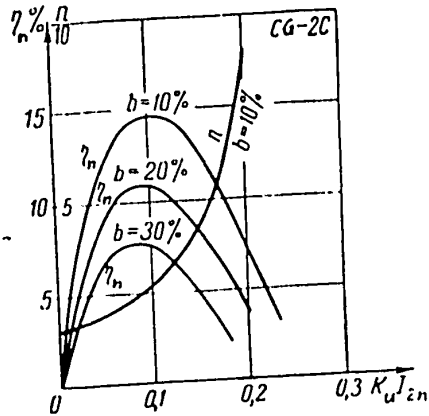


Fig. 2

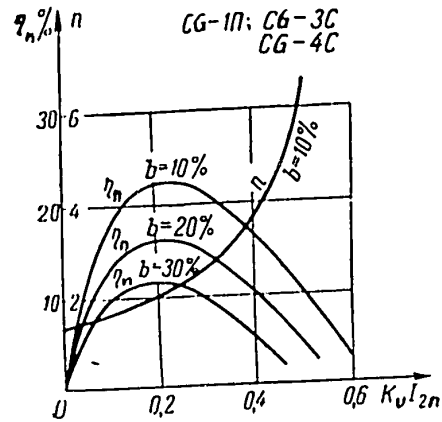


Fig. 3

3. We will next find the connection between K_u and η_n . The efficiency of the stabilivolt at rated operation is equal to

$$\eta_n = \frac{U_{2n} I_{2n}}{U_{1n} (I_{2n} + I_{cn})} = \frac{1}{n} \cdot \frac{I_{2n}}{I_{2n} + I_{cn}}, \tag{7}$$

where I_{cn} is the current across the stabilivolt at rated operation or, considering that

$$K_u = \frac{r}{n K_i} = \frac{U_{2n} (n-1)}{(I_{2n} + I_{cn}) n R_i}, \tag{8}$$

eqs.(7) and (8) will yield η_n in the form

$$\eta_n = \frac{K_u}{n-1} \cdot \frac{R_i}{U_{2n}} \cdot I_{2n}. \tag{9}$$

From eq.(9), using eq.(6), we get

$$\eta_n = \frac{K_u \frac{R_i}{U_{2n}} I_{2n} \left[\frac{U_{2n}}{U_s} \left(1 - \frac{b}{100} \right) - K_u \frac{R_i}{U_{2n}} I_{2n} \left(1 + \frac{c}{100} \right) \right]}{1 - \frac{U_{2n}}{U_s} \left(1 - \frac{b}{100} \right) + K_u \frac{R_i}{U_{2n}} I_{2n} \left(1 + \frac{c}{100} \right)}. \tag{10}$$



In eq.(10), η_n depends at least on the given magnitudes and on the stabilizer parameters.

If η_n is determined at the end of the calculation, then eq.(9) is a simple and suitable formula for this circuit. However, for evaluating the stabilizer, it is of interest to determine η_n at the beginning of the calculation when n has not yet been found. In this case, it follows that eq.(10) should be used.

For a direct evaluation of the magnitude of η_n , the relations set up $\eta_n(K_u I_{2n})$ are derived for $b = 10, 20, \text{ and } 30\%$; $c = 10\%$ for the stabilivolt CG-1P, CG-3C, and CG-4C (Fig.2)*, CG-2C (Fig.3), and CG-5B (Fig.4).

From eq.(6) it is clear that firing is at least possible when the following condition is satisfied:

$$K_u I_{2n} < (K_u I_{2n})_{\max} \Rightarrow \frac{\frac{U_{2n}}{U_3} \left(1 - \frac{b}{100}\right)}{\frac{R}{U_{2n}} \left(1 + \frac{c}{100}\right)}, \quad (11)$$

due to the fact that while plotting $\eta_n(K_u I_{2n})$, the value η_n was not determined for all values of $K_u I_{2n}$, not satisfying the inequality (11), since these regimes have no meaning.

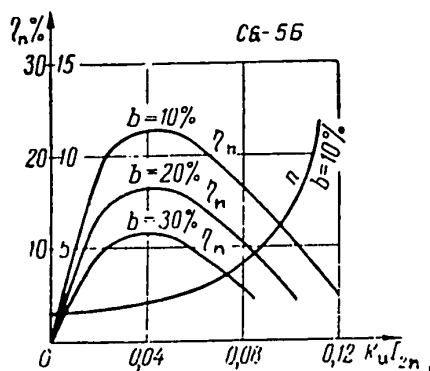


Fig.4

The values of $(K_u I_{2n})_{\max}$ result in certain types of stabilivolt at $c = 10\%$, as given in Table 1. The parameters of the stabilivolt are listed in Table 2.

From the curves of $n(K_u I_{2n})$ plotted in Figs.2, 3, and 4 for $b = 10\%$ and $c = 10\%$, it follows that η_n cannot be greater

*Since, in the working band of currents (5 - 30 ma) of the stabilivolt, the magnitude $\frac{i_1}{U_{2n}}$ for CG-1P, CG-3C, and CG-4C is roughly the same, general curves can be constructed for these.

than 22% for the stabilivolt CG-1P, CG-3C, CG-4C, and CG-5B, and not greater than 15% for the stabilivolt CG-2C. The magnitudes of η_n and $K_u I_{2n}$ are strictly correlated and the maximum efficiency of the circuit corresponds to $n = 2 - 3$; a further growth in the magnitude of $K_u I_{2n}$ leads to such a sharp increase in n and a drop in η_n that this leads to the necessity of a high input voltage, which is not economical.

Table 1

a)	$b = 5\%$	$b = 10\%$	$b = 15\%$	$b = 20\%$	$b = 30\%$
CG-1P, CG-3C, CG-4C	0,66	0,62	0,59	0,55	0,48
CG-2C	0,25	0,24	0,23	0,22	0,19
CG-5B	0,134	0,125	0,12	0,113	0,1

a) Type of stabilivolt

Table 2

a)	U_{2n}, V	U_3, max, V	$I_{c, \text{min}}, \text{perm}, \text{mA}$	$I_{c, \text{max}}, \text{perm}, \text{mA}$	$R_{i, \text{max}}, \text{ohm}$	$\frac{U_{2n}}{R_{i, \text{max}}}$	$K_u, \text{max}, \text{lim}$	$K_u, \text{min}, \text{lim}$
CG-1P	150	180	5	30	160	0,93	31	5,2
CG-2C	75	105	5	30	180	0,42	24	4
CG-3C	105	127	5	40	170	0,44	25	3,1
CG-4C	150	180	5	30	120	0,88	30	5
CG-5B	150	180	5	10	800	1,05	36	4,5
						0,93	31	5,2
						0,19	6,2	3,1

Note: The parameters of the stabilivolt have a large spread, so that, before starting the calculation, it is preferable to check the magnitudes of U_{2n} , U_3 , and R_i .

a) Type of stabilivolt

4. We will determine the rated, minimum, and maximum currents across the stabilivolt.

The input voltage U_{1n} and the ballast resistance were determined from the conditions guaranteeing the proposed integral stabilization factor and firing of the

stabilivolt under more difficult circumstances. There still remains the requirement that the rated current I_{cn} across the stabilivolt guarantee its rated regime with the earlier found I_{1n} and r . For this, it is necessary that

$$(I_{cn} + I_{2n})r = U_{1n} - U_{2n}. \quad (12)$$

Taking into account eqs.(4) and (5), we get from eq.(12)

$$I_{cn} = \frac{(n-1)U_{2n}}{nK_u R_l} - I_{2n}. \quad (13)$$

From eq.(13) it is clear that the rated current I_{cn} across the stabilivolt depends on K_u and I_{2n} and it is necessary to calculate it for each concrete case.*

Taking into account eq.(2a), we get

$$I_{c_{min}} = I_{cn} - \frac{U_{1n}b}{r \cdot 100} - I_{2n} \frac{c}{100}, \quad (14a)$$

$$I_{c_{max}} = I_{cn} + \frac{U_{1n}a}{r \cdot 100} + I_{2n} \frac{d}{100}. \quad (14b)$$

From eqs.(13) and (14a), taking into account eqs.(4) and (5), we get

$$I_{c_{min}} = \frac{U_{2n}}{K_u R_l} \left(1 - \frac{b}{100} - \frac{1}{n}\right) - I_{2n} \left(1 + \frac{c}{100}\right). \quad (15a)$$

From eqs.(13) and (14b), taking into account eqs.(4) and (5), we get

$$I_{c_{max}} = \frac{U_{2n}}{K_u R_l} \left(1 + \frac{a}{100} - \frac{1}{n}\right) - I_{2n} \left(1 - \frac{d}{100}\right). \quad (15b)$$

Naturally, we must satisfy the conditions

$$I_{c_{min}} > I_{c_{min perm}} \quad (16a)$$

Consequently, it is impossible to take I_{cn} as equal to half the sum of the maximum and minimum permissible currents across the stabilivolt (Bib.2) or to set the current I_{cn} equal to any other arbitrary magnitude, without having determined its values (Bib.1).

$$I_{c_{max}} \leq I_{c_{max\ perm}} \tag{16b}$$

Taking into account eqs.(16a) and (6), we get from eq.(15a)

$$K_u \leq K_{u_{max_2}} = \frac{U_{2n} \left[1 - \frac{b}{100} - \frac{U_{2n}}{U_3} \left(1 - \frac{b}{100} \right) \right]}{R_i I_{c_{min\ p}}} \tag{17a}$$

Taking into account eqs.(16b) and (6), we get from eq.(15b)

$$K_u > K_{u_{min}} = \frac{U_{2n} \left[1 + \frac{a}{100} - \frac{U_{2n}}{U_3} \left(1 - \frac{b}{100} \right) \right]}{R_i \left[I_{c_{max\ perm}} - I_{2n} \left(\frac{c+d}{100} \right) \right]} \tag{17b}$$

From eqs.(17a) and (17b) we determine the limiting (though in practice unattainable) integral stabilization factors of the stabilivolt in hookup:

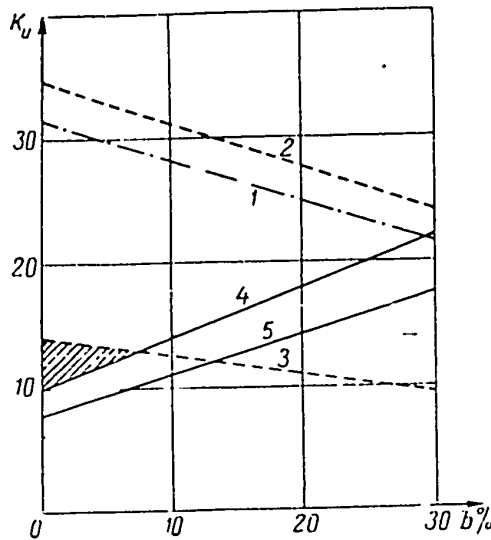


Fig.5

$$K_{u_{max_2\ lim}} = \frac{U_{2n} \left(1 - \frac{U_{2n}}{U_3} \right)}{R_i \cdot I_{c_{min\ perm}}} \tag{18}$$

$b \rightarrow 0$

$$K_{u_{min\ lim}} = \frac{U_{2n} \left(1 - \frac{U_{2n}}{U_3} \right)}{R_i \cdot I_{c_{max\ perm}}} \tag{19}$$

$a \rightarrow 0,$

$b \rightarrow 0,$

$I_{n2} \rightarrow 0.$

Table 2 contains the values of the limiting integral stabilization factors for certain types of stabilivolts. The possible values of \$K_u\$ depend on \$I_{2n}\$, and

a, b, c and d should lie between $K_{u_{max_2\ lim}}$ and $K_{u_{min\ lim}}$.

For orientation in the selection of a permissible value for \$K_u\$, the plotted values in Fig.5 \$K_{u_{max}}\$ (b), line 1, and \$K_{u_{min}}\$ (\$bI_{2n}\$), at $a = 5\%$, $c = d = 10\%$, lines 4



and 5, are common for CG-1P, CG-3C, and CG-4C in the working band of the currents 5 - 30 ma. Line (1) denotes $K_{u_{max2}}$ for any currents; line (2) is the $K_{u_{max1}}$ for $I_{2n} = 20$ ma (from the condition guaranteeing firing); line (3) is the $K_{u_{max1}}$ for $I_{2n} = 50$ ma; line (4) is the $K_{u_{min}}$ for $I_{2n} = 50$ ma; and line (5) is the $K_{u_{min}}$ for $I_{2n} = 20$ ma. The region of possible K_u at $I_{2n} = 50$ ma, is deleted.

If for finding $K_{u_{max2}}$ according to eq.(17a) it is possible to use Fig.5 for any values of I_{2n} ; a, c, and d, then the values of $K_{u_{min}}$, determined from Fig.5, are correct at least for the quantities I_{2n} , a, c, and d, indicated on the graph. In other cases, $K_{u_{min}}$ is determined from eq.(17b).

5. The proposed K_u should be smaller than $K_{u_{max2}}$ obtained from eq.(17a); in addition, the proposed $K_u I_{2n}$ should be smaller than $(K_u I_{2n})_{max}$, determined from eq.(11). Naturally, the K_u with the proposed I_{2n} should at the same time satisfy both inequalities (11) and (17a). For the same values of I_{2n} , $K_{u_{max1}}$ from eq.(11) will be the limit; for others, it will be $K_{u_{max2}}$ from eq.(17a).

In Fig.5, $K_u(b)$ is plotted for $I_{2n} = 20$ ma (line 2) and for $I_{2n} = 50$ ma (line 3). Thus it follows from Fig.5, for $I_{2n} = 20$ ma, that K_u will be defined by $K_{u_{max2}}$ from eq.(17a), i.e., line 1, while for $I_{2n} = 50$ ma, the value of K_u will be defined by $K_{u_{max1}}$ from eq.(11), i.e., line 3. The permissible magnitudes of K_u should lie in the region bordered by $K_{u_{min}}$ and by the smallest values of $K_{u_{max}}$.

Based on the above statements, the calculation of a stabilizer should begin by checking whether it conforms to the inequality (11). Then, the value $K_{u_{max1}}$ for the given I_{2n} , is obtained from eq.(11). Using eq.(17a), find $K_{u_{max2}}$. For an estimate, take the smaller of these two $K_{u_{max}}$.

If $K_u > K_{u_{max}}$ of the fact that firing is not guaranteed (11) or because of the fact that $I_{c_{min}} < I_{c_{min} \text{ lim}}$ (17a), then it is impossible to design the wanted stabilizer.

If $K_u < K_{u_{min}}$ ($I_{c_{max}} > I_{c_{max} \text{ lim}}$), then it is possible to construct the stabilizer, if the proposed magnitude of K_u is obtained, considering for this that $K_u =$

$= K_{u_{min}}^*$. At constant values for a and b, this leads to a decrease in the values of e, f and $I_{c_{max}}$.

With this specification, K_u can be approached to a definite magnitude n, and the calculation can be completed.

The suggested method frees the designer from recalculations, which are frequently necessary at the end of the calculation, due to incompleteness of one of the inequalities, (16a) or (16b)**.

6. Approximate calculation of a stabilizer.

Given $U_{2n} = 150$ B, $I_{2n} = 20$ ma, $a = 5\%$, $b = 15\%$, $c = d = 10\%$, $e = f = 1\%$, from this:

$$K_u = \frac{a+b}{e+f} = 10 \text{ and } K_u I_{2n} = 0,2.$$

*This is correlated with the increase in n, U_{1n} , and the decrease in γ_n (cf. Figs. 2, 3, 4), with which it must be reconciled, or else it is impossible to complete the projected assignment.

**If $K_{u_{max}}$ is determined from eq. (17a), and not from eq. (11), then $I_{2n_{max}}$ can be found from eqs. (17a) and (17b), by which stabilization is still possible. In this regime, $I_{c_{min}} = I_{c_{min} \text{ lim}}$ and $I_{c_{max}} = I_{c_{max} \text{ lim}}$ and the full band currents of the stabilizer are used.

Having equated the right-hand sides of eqs. (17a) and (17b), we get

$$I_{2n_{max}} = \frac{1}{\left(1 - \frac{b}{100}\right) \cdot \left(\frac{c+d}{100}\right)} \left[I_{c_{max} \text{ perm}} \left(1 - \frac{b}{100}\right) - I_{c_{min} \text{ perm}} \left(1 + \frac{\frac{a}{100} + \frac{U_{2n}}{U_3} \cdot \frac{b}{100}}{\frac{U_{2n}}{U_3}}\right) \right] \quad (20)$$

In Fig. 5, this extremely rare state is determined by the intersection of the line $K_{u_{min}}$ for $I_{2n_{max}}$ and line 1.

It is necessary to determine: U_{1n} , r , $I_{c_{min}}$, $I_{c_{max}}$, I_{cn} , η_n .

Calculation Sequence

1. Select the stabilivolt CG-4C (cf. Table 2).
2. From eq. (11) we have $(K_u I_{2n})_{max} = 0.59$; $0.59 > 0.2$ and the inequality (11) is satisfied.
3. When $I_{2n} = 20$ ma from $K_u I_{2n_{max}} = 0.59$, we get $K_{u_{max}1} = 29.5$.
4. From eq. (17a), we have $K_{u_{max}2} = 26.5$.
5. We then take $K_{u_{max}} = 26.5$; $26.5 > 10$ so that the inequality (17a) is satisfied.
6. From eq. (17b), we have $K_{u_{min}} = 12.3$; $10 < 12.3$ so that inequality (11b) is not satisfied; consequently, it is necessary to raise I_{2n} to $K_{u_{min}}$.
7. We then take $K_u = 12.3$, and by this obtain $K_u I_{2n} = 0.246 < 0.59$.
8. From eq. (6), we have $n = 2.38$.
9. From eq. (13), $I_{cn} = 24$ ma.
10. From eq. (15a), $I_{c_{min}} = 11$ ma; 11 ma $>$ 5 ma.
11. From eq. (15b), $I_{c_{max}} = 30$ ma; 30 ma $= 30$ ma.
12. From eq. (5), $U_{1n} = 357$ volts.
13. From eq. (4), $r = 1,680$ ohms.
14. From eq. (9), $\eta_n = 0.19$.

CONRECTION:

From eq. (3) for $I_{c_{min}} = 11$ ma and $I_{c_{max}} = 30$ ma, we have $\Delta U_2 = 3.04$ volts.
Then, $e + f = 2.025$; 2.0 had been given.

Article received by the Editors 7 January 1955.

BIBLIOGRAPHY

1. Mazel', K.B. - Calculation of a Voltage Stabilizer with Glow Discharge Tubes.
Vestnik Svyazi, issue of Tekhnika Svyazi No. 11 (1949)

2. Efrussi, M. - Gas Voltage Stabilizers. "Radio" No. 6 (1951)
3. Gol'dreer, I.G. - Voltage Stabilizers. DEI (1952)
4. Bonch-Bruyevich, A.M. - The Use of Electron Tubes in Experimental Physics.

GITTL (1954)

A METHOD FOR INCREASING THE ACCURACY OF FREQUENCY ANALYZERS WITH AN ELECTRON-BEAM INDICATOR

by

H.F.Vollermer

Active Member of the Society

In the article a schematic is examined for raising the accuracy of a frequency analyzer with an electron-beam indicator, possessing a higher degree of accuracy as a result of excluding the error of the frequency scale.

In modern radio engineering, a wide range of different frequency analyzers exists in addition to various types of spectrometers, panoramic receivers, and cathode-ray curve tracers, permitting observation on a screen of the spectrum, characteristics, etc. being studied.

The basic elements of such devices are a frequency-modulating (FM) generator - voltage source with constant amplitude and a frequency varying within a given interval - and an electron-beam tube functioning as an indicator. On the tube screen the studied characteristics, frequency spectrums, etc. are observed. Block diagrams of such devices are very well-known (Fig.1).

The accuracy of frequency metering in devices carried out according to such a block diagram, is primarily determined by the stability of the modulating characteristic of the FM generator $\omega = \psi(u)$.

We will consider this question in more detail. The deviation of the beam along the x-axis, proportional to the instantaneous value of the voltage (current) at the amplifier outlet of the channel x, is used for determining the instantaneous frequency. From the deviation of the beam along the y-axis, the level of the frequency components of the examined voltage can be determined; or else the transmission fac-

tor at the given frequency of the examined quadripole.

The input voltage of the amplifier channel x, determining the deviation of the

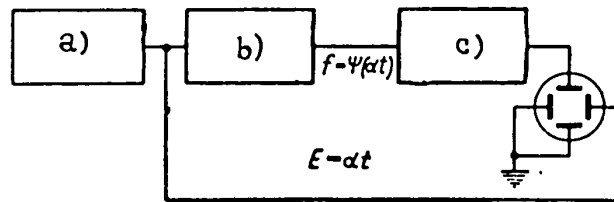


Fig.1

a) Sawtooth-voltage generator; b) FM generator; c) Investigated object

beam along the x-axis (and consequently also the frequency metering) and appearing at the same time as the modulating voltage of the FM generator, is connected at least indirectly through the modulation characteristic $\psi(u)$ with the instantaneous frequency. If, for some reason, the modulation characteristic of the FM generator changes, significant errors arise during frequency metering in accordance with the pre-charted scale. This is the main shortcoming of frequency analyzers constructed

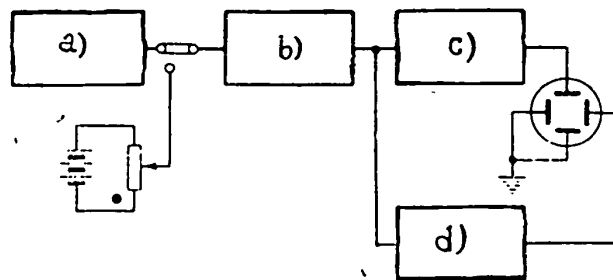


Fig.2

a) Sawtooth-voltage generator; b) FM generator; c) Examined object;

d) Frequency discriminator

according to a block diagram such as that shown in Fig.1, especially when the tubes in the frequency modulation circuit vary, since the modulation characteristic of

the FM generator in this case depends mainly on the form of the tube characteristic, which changes significantly during operation and varies with changes in the state of the power supply.

The block diagram in Fig. 2, which uses connection in series, is free of the indicated shortcomings (Bibl. 3). In this hookup, the error of the frequency scale, caused by a change in the shape of the modulating characteristic $\omega = \psi(u)$, is practically excluded. The voltage for the deviation along the x-axis, i.e., the frequency scale, is taken from the output of the frequency discriminator, so that the coupling between the instantaneous voltage frequency, created by the FM generator, and the instantaneous voltage (current) in the channel x is of the direct type; this coupling is determined by the frequency discriminator characteristic $u_d = \psi_1(\omega)$.

~~Inasmuch as the slope of the characteristic of the frequency discriminator during~~
reasonable performance does not depend on the form of the electron tube characteristics, the stability of the discriminator can be significantly higher than the stability of the modulation characteristic of the FM generator.

The suggested schematic is also interesting in that, with the proper choice of the discriminator characteristic, a stable frequency scale of the analyzer with the necessary degree of accuracy for example, can be obtained, such as an evenly divided (linear) scale, close to the logarithmic scale, etc.

When designing frequency analyzers in accordance with the block diagram of Fig. 2, it is not necessary to make strict requirements as to the form of the modulating characteristic of the FM generator; it is correct within the limits in which, due to the change in form (slope) of the modulating characteristic, the rate of change of the frequency, influencing the resolution and other parameters of the analyzer, is not observed to vary (Bibl. 1 and 2). The value of this block diagram lies also in the possibility of changing the frequency scale of the device, without additional errors, by proper selection of the separate sections of the scale for a detailed analysis, by a change in the mean frequency of the FM generator, or by a

decrease in the frequency deviation and an increase of the amplification in the channel of the frequency axis (correspondingly shortening, if necessary, the analyzing time). At correctly selected parameters of the spectrometer, this block diagram permits, without additional errors, changing from automatic scanning to manual scanning by replacing the sawtooth voltage leading to the FM generator with a constant voltage, whose magnitude varies during adjustment of the analyzer to manual scanning (for example, by the potentiometer).

In designing frequency analyzers according to the block diagram in Fig.2, broad-band frequency discriminators (with a large $\frac{\Delta f}{f}$, where Δf is the pass band and f is the mean frequency) must be used.

Broad-band discriminators can be completed in the same manner as a network with ~~detuned and thus strongly coupled circuits (phase discriminator); (Bibl.4).~~ For obtaining a broad-band frequency discriminator its circuit must have a low resistance and thus also a low equivalent resistance. As a result of this, the transmission factor of the discriminator drops sharply, and to obtain significant voltages at its output relatively powerful tubes, with a large current, must be used. One can roughly double the output voltage of the discriminator with strongly coupled circuits, at given Q-factors of the circuits and the current of the tubes, by connecting the first circuit of the discriminator in the cathode of the tube. This arrangement (a circuit with a grounded plate) eliminates the necessity of a special shunting resistance, lowering the Q-factor of the first circuit to the required magnitude.

Article received by the Editors 7 July 1955

BIBLIOGRAPHY

1. Beranek, L.A. - Acoustic Measurements. IL (1952)
2. Kharkevich, A.A. - Spectra and Analysis. GTTI (1952)
3. - Description of Heterodyne Spectrometers in the Bands 0.3 - 10 kc, 4 - 100 kc, and 30 - 500 kc Kiev Political Institute. Faculty for Radio Receiver

Design (1950 - 1952)

A. Goncrowskiy, I.S. - Frequency Modulation and its Application. Svyazizdat (1946)

!

THE EFFECT OF CAPACITANCE OF A SPACE CHARGE AND NONLINEARITY OF A TUBE
CHARACTERISTIC ON THE FREQUENCY OF A SELF-OSCILLATOR

by

G.T.Shitikov

Active Member of the Society

The causes of the effect of power-supply voltages on the frequency of a self-oscillator in wide frequency spacing are examined. It is demonstrated that the capacitance, produced by the space charge of a tube, is the main destabilizing factor in the meter and short-wave band.

Ways are shown of decreasing the destabilizing effect of the power-supply voltages for optimum coupling of the tube with the circuit. Mathematical formulas are given and experimental material is cited, which agree closely with the computed data.

1. Basic Principles

The dependence of the frequency of the self-oscillator on its operating state is one of the most important destabilizing factors which determine the magnitude of its instability as a whole. The problem of the causes of this dependence of the oscillator frequency on its operating state has been repeatedly examined in the technical literature (Bibl.1, 2, 3, 4). However, such studies consisted in comparisons of schematics with complete coupling of the tube to the circuit mainly concerned the destabilizing effect of higher harmonics, caused by the nonlinearity of the tube characteristic.

As for the destabilizing influence of the capacitance produced by the space

charge of the tube (dynamic capacitance), this problem is not quantitatively investigated in the technical literature; there is merely an indication of the presence of such an influence.

Our task is a quantitative evaluation of all destabilizing factors connected with the operation of the self-oscillator at optimum tube coupling with the circuit ("optimum link" is what we call the minimum coupling for obtaining stable self-oscillations). The problem of decreasing the coupling of a tube with a circuit is of great significance, inasmuch as the partial (optimum) coupling of a tube with a circuit basically permits a decrease in the destabilizing effect of the oscillator tube as a whole, as established previously (Bibl. 5, 6)*.

The upper frequency limit, which will be investigated here, are frequencies of the order of tens of megacycles. One can consider that up to these frequencies the effect produced by the electron transit time of the tube, is negligible. The dependence of the frequency of the oscillator on its operating state when the transit time of the electrons between the electrodes of the tube is commensurable with the period of oscillation, demands special investigation.

Since we are primarily concerned with finding ways of increasing the frequency stability of the self-oscillator rather than with determining the amount of frequency instability of unstable self-oscillators, the general prerequisite for the initial operating conditions of the oscillator is its operation in the left-hand segment

*In the paper (Bibl. 6), published in the magazine "IEEST" No. 12 for 1940, I made the deduction "...the stability of an oscillator during changes in the tube parameters and its operating conditions does not depend on the L/C ratio of the oscillatory circuit". Clapp, in his historic survey "Frequency-Stable L,C Oscillators", published in PIPE (August 1954) writes: "Vackar (1949), Gouriet (1950), and Edson (1953) established that, while working in a linear state, the stability does not depend on the ratio of L to C". In this way, we have an almost complete coincidence in deductions; however, my deductions were made 9 to 14 years earlier.

of the tube characteristic. This practically prevents one of the most important destabilizing factors - the influence of grid currents.

The practical realization of such an operating state of the oscillator encounters no serious difficulties.

2. Effect of Dynamic Capacitance on the Oscillation Frequency of an Oscillator

For studying the effect of dynamic capacitance on the frequency of an oscillator, it is primarily necessary to know the magnitude of this capacitance and its correlation with other characteristics of the tube. Research shows that this capacitance, for each type of tube and for each given tube, is determined just like any other parameter of the tube. As far as the nature of its dependence on the operating state of the tube, is concerned, it most closely resembles the transconductance of the characteristic; this is due to the transconductance of the characteristic which, in turn, is closely related to the presence of a space charge.

In Figs.1, 2 and 3 are plotted the interdependence of the transconductance of

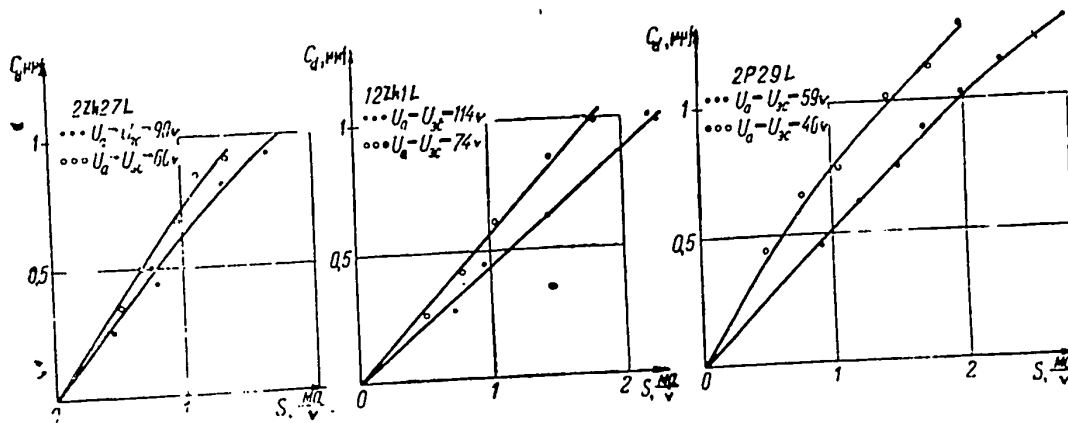


Fig.1

Fig.2

Fig.3

the characteristic and the dynamic capacitance with various voltages on the first grid for certain modern pentodes, including the equivalent triode. As is seen from the graphs, these dependences are close to linear; however, their slope is essen-

tially different for various plate voltages, by which the transconductance of the slope increases on lowering the plate voltage. This means that, on lowering the voltage, the transconductance of the characteristic decreases faster than the magnitude of the dynamic capacitance.

With a change in the filament voltage (Fig. 4) within the limits permissible for normal operation of the tube, the slope of the characteristics of the interdependence of the dynamic capacitance and the transconductance changes less, and then to the opposite side, i.e., with a lowering of the filament voltage, the magnitude of the dynamic capacitance declines more rapidly.

Under actual operating conditions of the tube generator (working with plate-current cutoff) the alternating voltage on the grid significantly overlaps the linear part of the tube characteristic, so that this voltage reacts on the nonlinear capacitive reactance of the tube. If the grid voltage is considered sinusoidal (it will be shown below that in practical situations it is always close to sinusoidal), then the current, flowing across the nonlinear capacitive reactance, can be expanded into a Fourier series and, after separating the first harmonic of this current, the mean magnitude of the dynamic capacitance can be determined for the period. This capacitance (designated below as active dynamic capacitance) will be connected by a given transmission factor to the fundamental capacitance of the oscillator circuit, since every other interelectrode capacitance of the tube is connected to it. The only difference is that, in practice, the statistical interelectrode capacitances do not depend on the magnitude of the power-supply voltages, while the active value of the dynamic capacitance does.

Here the main point of the mechanism of the power supply voltage influence on the frequency of the oscillator is due to the dynamic capacitance of the tube.

We will next discuss this problem quantitatively. We will assume at first that the dynamic capacitance increases during a change in the grid voltage in jumps rather than continuously, immediately attaining its maximum value. The justification for

such an assumption is that the entire existing system of calculating tube generators according to the broken-line characteristics is based on this, considering that the transconductance of the characteristic is either equal to zero or has a completely determined constant value. Then, based on the dependence between the current and the voltage under a capacitive load, we get

$$i = -\omega C_d U_{c\kappa} \sin \omega t, \quad (1)$$

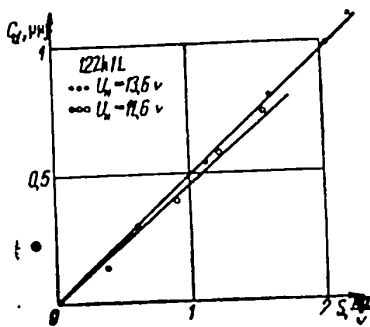


Fig. 4

where C_d is the dynamic capacitance of the tube (in the beginning it is assumed that it has a constant value when the grid voltage is equal to or greater than the cutoff voltage and that it is equal to zero when the grid voltage is equal to or less than the cutoff voltage; $U_{c\kappa}$ denotes the

amplitude value of the grid voltage.

If we designate by θ that half of the period during which the capacitive current is flowing, then the maximum value of this current, based on eq.(1), is equal to

$$i_m = -\omega C_d U_{c\kappa} \sin \theta \quad (2)$$

(at values of $\theta \geq 90^\circ$ the magnitude of the current i_m will be highest when $\omega t = 90^\circ$; however this does not change the final results).

From eqs.(1) and (2) we find

$$i = \frac{i_m \sin \omega t}{\sin \theta} \quad (3)$$

After an expansion into series, we find the amplitude of the first harmonic

$$i_1 = \frac{i_m}{\pi \sin \theta} \int_{-\theta}^{+\theta} \sin^2 \omega t dt = \frac{i_m}{\pi \sin \theta} (\theta - \sin \theta \cos \theta) \quad (4)$$

or, after corresponding substitutions, we conclusively get the magnitude of the capacitive susceptance for the first harmonic of the current:

$$g_c = \frac{i_1}{U_{c\kappa}} = -\omega C_d \frac{\theta - \sin \theta \cos \theta}{\kappa} \tag{5}$$

The magnitude $\frac{\pi}{\theta - \sin \theta \cos \theta} = \alpha_i$, where α_i is the reduction factor which, as is well known from the theory of transmitters, is equal to the ratio of the maximum transconductance of the characteristic for the period to the mean transconductance.

Completing the substitution, we get

~~$$g_c = -\omega C_d \alpha_i$$~~

In this way, the magnitude of the active dynamic capacitance can be presented

as

$$C_{d\alpha} = \frac{C_d}{\alpha_i} \tag{6}$$

Equation (6) shows that, at a linear dependence between the transconductance of the characteristic and the dynamic capacitance, the active value of the dynamic capacitance has the same dependence on its maximum value as the mean transconductance. Although these deductions are made on the basis of an examination of idealized characteristics of the transconductance and the dynamic capacitance, nonetheless they are

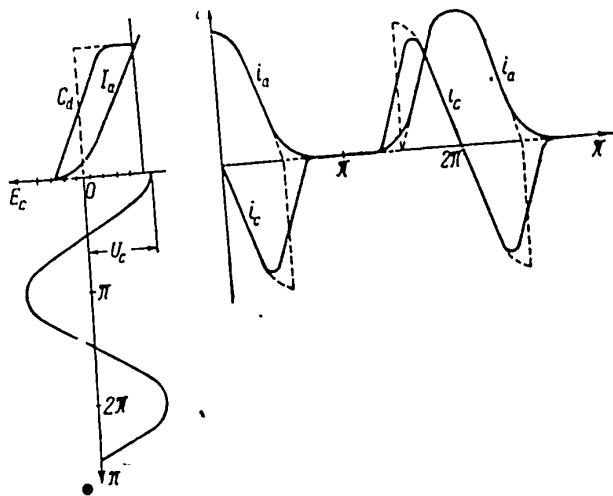


Fig.5

completely correct for the actual characteristics of the tube.

As an illustration of the explanation, Fig.5 gives the characteristics of the

current i_c , flowing through the dynamic capacitance with its actual (solid line) and idealized (broken line) characteristic, in the case of operation of the generator with a cutoff of $\theta = 90^\circ$ (according to the idealized characteristic). In the same graph, the plate current i_a of the tube for the idealized and the actual characteristics is plotted.

If the dependence between S and C_d is not linear, there will not be a complete identity of the coefficients α_i for the dynamic capacitance and the transconductance of the characteristic. However, for the majority of modern tubes this discrepancy is not great and can be disregarded. For example, for the dependence plotted in Fig.3 (an unfavorable case), the discrepancy of α_i for C_d and S does not exceed 10%.

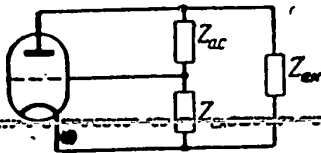


Fig.6

We will next discuss a study of actual schematics of tube generators with self-excitation. For any circuit of a triode generator (generalized schematic shown in Fig.6) during its steady state, there should exist equality between the negative resistance of the tube and the positive resistance of the circuit in the plate-cathode section

$$\frac{\sigma \gamma_i}{S - \frac{\sigma}{R_i}} = Z_\alpha \quad (7)$$

where S is the transconductance of the tube characteristic; R_i is the internal resistance of the tube; σ is the ratio of the voltage between the cathode and the anode to the voltage of the grid-cathode, i.e.,

$$\sigma = \frac{U_{ak}}{U_{ck}} \quad (8)$$

$$Z_\alpha = \frac{Z_{ak}(Z_{ck} + Z_{gr})}{Z_{ck} + Z_{dc} + Z_{ak}} \quad (9)$$

When the generated frequency is close to the frequency of the oscillatory cir-

circuit, we can write

$$Z_{\alpha} \approx R_{\alpha} = p_{\alpha}^2 R_0, \quad (10)$$

where R_0 is the complete resistance of the oscillatory circuit during resonance,

$$p_{\alpha} = \frac{U_{\alpha k}}{U_0}, \text{ where } U_0 \text{ is the voltage in the entire circuit.}$$

We will designate

$$p = \frac{U_{ac}}{U_0}, \quad (11)$$

where U_{ac} is the voltage between the grid and plate of the tube.

We will denote by p the coupling factor of the tube with the circuit. Then, on the basis of eqs. (7), (8), (10), and (11) and taking into account that $U_{ac} = U_{ck} +$

$+ U_{ak}$, we get

$$p^2 = \frac{(1 + \sigma)^2 r_i}{\sigma \left(S - \frac{\sigma}{R_i} \right) R_0}. \quad (12)$$

Since, during resonance, we have

$$R_0 = \frac{Q}{\omega C_0}, \quad (13)$$

where Q is the Q -factor of the circuit and C_0 is the total capacitance of the oscillatory circuit, then

$$p^2 = \frac{(1 + \sigma)^2 \sigma_i \omega C_0}{\sigma \left(S - \frac{\sigma}{R_i} \right) Q}. \quad (14)$$

Equation (14) characterizes the dependence of the coupling factor p of the tube with the circuit on the parameters of the circuit, the tube, and its operating state. Based on this expression, it is possible to calculate the magnitude inserted into the capacitance circuit from any interelectrode capacitance and the extent of its effect on the generator frequency. The magnitude of the insertion into the circuit of the capacitance from the interelectrode grid-cathode capacitance is determined,

with sufficient accuracy, by the expression

$$\Delta C_{ck} = \frac{p^2}{(1 + \sigma)^2} C_{ck}. \quad (15)$$

Furthermore, using the simple correlation

$$\frac{\Delta f}{f} = - \frac{\Delta C_{ck}}{2 C_0}, \quad (16)$$

(where f is the fundamental frequency and Δf is the change in frequency) and using eqs.(14) and (15), the magnitude of the frequency correction for the interelectrode capacitance C_{ck} can be obtained:

$$\frac{\Delta f}{f} = - \frac{\pi f C_{ck} \eta_1}{\sigma Q \left(S - \frac{\sigma}{R_i} \right)}. \quad (17)$$

However, in the given case we are interested in the effect of the dynamic capacitance of the tube on the generator frequency. It was established above that the dependence of the active value of this capacitance on the operating conditions is determined by eq.(6), under the condition that a sinusoidal voltage

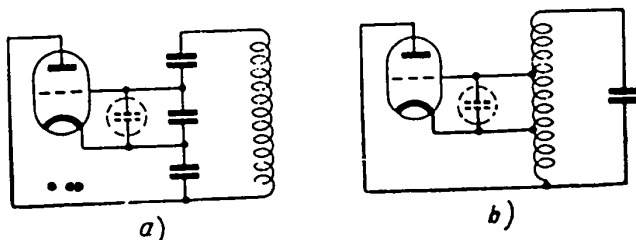


Fig.7

is supplied to the grid of the tube. We will now examine to what degree this condition is satisfied in actual networks of tube generators having partial coupling of the tube with the circuit. For the analysis, we will take the two most characteristic schematics of the triode generator - the hookup with capacitive coupling and the hookup with inductive coupling shown respectively in Figs.7a and 7b. In these hookups, the dynamic capacitances are indicated by the circular broken lines. Applying eq.(1) for the fundamental frequency and higher harmonics to the grid circuit of

these hookups, and using eqs. (14), (15) and (16), we find: for the hookup with capacitive coupling

$$\frac{U_n}{U_{ck}} = - \frac{C_d}{C_2 a_1} \sum_{n=2}^{n=\infty} \frac{I_n}{I_1 n} = - \frac{\rho C_d}{(1 + \sigma) C_2 a_1} \sum_{n=2}^{n=\infty} \frac{I_n}{I_1 n}, \quad (18)$$

for the hookup with inductive coupling

$$\frac{U_n}{U_{ck}} = - \frac{\rho C_d}{(1 + \sigma) C_2 a_1} \sum_{n=2}^{n=\infty} \frac{I_n}{I_1} n, \quad (18a)$$

where U_n is the voltage in the grid circuit from the n^{th} harmonic of the current flowing through the nonlinear (dynamic) capacitance: n is the number of the harmonic; I_n is the current of the n^{th} harmonic; I_1 is the current of the first harmonic; C_2 is the general capacitance of the grid-cathode section of the tube.

It is not difficult to see that, at normal operation of the generator, and at a sufficiently high Q -factor of the circuit, the left-hand side of eqs. (18) and (18a) does not exceed 1. Such a numerical order can be obtained in any other hookup of a triode generator with partial coupling of the tube to the circuit.

This proves the reliability of the magnitude of the active dynamic capacitance determined from eq. (6). Then, substituting in eq. (17) the value of C_{doe} from eq. (6) for C_{ck} , we get

$$\frac{\Delta f}{f} = - \frac{\rho C_d}{\sigma Q \left(S - \frac{\sigma}{H_i} \right)}. \quad (19)$$

Equation (19) is used for determining the frequency correction due to the dynamic capacitance; it is deduced on the basis of the general theory of triode generators and is therefore applicable to any form of hookup with partial coupling of the tube to the circuit and with operating conditions of the generator close to normal.

Using Eq. (19), knowing the values of the quantities entering into this formula, and having determined the dependence S , C_d , and R_i of the given tube on the applied

voltages (according to statistical characteristics), one can easily calculate the change in the generator frequency during a change in the power-supply voltages. Inasmuch as, during a decrease in the plate voltage, the transconductance of the characteristic decreases faster than the dynamic capacitance, while this decrease is slower during a drop in the filament voltage, then [in agreement with eq.(19)] a lowering of the plate voltage will lead to a lowering of the frequency, while a lowering of the filament voltage will result in an increase in frequency.

3. Influence of the Higher Harmonics on the Generator Frequency, at Optimum Coupling of the Tube with the Circuit

For the generalized hookup of a tapped-coil oscillator (Fig.6), based on the condition that balance of the phases is present, the following expression is valid (Bibl.7, 8):

$$= - \sum_{n=1}^{n=\infty} n \left[\frac{Z_{akn}(Z_{ckn} + Z_{acn})}{Z_{ckn} + Z_{acn} + Z_{akn}} \left(\frac{Z_{ckn}}{Z_{ckn} + Z_{acn}} + \frac{1}{\mu} \right) \right] \left(\frac{I_{an}}{I_{a1}} \right)^2, \quad (20)$$

where I_{a1} is the component of the first harmonic of the plate current;

I_{an} is the component of the n^{th} harmonic of the plate current;

μ is the amplification factor of the tube;

Z_{ak} , Z_{ck} , Z_{ac} are the impedances of the corresponding sections of the hookup for the fundamental frequency;

Z_{akn} , Z_{ckn} , Z_{acn} are the same for the n^{th} harmonic.

The discussion below is applicable to actual circuits of generators. We will pay special attention to the tapped-capacitor network, which offers the possibility of obtaining the best indexes for frequency stability and for simplicity in structural solutions. In its most general outline, this schematic is shown in Fig.8; as indicated below, every other network of a tapped-capacitor oscillator (Colpitts

oscillator) is a special case of this schematic. The necessity of inserting the capacitance C_1 into the circuit is due to the fact that, at sufficiently small values

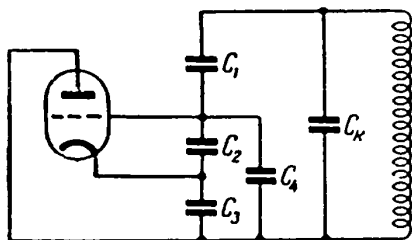


Fig. 8

of the capacitances C_2 and C_3 , the capacitance C_1 (i.e., the plate-grid capacitance of the tube) may greatly affect the final results. We will assume that the active resistance of the circuit is concentrated in the inductance (that it does not have a noticeable limit, since the Q-factor of modern capacitors is many times larger than

the Q-factor of the inductance coils. Then, after certain transformations of eq.(20), we get for the imaginary part:

$$\frac{r_0^2 + x_0[x_{ck}(\mu + 1) + x_{ac}]}{x_0^2 + r_{ac}^2} = \frac{1}{x_{ak}} \sum_{n=2}^{n=\infty} n x_{akn} [r_n^2 + x_{on} x_{ckn}(\mu + 1) + x_{on} x_{ackn}] \left(\frac{I_{on}}{I_{a1}} \right)^2 \quad (21)$$

where I_{ac} is the active resistance of the entire circuit for the fundamental frequency;

r_n is the same for the corresponding number of the harmonic;

x_{ak} , x_{ac} , x_{ck} are the reactances of the corresponding chain circuits for the fundamental frequency;

x_{akn} , x_{ackn} , x_{ckn} are the same for the n^{th} harmonic;

$x_0 = x_{ak} + x_{ac} + x_{ck}$ is the reactance impedance of the entire circuit for the fundamental frequency;

$x_{on} = x_{akn} + x_{ackn} + x_{ckn}$ is the same for the n^{th} harmonic.

Before continuing with the transformations of eq.(21), we will designate

$$\omega = \omega_0 + \Delta\omega, \quad (22)$$

where ω is the working angular velocity; ω_0 is the resonant angular velocity of the circuit.

Since the magnitude $\Delta\omega$ is small in comparison to ω , it is not difficult to find

$$\omega^2 = \omega_0^2 \left(1 + \frac{2\Delta f}{f} \right), \quad (23)$$

We will further designate

$$a = \frac{C_4}{C_2}, \quad (24)$$

$$m = \frac{C_{\alpha}}{C_0}, \quad (25)$$

where C_{0e} is the total capacitance of the link, comprised of C_1, C_2, C_3 , and C_4 .

We will assume the following limiting condition:

$$m \gg \frac{1}{Q}, \quad (26)$$

i.e., we stipulate that the ratio of the total capacitance of the divisor to the entire circuit capacitance must not be less than the determined magnitude (nonobservance of this condition leads to a sharp increase in the frequency correction of the generator and to instability of its operation).

We will further take into account that, for a fractional frequency change due to a nonlinear correction, the inequality $\frac{\Delta f}{f} \ll \frac{1}{Q}$ is valid, from which it follows that $x_0 \ll r_{ac}$ and that, for the higher harmonics, we have $x_{on} \gg r_n$, since the system for the higher harmonics is located far from resonance (excluding special points, where the capacitance C_k together with the circuit inductance L_0 will be in resonance on the frequency of one of the higher harmonics). Then, after several calculations and transformations of eq.(21), we get finally

$$\frac{\Delta f}{f} = \frac{[1 + a(1 + \sigma)] \sum_{n=2}^{n=\infty} \left[\frac{\mu + 1}{1 + \sigma} \right]}{\rightarrow}$$

$$\begin{aligned} & + \frac{(n^2 - 1)(1 - p) + n^2 mp}{p[n^2(1 - m) - 1] + a(1 + \sigma)(n^2 - 1)} \left[p \left[n^2(1 - m) - 1 \right] + \right. \\ & \left. \frac{2Q^2 \left[1 + m(1 - p) + a(1 + \sigma) \right] pm \left[\frac{\mu + 1}{1 + \sigma} - 1 \right]}{+ a(1 + \sigma)(n^2 - 1)} \right] \frac{1}{n^2 - 1} \left(\frac{I_{an}}{I_{a1}} \right)^2 \end{aligned} \quad (27)$$

Equation (27) offers the opportunity of calculating the correction of the frequency due to the influence of the higher harmonics for the generalized network of

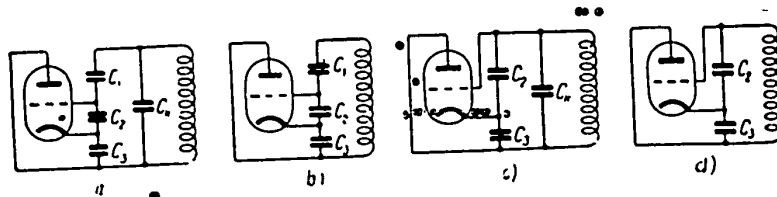


Fig. 8

a tapped-capacitor oscillator (Fig. 8). We will assume that the capacitances C_2 and C_3 are significantly larger than the capacitance C_1 , i.e., in compliance with eq. (27), the quantity a will be small. Then, equating the term a in eq. (27) to zero, we get the frequency correction for the schematic in Fig. 9a, i.e.,

$$\frac{\Delta f}{f} = \frac{\sum_{n=2}^{n=\infty} \left[\frac{\mu + 1}{1 + \sigma} + \frac{(n^2 - 1)(1 - p) + n^2 mp}{p[n^2(1 - m) - 1]} \right] \left[n^2(1 - m) - 1 \right] \frac{1}{n^2 - 1} \left(\frac{I_{an}}{I_{a1}} \right)^2}{2Q^2 m \left[1 + m(1 - p) \right] \left[\frac{\mu + 1}{1 + \sigma} - 1 \right]} \quad (28)$$

We then assume that $m = 1$ (the schematic in Fig. 9b corresponds to this case), so that the frequency correction will be

$$\frac{\Delta f}{f} = - \frac{\sum_{n=2}^{n=\infty} \left[\frac{\mu + 1}{1 + \sigma} - \frac{(n^2 - 1)(1 - p) + n^2 p}{p} \right] \frac{1}{n^2 - 1} \left(\frac{I_{an}}{I_{a1}} \right)^2}{2Q^2 (2 - p) \left[\frac{\mu + 1}{1 + \sigma} - 1 \right]} \quad (29)$$

Further we will consider the case when $m \neq 1$, $p = 1$ (Fig. 9c); then the frequen-

cy correction is

$$\frac{\Delta f}{f} = \frac{\sum_{n=2}^{n=\infty} \left[\frac{\mu+1}{1+\sigma} + \frac{n^2 m}{n^2(1-m)-1} \right] [n^2(1-m)-1] \frac{1}{n^2-1} \left(\frac{I_{an}}{I_{a1}} \right)^2}{2Q^2 m \left[\frac{\mu+1}{1+\sigma} - 1 \right]} \quad (30)$$

Lastly, for the usual tapped-capacitor network, (Fig.9d), i.e., when $a = 0$, $p = 1$, $m = 1$, we have

$$\frac{\Delta f}{f} = \frac{\sum_{n=2}^{n=\infty} \left[\frac{\mu+1}{1+\sigma} - n^2 \right] \frac{1}{n^2-1} \left(\frac{I_{an}}{I_{a1}} \right)^2}{2Q^2 \left[\frac{\mu+1}{1+\sigma} - 1 \right]} \approx \frac{\sum_{n=2}^{n=\infty} \frac{1}{n^2-1} \left(\frac{I_{an}}{I_{a1}} \right)^2}{2Q^2} \quad (31)$$

Equations (27) - (31) permit computing the frequency correction due to higher harmonics for any hookup of a tapped-capacitor oscillator. It is not difficult to prove that the frequency corrections can be actually separated not only according to magnitude but also according to sign, for various networks as well as for the same network at various values entering into it.

It must be remarked that, due to the presence of the interelectrode capacitance of the tube and the self-capacitance of the coil, the inductance of the schematics in Fig.9a, b, g does not exist in the pure form. The error in calculating the frequency correction due to the higher harmonics, produced by disregarding these capacitances can be quite significant, especially at high frequencies (almost up to a change in sign of the correction). Therefore, the frequency correction for the usual tapped-capacitor network [eq.(31)] well-known in the theory (Bibl.3, 4), is not applicable in practice for short and meter waves; for these wavelengths, eq.(30) must be used.

We will next examine the network of a tapped-coil oscillator with partial coupling of the tube to the circuit (Fig.10). Based on eq.(20) and applying such methods as used for deducing the expressions for tapped-capacitor networks, we find the

frequency correction

$$\frac{\Delta f}{f} = - \frac{\sum_{n=2}^{n=\infty} \left[\frac{(\mu+1)p}{1+\sigma} - \frac{1}{n^2} + (1-p) \right] \frac{n^4}{n^2-1} \left(\frac{I_{an}}{I_{a1}} \right)^2}{2Q^2 p \left[\frac{\mu+1}{1+\sigma} - 1 \right]} \approx - \frac{1}{2Q^2} \sum_{n=2}^{n=\infty} \frac{n^4}{n^2-1} \left(\frac{I_{an}}{I_{a1}} \right)^2 \quad (32)$$

In deriving eq.(32), we consider that, for the fundamental frequency and the nearest higher harmonics (the second and third harmonics), the capacitive reactance of the interelectrode capacitances (in Fig.10 these are shown as broken lines) are actually larger than the inductive reactance of the sections of the inductance connected in parallel to them. With a sufficiently high Q-factor of the circuit, this limiting is not essential.

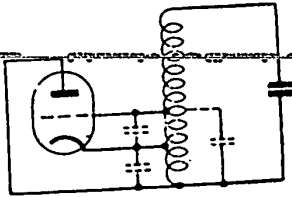


Fig.10

From eq.(32) it can be seen that, in the given case, the frequency correction is actually the same as for a tapped-coil network with total coupling of the tube to the circuit. In contrast to the frequency correction due to dynamic capacitance, the frequency correction due to higher harmonics has the same sign with a one-sign change of the plate and filament voltages, since the transconductance of the characteristic (and consequently the coefficients of the harmonics) decreases with a decrease in the plate voltage as well as with a decrease in the filament voltage.

4. Variation in the Generator Frequency, due to the Shunting Action of the Internal Resistance of the Tube

The shunting action of the internal resistance of the tube introduces the additional reactance $x_0 = - \frac{r_{ac} x_{ak}}{r_{ia1}}$ into the oscillatory circuit. After substituting,

in this expression, the quantities x_0 , r_{ac} , and x_{ak} it takes the following form, for the schematic given in Fig.8:

$$\frac{\Delta f}{f} = \frac{\rho \sigma |1 + a(1 + \sigma)|}{4 \pi f Q m C_0 (1 + \sigma) R_i a_i} \quad (33)$$

For a tapped-coil network (Fig.10) we will have

$$\frac{\Delta f}{f} = \frac{\rho \sigma}{4 \pi f Q C_0 (1 + \sigma) R_i a_i} \quad (34)$$

It is not difficult to see that the frequency correction (33) can change during a change in the operating condition of the generator only because of the value $R_i a_i$.

We will transform this value

$$R_i a_i = \frac{\mu a_i}{S} \quad (35)$$

The amplification factor μ of the tube is expressed, as is well known, by a ratio of the interelectrode grid-cathode capacitance to the plate-cathode capacitance. Undoubtedly, we should include the static as well as the dynamic capacitance in the interelectrode grid-cathode capacitance. Then, during operation of a tube with a cutoff we get the following value for μ

$$\mu = \frac{C_{ck} + \frac{C_d}{a_i}}{C_{ak}} \quad (36)$$

Taking into account the values for μ , eq.(33) takes the form

$$\frac{\Delta f}{f} = \frac{\rho \sigma C_{ak} S |1 + a(1 + \sigma)|}{4 \pi f Q m C_0 (1 + \sigma) (a_i C_{ck} + C_d)} \quad (37)$$

Equation (37) permits computing the magnitude of the frequency change during a change in the power-supply voltage, due to the shunting action of the plate resistance. For this it is necessary to know the change in the magnitude of C_d , a_i and S , which, as we have seen, is necessary also for calculating other frequency correc-

tions.

The peculiar feature of the given frequency correction is that its absolute magnitude does not depend directly on the frequency. Therefore, it will have a more relative valuation at comparatively low frequencies.

Besides the above frequency corrections, there is room for a frequency correction due to the currents of the higher harmonics, formed in the grid circuit on account of the nonlinearity of the dynamic capacitance. These currents create an additional shift in the phase of the grid voltage. The magnitude of this correction changes comparatively little with a change in frequency; in the overall sum of frequency corrections, its relative magnitude is not great, so that it can be disregarded in the discussion.

5. Comparative Evaluation of the Obtained Results

From the above explanation, it follows that the mechanism of the effect of a change in the power supply voltages is characterized by a series of frequency corrections, determined by eq.(19) for the frequency correction due to the dynamic capacitance of the tube, by eqs.(27) - (32) for the frequency correction due to the nonlinearity of the tube characteristic, and by eq.(37) for the frequency correction due to the shunting action of the internal resistance of the oscillating tube.

Taking into account that all these corrections are individually and in total sufficiently small, it is possible to assume that they act independently of each other. Therefore a computation of the change in frequency of the generator, for each factor, can be made separately and later combined.

Considering the diversity of the factors influencing the change in frequency, it is difficult to determine in a general form the relative magnitude of each of these corrections in different zones of the band and for various values of the quantities entering them. Actually, it is possible to state only one: the relative magnitude of the frequency correction, due to dynamic capacitance, increases with an

increase in the operating frequency.

However, the problem can be greatly simplified (nonetheless evaluating by this the whole pattern), if the calculations of the changes in the generator frequency during changes in the power-supply voltages are carried out for the most characteristic cases in practice and in a wide interval of operating frequencies.

We will assume as the limit of variation in the working frequencies, the range from 0.2×10^6 cycles to 60×10^6 cycles. We will take into account that, for the frequency 0.4×10^6 cps, the Q-factor of the oscillating circuit of the generator is equal to $Q = 125$ and the full circuit capacitance $C_0 = 300 \mu\text{f}$. We will further take into account that the Q-factor of the circuit changes monotonously in proportion to the root of the fourth power of the frequency, while the circuit capacitance is inversely proportional to the square root of the frequency. The circuit coils are of the single-layer type, without a core, and their inductance is determined by the given frequency and the capacitance of the circuit. We will consider that the special (distributed) capacitance of the circuit coil changes according to a law opposite to the change of its Q-factor. As the oscillating tube we will use a tube of the type 12Zh1L, working equally well in all given intervals of the operating frequencies.

Inasmuch as we are not interested in the frequency corrections themselves but only in their change with a deviation in the power-supply voltages from the rating for the given relative magnitude, the magnitude of the change in these voltages must be known. In operation, the latter constitutes 10 - 20%. We will take it as equal to 20%.

Let us make calculations applicable to two cases - to a hookup with a capacitive coupling (Fig.8) in the most general form, when $m = 0.2$ and to the same network but with the a capacitance C_k , decreased to the possible limit ($m = 1$), i.e., at self-capacitance of the inductance coil. As for the capacitance C_k , it is in both cases taken equal to the interelectrode capacitance of the tube C_{ac} (counting the

capacitance between the leads and the capacitance of the tube socket), since the artificial increase of this capacitance can in no way be justified.

In Figs. 11 and 12 the results of the above calculations are plotted in the form of a graph. Here a denotes the curves for the frequency change due to the influence of the higher harmonics, r those due to the shunting action of the plate resistance, c those due to the dynamic capacitance and S is the total change in frequency. In both cases, the generator was examined under two operating conditions

$$\sigma = 0.5 \quad \text{and} \quad \sigma = 2.$$

From the analysis of the obtained results it follows that

1. Both networks are of equal value in an evaluation of the frequency change due to the dynamic capacitance of the tube; at the same time, they are basically different in an evaluation of the destabilizing influence of the higher harmonics. The influence of the interelectrode capacitances and the self-capacitance of the inductance coil (C_L and C_K) in the second case is so significant that it cannot be ignored without committing a serious error, especially at the higher frequencies.
2. At a properly selected schematic, the frequency change due to the influence of the dynamic capacitance is dominant in the entire band of the short and meter waves.

6. Material for Experimental Research

To check experimentally the above cases, a working circuit, based on the basic diagram in Fig. 8, was selected. At a proper selection of the quantities entering into it, this hookup can be converted into the schematic shown in Fig. 9.

The research was carried out on the tube 12Zh1L, including the equivalent triode. In order to decrease measuring errors as much as possible, the plate voltage did not vary by 20%, but by 84% (from 60 to 110 v), which corresponded to a variation in the transconductance of the tube characteristic S from $\frac{2.3 \text{ ma}}{B}$ to $\frac{3.13 \text{ ma}}{B}$.

The maximum dynamic capacitance of the tube $C_d - 1.2 \mu\mu f$ (at $U_{c1} = 0$) was practically constant for various values of the plate voltage. At a variation in the quantities entering eqs.(19), (27) - (31), and (37) the capacitances of the network were changed in a corresponding manner. The interelectrode capacitances of the tube and the self-capacitance of the inductance coil, were used as the lower limit of the values for the capacitances $C_2, C_3, C_4,$ and C_k ; here likewise eq.(26) was valid. The inductance coil was in all cases of the single-layer, cylindrical (except in the specified cases) type, in a red copper shield.

The calculated and measured values of the frequency change for the self-oscillator are presented in Tables 1, 2, and 3.

Table 1

Fundamental frequency: $f = 26.2 \times 10^6$ cps; inductance of the circuit $L = 1.05 \times 10^{-6}$ henry; Q-factor of the circuit $Q = 200$ (measured values)

m	0,107	0,113	0,111	0,23	0,294	0,11	0,133	a)
p	0,375	0,5	0,38	0,33	0,337	0,35	0,117	
c	0,98	0,98	0,98	0,98	0,53	0,62	1,51	
a	0,44	0,44	0,28	0,109	0,116	0,11	0,28	
$\Delta \Sigma \left(\frac{f_{an}}{f_{a1}} \right)^2$	0,16	0,21	0,145	0,121	0,12	0,134	0,17	b)
$\Delta \Delta f_m, \text{ cps}$	1650	1320	827	275	160	1220	1190	c)
$\Delta \Delta f_r, \text{ cps}$	50	16	33	22	23	55	28	d)
$\Delta \Delta f_c, \text{ cps}$	1730	1730	1730	1730	2970	2570	1160	e)
$\Delta \Delta f_s, \text{ cps}$	3430	3066	2590	2027	3153	3845	2378	$\Delta \Delta f_s = \Delta \Delta f_r + \Delta \Delta f_a + \Delta \Delta f_r$
$\Delta \Delta f_4, \text{ cps}$	3320	3180	2620	2250	3400	3500	2490	f)
$\frac{\Delta \Delta f_s - \Delta \Delta f_4}{\Delta \Delta f_4}, \%$	+ 3,3	- 3,6	- 1,1	- 10	- 7,3	+ 9,9	- 4,5	

a) Remarks; b) Calculated; c) Calculated according to eq.(27); d) Calculated according to eq.(37); e) Calculated according to eq.(19); f) Measured.

The Tables indicate that the discrepancy between the calculated and measured values of the frequency change of the self-oscillator lies within the limits of the accuracy of the measurements, taking into account the diversity of the factors influencing this change.

In order to determine the possibility of using inductance coils with a carbonyl

Table 2

f , cps	$L = 12,2 \cdot 10^{-6}$ cps				a)
	$6,95 \cdot 10^6$	$4,95 \cdot 10^6$	$4,99 \cdot 10^6$	$4,98 \cdot 10^6$	
Q	138	124	124	124	
m	0,126	0,485	0,473	0,473	
ρ	0,223	0,267	0,29	0,29	
σ	0,975	1,065	2	0,5	
a	0,12	0,115	0,11	0,12	
$\Delta \Sigma \left(\frac{I_{an}}{I_{an}} \right)^2$	0,12	0,11	0,11	0,12	b)
$\Delta \Delta f_a$, cps	394	32	32	21	c)
$\Delta \Delta f_r$, cps	37	6	8	4	d)
$\Delta \Delta f_c$, cps	172	90	54	185	e)
$\Delta \Delta f_s$, cps	603	128	94	210	$\Delta \Delta f_s = \Delta \Delta f_c + \Delta \Delta f_a + \Delta \Delta f_r$
$\Delta \Delta f_4$, cps	510	127	94	220	f)
$\frac{\Delta \Delta f_s - \Delta \Delta f_4}{\Delta \Delta f_4}$, %	+ 18	+ 1	0	- 4,5	

a) Remarks; b) Calculated; c) Calculated according to eq.(27); d) Calculated according to eq.(37); e) Calculated according to eq.(19); f) Measured

iron core for the experiment, whose results are presented in Table 3, a single-layer coil was replaced by an inductance coil with a carbonyl iron core. A closed (pot-shaped) core of a diameter of 22 mm was selected; the inductance of the coil in this core and its Q-factor were roughly the same as the inductance and the Q-factor of the single-layer coil. The frequency in this case changed a few tens of times more

than in a single-layer inductance coil. This could have been merely due to the non-linearity of the magnetic permeability of the core.

Consequently, when using carbonyl iron cores in contour coils, the instabilities of the generator frequency are of a much higher order, incompatible with the

Table 3

$L = 260 \cdot 10^{-6}$ cps

f , cps	$0,77 \cdot 10^6$	$0,756 \cdot 10^6$	$0,405 \cdot 10^6$	a)
Q	160	160	106	
m	0,97	0,9	0,343	
ρ	0,18	0,14		
ϵ	0,37	1,06	0,53	
n	0,001	0,002	0,001	
$\Delta \Sigma (I_{an})^2$	0,15	0,13	0,13	b)
$\Delta \Delta f_a$, cps	0,03	0,3	4,36	c)
$\Delta \Delta f_r$, cps	0,22	0,45	0,70	d)
$\Delta \Delta f_c$, cps	1,5	1,6	1,44	e)
$\Delta \Delta f_s$, cps	4,69	2,35	6,50	$\Delta \Delta f_s = -\Delta \Delta f_a + \Delta \Delta f_c + \Delta \Delta f_r$
$\Delta \Delta f_i$, cps	5	3	6	f)

a) Remarks; b) Calculated; c) Calculated according to eq.(27); d) Calculated according to eq.(37); e) Calculated according to eq.(19); f) Measured

concept of a high-stability oscillator. The given theory is naturally not extended to this case.

7. General Conclusions

The influence of power-supply voltages on the frequency of an oscillator is determined basically by three unstabilizing factors: the active value of the dynamic

POOR ORIGINAL

than in a single-layer inductance coil. This could have been merely due to the non-linearity of the magnetic permeability of the core.

Consequently, when using carbonyl iron cores in contour coils, the instabilities of the generator frequency are of a much higher order, incompatible with the

Table 3

 $L = 260 \cdot 10^{-6}$ cps

f , cps	$0,77 \cdot 10^6$	$0,756 \cdot 10^6$	$0,405 \cdot 10^6$	a)
Q	160	160	106	
m	0,97	0,9	0,343	
p	0,18	0,14		
s	0,37	1,06	0,53	
a	0,001	0,002	0,001	
$\Delta \Sigma \left(\frac{I_{an}}{I} \right)^2$	0,15	0,13	0,13	b)
$\Delta \Delta f_a$, cps	0,03	0,3	4,36	c)
$\Delta \Delta f_r$, cps	0,22	0,45	0,70	d)
$\Delta \Delta f_c$, cps	1,5	1,6	1,44	e)
$\Delta \Delta f_s$, cps	4,69	2,35	6,50	$\Delta \Delta f_s = - \frac{\Delta \Delta f_a}{+ \Delta \Delta f_r} + \Delta \Delta f_c +$
$\Delta \Delta j_a$, cps	5	3	6	f)

a) Remarks; b) Calculated; c) Calculated according to eq.(27); d) Calculated according to eq.(37); e) Calculated according to eq.(19); f) Measured

concept of a high-stability oscillator. The given theory is naturally not extended to this case.

7. General Conclusions

The influence of power-supply voltages on the frequency of an oscillator is determined basically by three unstabilizing factors: the active value of the dynamic STAT

capacitance of the tube; the higher harmonics; the internal resistance of the generator.

For short and especially for meter waves, the main factor determining the variation in the generator frequency due to power-supply voltages, is the change in the active value of the dynamic capacitance of the tube.

The variation in frequency due to the dynamic capacitance is characterized by its independence (at optimum coupling of the tube with the circuit) from the form of the network and from the characteristic of the circuit (L/C ratio); at a given frequency, this variation is determined only by the basic parameters of the tube and the circuit (S, C_d , and Q), and likewise by the relationship between the grid and plate coupling σ .

The material presented in the present article proves the feasibility of designing continuous-band oscillators with very small frequency variations during a change in the power-supply voltages (up to 1×10^{-6}) and permits a calculation of this variation with a sufficient degree of accuracy.

Article received by the Editors 20 July 1955

BIBLIOGRAPHY

1. KoBzarev, Yu.B. - The Dependence of the Oscillator Frequency on its Operating Conditions. Vestnik Elektrotehniki, No.10 (1931)
2. Krylov, I.M. and Bogolyubov, N.N. - New Methods in Nonlinear Mechanics. ONTI (1934)
3. Shembel', B.K. - Deviation of the Generator Oscillation Frequency from the Natural Frequency of the Linear Circuit. ZhTF (Zh.Tekhn.Fiz.) Vol.IX, No.7 (1939)
4. Yevtyanov, S.I. - Calculation of Self-Oscillation Frequency. Radiotekhnika, No.2 (1946)
5. Shitikov, G.T. - Investigation of the Influence of the Tube on the Oscillator Frequency. IEST No.8 (1940)
6. Shitikov, G.T. - Influence of the Circuit Characteristic on the Oscillator Stabil-

ity and the Permissible Amplification Factor in Systems with Single-Element Tuning. IEST No.12 (1940)

7. Groshkovskiy, Ya. - Generation of High-Frequency Oscillations and Frequency Stabilization. IL (1953)

8. Yevtyanov, S.I. - Radio Transmitting Systems. Svyazizdat, Moscow (1950)

CALCULATION OF THE AMPLITUDE CHARACTERISTICS OF LIMITERS

by

Ya.Z. Tsypkin

Active Member of the Society

The amplitude characteristic of a limiter is expressed indirectly by the dynamic characteristic of the tube, which simplifies calculations and establishes a link between the properties of these characteristics.

The amplitude of the output voltage of a limiter, consisting of a tube and a filter and passing the first harmonic (Fig.1), as is well known (Bibl.1), is equal to

$$U_{m \text{ out}} = B I_1, \quad (1)$$

where B is a constant, determined by the network of the filter;

I_1 is the amplitude of the first harmonic of the plate current of the tube.

This amplitude depends on the fixed bias E_{sm} and the amplitude of the input voltage $U_{m \text{ in}}$ and is determined according to the dynamic characteristic of the tube

$$i = F(e), \quad (2)$$

on the basis of the well-known formula:

$$I_1 = \frac{2}{\pi} \int_0^{\pi} F(E_{sm} + U_{m \text{ in}} \cos \varphi) \cos \varphi d\varphi. \quad (3)$$

For an analysis of I_1 , a previous report (Bibl.1) derives an approximation of the dynamic characteristic by straight-line segmenting and integration by sections, analogous to the method used in the simplest case in courses on the theory and com-

putation of transmitting systems (Bibl.2).

A similar method was used in another paper (Bibl.3) for determining the higher as well as the first harmonics of the plate current.

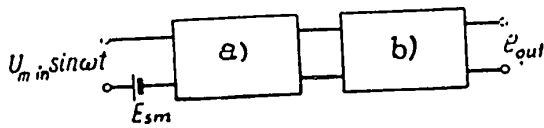


Fig.1

a) Tube; b) Filter

straight line E_k , the bias E_{sm} and the amplitude of the oscillating component U_m in; to determine the value, according to the formula or tabular functions

$$i(\cos \theta_k) = \frac{1}{\pi} \left[\theta_k \cdot \frac{1}{2} \sin 2\theta_k \right]_{k=1,2,3,\dots}$$

multiply these functions by the change of slope of the segment of the approximation straight line and add the obtained products.

All these operations must be repeated for each value of U_{min} , which makes a calculation of I_1 quite cumbersome. To clarify the influence of E_{sm} or of the form of the dynamic tube characteristic on the amplitude characteristic, the calculation must be repeated.

Nonetheless, it is possible to express I_1 , with sufficient accuracy for practice, indirectly through the dynamic characteristic of the tube F and by this not only simplify the calculation, but also establish a definite link between I_1 and both U_m out and $F(e)$. This possibility was used by the author for establishing a close connection between the "mean transconductance" or, as it is called in the theory of automatic control, the complex amplification factor, and the characteristic of the nonlinear element (Bibl.4).

We will substitute the variable $\cos \varphi = y$. Then, after elementary calculations (Bibl.4) and substitution of the value of I_1 in eq.(1), we can put the expres-

sion of the amplitude characteristic of the limiter in the form

$$U_{m \text{ out}} = BI_1 = \frac{2B}{\pi} \int_{-1}^1 \frac{F(E_{sm} + U_{m \text{ in}} y) y}{\sqrt{1-y^2}} dy. \quad (4)$$

For computing this expression the quadratic equations of V.A. Steklov, can be used:

$$\frac{1}{\pi} \int_{-1}^1 \frac{f(y)}{\sqrt{1-y^2}} dy = \frac{1}{6} \left[f(1) + f(-1) + 2f\left(\frac{1}{2}\right) + 2f\left(-\frac{1}{2}\right) \right] + R_6, \quad (5)$$

where

$$R_6 = \dots \frac{f^{(6)}(\xi)}{2^6 \cdot 6!},$$

$$|\xi| < 1,$$

or

$$\frac{1}{\pi} \int_{-1}^1 \frac{f(y)}{\sqrt{1-y^2}} dy = \frac{1}{6} \left[\frac{f(1) + f(-1)}{2} + f\left(\frac{1}{2}\right) + f\left(-\frac{1}{2}\right) + f\left(\frac{\sqrt{3}}{2}\right) + f\left(-\frac{\sqrt{3}}{2}\right) + f(0) \right] + R_{12},$$

where

$$R_{12} = \dots \frac{f^{(12)}(\xi)}{2^{11} \cdot 12!},$$

$$|\xi| < 1.$$

If we eliminate the remaining terms R_6 and R_{12} , we will find the approximate expressions of the integral in the wanted form. Obviously, the expression obtained from eq.(6) in the usual case will be more accurate than that obtained from eq.(5).

Putting, in eqs.(5) and (6)*,

$$f(y) = F(E_{sm} + U_{m \text{ in}} y) y^{11},$$

*Further, it is assumed that $F(e)$ corresponds to a continuous curve.

we get, after substituting them in eq.(4) and eliminating the remaining terms, the approximate expressions for the amplitude characteristic of the limiter in the form

$$U_{m \text{ out}} = \frac{B}{3} \left[F(E_{sm} + U_{m \text{ in}}) - F(E_{sm} - U_{m \text{ in}}) + F\left(E_{sm} + \frac{1}{2} U_{m \text{ in}}\right) - F\left(E_{sm} - \frac{1}{2} U_{m \text{ in}}\right) \right] \quad (7)$$

and, with greater accuracy,

$$U_{m \text{ out}} = \frac{B}{3} \left\{ \frac{1}{2} \left[F(E_{sm} + U_{m \text{ in}}) - F(E_{sm} - U_{m \text{ in}}) + F\left(E_{sm} + \frac{1}{2} U_{m \text{ in}}\right) - F\left(E_{sm} - \frac{1}{2} U_{m \text{ in}}\right) \right] + \frac{\sqrt{3}}{2} \left[F\left(E_{sm} + \frac{\sqrt{3}}{2} U_{m \text{ in}}\right) - F\left(E_{sm} - \frac{\sqrt{3}}{2} U_{m \text{ in}}\right) \right] \right\}. \quad (8)$$

The presented formulas indirectly connect the amplitude characteristic of the limiter $U_m \text{ out}$ with the dynamic characteristic of the tube $i = F(e)$. Equation (7) is relatively simple. In cases where its accuracy is not sufficient, one can use eq.(8)* which, disregarding the factor $\frac{1}{2}$, differs from eq.(8) by the last two terms:

$$\frac{\sqrt{3}}{2} F\left(E_{sm} + \frac{\sqrt{3}}{2} U_{m \text{ in}}\right) - \frac{\sqrt{3}}{2} F\left(E_{sm} - \frac{\sqrt{3}}{2} U_{m \text{ in}}\right).$$

If the dynamic characteristic of the tube is given analytically, then by substituting its expression in eqs.(7) or (8), we find the approximate analytical expression for the amplitude characteristic of the limiter.

If, as usually happens, the dynamic characteristic of the tube is given graphically (Fig.2a), it is possible to find the amplitude characteristic of the limiter by a simple plotting of the graph. For this, using the dynamic characteristic of $F(e)$, the curve $F\left(\frac{1}{2}e\right)$ is constructed by doubling the abscissas of $F(e)$. In-

*Equations (7) and (8) become accurate if $F(e)$ can be represented by polynomials of the 4th and 10th degree, respectively; then, eq.(7) will yield the "formula of the five ordinates" (Bibl.5).

serting the ordinates of these curves (Fig.2b), we get $F(e) + F(\frac{1}{2}e)$. Displacing the origin of the coordinates by the amount E_{sm} (to the right at $E_{sm} > 0$ and to the left at $E_{sm} < 0$), we find $F(E_{sm} + e) + F(E_{sm} + \frac{1}{2}e)$, (curve 1 in Fig.2b). The curve $F(E_{sm} - e) + F(E_{sm} - \frac{1}{2}e)$ is obtained by the mirror image of the curve obtained earlier relative to the ordinates (curve 2 in Fig.2b). Since it is assumed

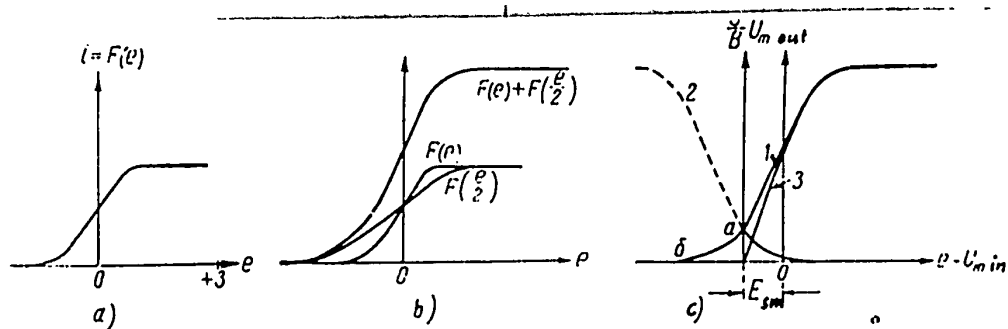


Fig.2

that $U_{m \text{ in}} = e > 0$, it is sufficient to get a mirror image of the section oa of curve 2, lying to the left of the ordinates (the mirror section is indicated by the solid line). The difference between curves 1 and 2 at $U_{m \text{ in}} = e > 0$ (curve 3 in Fig.2b), in agreement with eq.(7), is equal to $\frac{3}{B} U_{m \text{ out}}$. Changing the scale along the ordinates $\frac{B}{3}$ times, we get a graph for the amplitude characteristic of the limiter. If, for any reason, extreme accuracy in computing the amplitude characteristic of the limiter is necessary, then eq.(8) can be used.

In that case, the scale of curve 3 in Fig.2b changes along the ordinates $\frac{B}{6}$ times and the curve

$$\sqrt{3} \left[F \left(E_{sm} + \frac{\sqrt{3}}{2} U_{m \text{ in}} \right) - F \left(E_{sm} - \frac{\sqrt{3}}{2} U_{m \text{ in}} \right) \right],$$

is added to it, which is constructed in the same way as that obtained above.

Article received by the Editors 26 August 1955

BIBLIOGRAPHY

1. Sidorov, V.M. - Calculation of the Amplitude Characteristics of Limiters.
Radiotekhnika, Vol.8, No.5 (1953)
2. Berg, A.I. - Theory and Computation of Tube Generators (1935)
3. Person, S.V. - A Method for Expanding the Working Characteristics into a Fourier Series. Elektrichestvo No.3 (1948)
4. Tsyarkin, Ya.Z. - Concerning the Coupling of an Equivalent Complex Amplification Factor of a Nonlinear Element with its Characteristic. Automation and Telemechanics (in printing)
5. Krylov, N.N. - Electrical Processes in Nonlinear Elements of Radio Receivers (1949)

LIST OF THE ARTICLES WHICH APPEARED IN "RADIO ENGINEERING" JOURNAL
in 1955

Author	Title of Article	Journal Issue
Abramovich, G.P.	Concerning a Universal System of Units	1
Agafonov, V.M.	Matrix Coefficients for Two Types of Cells from the Cutoffs of Two Interacting Long Lines	4
Aizinov, M.M.	A Pulse Amplifier with a Two-Channel Feedback	7
Alterman, Ya.L. and Livshits, A.R.	Concerning the Broadening of the Frequency Transmission Band of an Input Transformer	5
Antseliovich, Ye.S.	Influence of the Nonlinearity of the Internal Resistance of a Tube, in Calculating Resistor-Coupled Amplifiers	3
Antseliovich, Ye.S.	Calculation of the Nonlinearity of the Internal Resistance of a Pentode During an Analysis of the Operation of Resistor-Coupled Amplifiers	7
Artym, A.D.	A New Method of Phase Modulation	1
Artym, A.D.	Raising the Efficiency of Reactance Tubes	6
Barchukov, A.I., Vasil'yev, G.A. Zhabotinskiy, M.E. and Osipov, B.D.	An Electromechanical Klystron Frequency	3
Baranul'ko, V.A. and Fedotov, I.V.	Letter to the Editor "Radio Echo from Lightning"	11
Belkin, B.G.	A New Generator of Noise Voltages	4
Belkin, B.G.	A New Method for Measuring Nonlinear Distortions in Loudspeakers	9
Blokh, E.L. and Kharkevich, A.A.	The Geometric Theory of the Threshold Carrying Capacity of a Link System	7
Blokh, E.L. and Kharkevich, A.A.	An Answer to the Reprimand by L.M.Finka	10
Borodich, S.V.	Concerning the Nonlinear Distortions Caused by Mismatching of the Antenna Feeder in Multichannel •FM Systems	10

Author	Title of Article	Journal Issue
Breytbart, A.Ya., Lyudmirskiy, I.L., Preobrazhenskiy, B.I.	Sources of Disturbances in Television Sets and Protective Devices	1
Bunimovich, V.I.	On Passage of a Signal and Noises through a Limiter and a Differentiating System	6
Veksler, G.S.	Calculation of an Ionic Voltage Stabilizer	12
Velikin, Ya. I., Gel'mont, Z.Ya. and Zelyakh, E.V.	A Piezoelectric Filter for the Upper Frequencies	3
Vereshchagin, Ya.M.	Quadratic Amplitude-Phase Modulation	3
Vol, V.A.	An Amplifier for a Stroboscopic Oscillograph	10
Vollermer, N.F.	A Method for Raising the Accuracy of Frequency Analyzers with an Electron-Beam Indicator	12
Vol'pert, A.R.	On the Phase Relationships in the Theory of Receiving Antennas and on Certain Applications of the Principle of Reciprocity	11
Vol'p'yan, V.G.	On the Sensitivity of Frequency Detectors with Resonant Circuits	10
Vol'f, V.M.	An Evaluation of the Qualitative Indexes of Sound Transmitting Devices	3
Vol'f, V.M.	The Nonlinear Conversion of Signals of a Compound Form	11
Gutkin, L.S. and Kuz'min, A.D.	The Influence of Electron Inertia in Diode Frequency Detection	9
Dekabrun, L.L.	K-Stabilizers for Voltage of Laboratory Rectifiers	10
Dement'yev, Ye.P.	Noises of Super-High Frequency Amplifiers	1
Zhitomirskiy, V.I.	Determining the Probability of Jamming, Caused by Interference Signals	10
Zingerenko, A.M.	Determining the Duration of the Build-Up of Transient Functions According to the Amplitude-Frequency Characteristics of Transmitting Systems	7
Zyuko, A.G.	A Comparative Evaluation of the Channels of a Link for Various Modulation Systems According to their Carrying Capacity	6

Author	Title of Article	Journal Issue
Ivanov, I.I.	Remarks on the Book by N.M. Izyumova	10
Ivanov, I.V.	Pulse Spark Excitation of Oscillations on the Centimeter Wave Band	12
Irisova, N.A., Zhabotinskiy, M.Ye., Veselago, V.G.	Frequency Stabilization of the Three-Centimeter Klystron with the Aid of Spectral Lines	4
Kalinin, A.I.	Calculation of the Field Strength of Ultrashort Waves in the "Illuminated" Region of Space	9
Kalikhman, S.G.	High-Frequency Broad-Band Transformers	12
Kashel', A.A.	Selection of Elements for Separating Filters During the Operation of Two Medium-Wave and Long-Wave Band Transmitters on One Antenna	11
Klyatskin, I.G.	On a Universal System of Units	1
Kogan, S.S.	Narrow-Band Quartz Filters for Intertube Connections	2
Kononovich, L.M.	Selection of a Hookup for Feedback in RC Generators	1
Kontorovich, M.I.	On the Basic Equations of a Tube Generator in an Established Regime in the Presence of Grid Currents	5
Kocherzhevskiy, G.N.	Radiation of a Slot in an Ideally Conductive Round Disk	4
Kravchenko, B.A.	Harmonic Analysis of the Plate Pulse Current of a Generator for Approximation of the Plate-Grid Characteristic of a Tube by a Straight-Line Break	9
Krize, S.N.	Transient Characteristics of Compound Pulse Systems Consisting of Heterogeneous Sections	12
Kriksunov, V.G.	On Establishing the Oscillation Amplitude in the Circuits of RC Oscillators	8
Kuznetsov, V.D.	Shunt Vibrators	10
Kulikovskiy, A.A.	Processes of Installation at Detection of Pulse Signals	6
Kulikovskiy, A.A.	A Comparison of the Theories of Tube and Semiconductor Amplifiers, and the Possibility of their Generalization	11

POOR ORIGINAL

Author	Title of Article	Journal Issue
Kushmanov, I.V.	Calculation of Correction Circuits for Broad-Band Amplifiers with the Help of RC Circuits	9
Levenstern, I.I., Kostandi, G.G.	Triode Converters of Meter Wave Frequencies	6
Levin, G.A., Levin, B.R.	The Time Characteristics of Pulse Signals, Having Passed Through a Linear System	1
Levitan, G.I.	Calculation of Rectifiers with Electron Stabilization	2
Levin, G.A., Golovchiner, M.M.	An Analysis of Quantum Noises with Pulse-Code Modulation	8
Leytes R.D., Gutman, L.N.	On a Method for Studying Transient Processes in a Linear System	6
Loshakov, L.N.	On a Case of Matching of Radio Waveguides	3
Mashkovtsev, Yu.P.	On the Amplitude-Frequency and Phase Characteristics of Broad-Band Amplifiers	3
Mizyuk, L.Ya.	Calculation of a Cathode Detector	5
Mikaelyan, A.L.	Calculation Methods for the Dielectric and Magnetic Permeability of Artificial Media	1
Mikaelyan, A.L., Pistol'kors, A.A.	Electromagnetic Waves in Magnetized Ferrite in the Presence of Conducting Planes	3
Mikaelyan, A.L.	Magneto-Optic Effects in a Rectangular Waveguide, Filled with an Electron Gas	9
Model', A.M.	The Propagation of Plane Electromagnetic Waves in Space, Filled with Plane-Parallel Grids	6
Model', Z.I., Nesvizhskiy, Yu.B.	Certain Features of Bridge T-Networks with Auxiliary Power from HF Generators	7
Morozov, I.I.	The Temperature-Frequency Characteristics of Electrolytic Capacitors	5
Nazarov, V.G.	Dielectric Amplifiers	8
Neyman, M.S.	Step-by-Step Method of Calculating Waveguide and Oscillatory Systems	1

STAT

POOR ORIGINAL

Author	Title of Article	Journal Issue
Lerman, M. S.	On the General Theory of Signals and the General Theory of Automatic Processes	5
Novozhenov, G. F.	On a Method for Determining the Power of Pulse Generators	2
Pongenden, I. G.	Investigation of Pulse Propagation in Magnetic Circuits	1
Pongenden, I. G.	Magnetic Recording of Rectified Pulses	11
Popov, A. V., Titov, A. V.	Calculation of Fourier Series of Coupled Pairs for Amplitude-Modulated Oscillations	6
Raupen, G. A., Petrov, G. V.	Analysis of Nonlinear-Frequency Amplifiers in Series-Resonant Circuits	12
Ragzin, A. A.	Selective Circuits	7
Titov, G. V.	Theory of Thermal Noises, Part I	2
Titov, G. V.	Theory of Thermal Noises, Part II	2
Zaslav, A. A.	On the Nonlinear Distortions of Unimodal Self-Oscillations in the Presence of Inertia Elements	3
Zinertov, I. M.	Part-Exchange Systems with Constant Pass Band	6
Korjenshin, V. A.	Calculation of Phase and Group Velocity of Surface Waves	7
Sokolik, A. I., Yakhanan, M. V.	Reproduction of a Square Pulse by an Amplifier with an RC Filter in the Plate Circuit of the Tube	11
Krasilernik, V. V., Kozlov, V. V.	On the Electro-Optic Action of Grid Systems	2
Kus, A. V., Didenko, V. V.	An Amplifier with a Logarithmic Characteristic	3
Kuslency, A. A.	The Transient Characteristics of Bridge-Connecting Networks	4
Tetelbaum, I. I.	The Dispersion of Radio Waves by a Plane Plate	1
Tetelbaum, I. I.	On Amplitude-Phase Modulation	6
Vikharev, V. I.	The Reaction of Square Pulses of Various Durations and Intervals on a Line Detector	12

STAT

Author	Title of Article	Journal Issue
Tyminskiy, R.M.	On Certain Features of Modulation	7
Fayzulayev, B.N.	The Pip of the Pulse Characteristic in Networks with a Correction of the Build-Up Front	11
Fayzulayev, B.N.	Calculation of a Cathode Repeater in Pulse Operation	5
Fedotov, Ya.A.	On Calculation Methods for Amplifying Networks with Crystal Triodes	8
Fedorov, N.N.	Nonlinear Distortions in Oscillation Generators with "Inertia Nonlinearity" in the Oscillating Circuit	11
Filippov, L.I.	Potential Noiseproof Feature for the Reception of Pulse Radio Signals	10
Fink, L.M.	Letter to the Editor	10
Fradin, A.Z., Olendskiy, V.A.	On the Antenna Effect of a Balanced Feeder	2
Khaykin, S.E.	Radioastronomy	4
Kharkevich, A.A., Blokh, E.L	On the Critical Carrying Capacity of a Link System	2
Khmel'nitskiy, Ye.P.	On a Method of Significantly Raising the Oscillating Power and Efficiency of an Oscillator, Operating in the Excess Voltage Regime	8
Khromykh, M.K.	Transient Processes in a Class B Power Amplifier	9
Tsykin, G.S.	Calculation of a Cathode Repeater	1
Tsykin, G.S.	Selection of Operating Conditions, Calculation of the Load, and Determination of the Nonlinear Distortions in Amplification Stages with Semiconductor Triodes of the Plane Type	8
Tsyppin, Ya.Z.	Calculation of the Amplitude Characteristics of Limiters	12
Chaykovskiy, V.I.	Reception of Pulse Signals by the Method of Reciprocal Correlation	6
Cherne, Kh.I.	On the Theory of a Single-Tube RC Oscillator	2
Shapiro, D.N.	Calculation of the Efficiency of Shield Cans	4

Author	Title of Article	Journal Issue
Shembel', B.K.	A Calculation Method for Generators with Piezoelectric Frequency Stabilization	7
Shitikov, G.T.	Effect of the Capacitance of a Space Charge and the Nonlinearity of the Tube Characteristic on the Generator Frequency	12
Shteyn, N.I., Eydus, G.S.	Theory and Calculation of a Transitron Generator	7
Yurov, Yu.Ya.	Equivalent Networks of Multigrid Electron Tubes	3 -
Yampolskiy, V.G.	An Approximate Method for Determining the Effect of Phase Distortions in the Aperture of a Space Antenna on its Radiation Characteristic	5
Yampolskiy, V.G.	The Oblique Incidence of a Plane Wave on a Wire Grid	9
Yastrebtsova, T.N., Galikin, O.P.	On a Method of Quenching the Free Oscillations of Quartz	7
OTHERS		
	P.I. Lukirski	1
	A.L. Mints. On his 60th Birthday	2
	Scientific-Technical Conference on Matters Pertaining to Television	2
	Sixty Years of Radio	4
	The All-Union Scientific-Technical Society of Radio Engineering and Telecommunication Imeni A.S. Popov	4
	A.G. Arenberg. On his 50th Birthday	5
	Scientific-Technical Conference on the Sound Quality of Radio Broadcasting Receivers	5
	All-Union Scientific Session Devoted to the "Dnyu Radio"	7
	F.A. Lbov. On his 60th Birthday	7
	All-Union Scientific Session Devoted to the "Dnyu Radio"	8
	I.G. Klyatskin. On his 60th Birthday	10
	Scientific-Technical Conference in Leningrad Devoted to the 60th Anniversary of the Invention of Radio	10

NEW BOOKS

Ya.S.Itskhokiy. Nonlinear Radio Engineering. Published by "Soviet Radio".
Moscow, 1955, 508 pp. Price: 18r. 50k.

The book is devoted to a study of the most important general properties of nonlinear elements, circuits and basic nonlinear conversions. The principal problems of self-excitation of self-oscillators (RC tube, klystron, TW tube, and magnetron) are explained. The reaction of the external efficiency on a nonlinear oscillating system (regeneration and holding of self-oscillation frequencies) is examined. About 500 problems with answers are given in the text; some of these with the solutions. Particular attention is given in the book to a through study of the essence of the physical processes in the basic nonlinear systems.

The book is designed for students of radiotechnological colleges and for radio engineers.

S.I.Bychkov. Magnetron Transmitters. Edited by S.A.Drobov. Voenizdat, Moscow, 1955, 216 pp. Price: 5r. 85k.

The principle of action and the classification of magnetron oscillators, the fundamentals of multiresonance magnetrons, the construction, electric characteristics and modulation of magnetron oscillators, a high-frequency assembly, and control of the operation of a magnetron transmitter are examined.

K.P.Yegorov and G.P.Tikhanov. Construction of Equipment for Long-Distance Links. Gosenergoizdat, Moscow-Leningrad, 1955, 423 pp. Price: 14r.

Basic data on the design of components and units of equipment for a long-distance link is explained as well as the construction of the apparatus as a whole. The book was compiled for engineers, but can also be used by technicians and students of advanced courses in the corresponding polytechnic institutes.

Dzh.K.Sausvort. Principles and Application of Waveguide Transmission. Pub-

POOR ORIGINAL

listed by "Soviet Radio", Moscow, 1955, 700 pp. Price: 33r. 50k.

In the book, the basic theories for transmitting electromagnetic energy by waveguides is explained, and the construction and operation of numerous waveguide elements and units, used in super-high frequency technique, are described. The book can be used as a reference and study guide by scientific workers, engineers, and students of advanced courses.

G.S. Tsypkin. Calculation of pulse amplification stages with a simple high-frequency correction. Sovnizdat, Moscow, 1955, 80 pp. Price: 2r. 30k.

Calculation of the stages in broad-band pulse amplification is discussed, including a structural computation of the correcting choke.

Circuit Engineering. Controlled Quartz Generators and Exciters for Frequency Radiotelegraphy. An informative collection. Sovnizdat, Moscow, 1955, 230 pp. plus 21 inserts (Ministry of Radio Links of the USSR, Technical Administration).

Price: 6r. 50k.

The collection includes articles devoted to the design and operation of the exciters VKhD-100 and VT-2, and also to the frequency control of generators with quartz stabilization. The collection is designed for engineer-technical workers, students of advanced courses, and those working with the technique of radio links.

STAT